HIGH PRESSURE SOLUBILITY MEASUREMENTS FOR SELECTED ASYMMETRIC MIXTURES AND EQUATION-OF-STATE DEVELOPMENT

By

WUZI GAO

Bachelor of Science
Xi'an Jiaotong University
Beijing, P. R. China
1990

Master of Science
Beijing University of Chemical Technology
Beijing, P. R. China
1993

Submitted to the Faculty of the
Graduate College of the
Oklahoma State University
in partial fulfillment of
the requirements for
the Degree of
DOCTOR OF PHILOSOPHY
December, 1999

HIGH PRESSURE SOLUBILITY MEASUREMENTS FOR SELECTED ASYMMETRIC MIXTURES AND EQUATION-OF-STATE DEVELOPMENT

Thesis Approved:

K.A.M. Gasem

Thesis Co-Adviser

Thesis Co-Adviser

Wayne B. Powell

Dean of the Graduate College

PREFACE

Measurements are reported for the solubilities of hydrogen, nitrogen and carbon monoxide in dodecane from 344.3 K to 410.9 K at pressures up to 13.2 MPa; of hydrogen in n-hexane and carbon monoxide in cyclohexane from 344.3 K to 410.9 K at pressures up to 15.1 MPa; and of nitrogen in cyclohexane, *trans*-Decalin, benzene, naphthalene, 1-methylnaphthalene, phenanthrene, and pyrene from 344.3 K to 433.2 K at pressures up to 22.8 MPa. Thorough evaluations indicate that the present data are both precise and in general agreement with existing literature measurements. Interaction parameters for both the Soave-Redlich-Kwong (SRK) and the Peng-Robinson (PR) equations of state (EOS) were determined for the systems studied, and the cubic EOS (CEOS) represent the data adequately. In general, the SRK and the PR EOS are capable of describing the data with RMSE within 0.001 in mole fraction, when two interaction parameters are used for each isotherm. The SRK and PR EOS are comparable in representing the mixtures studied.

The present efforts to improve CEOS predictions for asymmetric mixtures have been effective in many regards, including developing: (1) accurate correlations for predicting the heavy n-paraffin critical properties and acentric factors, (2) improved temperature-dependence α function for the PR EOS to predict accurately vapor pressures of heavy hydrocarbons (about 1% average absolute errors up to C_{28}), (3) an alternate EOS

combining rule, and (4) useful generalized-parameter correlations for two widely-used EOS.

I wish to extend my sincere thanks and expressions of gratitude to my adviser Dr. Khaled A. M. Gasem. His intelligent guidance, authoritative knowledge and depth of experience have contributed significantly to the completion of this work.

I would like to thank my co-adviser Dr. Robert L. Robinson, Jr. for the direction and supervision which he provided during the course of this study. His kind support and valuable suggestions are greatly appreciated. Thanks are also extended to Dr. Martin S. High and Dr. Larry H. Scott, Jr. for their help and encouragement during the course of this work.

My parents, Shunyu Gao and Xiaolan Wang, deserve my deep gratitude for being a constant source of support and love in my life. My appreciation goes to my wife, Liwei Cai, for her love, encouragement, and support.

The sponsorship from the Department of Energy of the United States under contract number DE-FG22-90PC90302 is greatly appreciated.

TABLE OF CONTENTS

Section I. Experimental Studies

Section II. Development of Cubic Equations of State

Chapter Page

LIST OF TABLES

Tables Page

Section I

Chapter 1

Chapter 2

Section II

Chapter 4

Chapter 5

Tables Page

Chapter 5 - *continued*

Chapter 6

LIST OF FIGURES

Figures Page

Section I

Chapter 2

Section II

Chapter 4

Chapter 5

Figures Page

Chapter 5 - *continued*

Chapter 6

NOMENCLATURE

a, b	Equation-of-state parameters
f	Fugacity
k, m	Intermediate function in equation of state
p	Pressure
v	Specific volume
z	Mole fraction
A, B, C, D, E, F, G	Model constants
CN	Carbon number
C_{ij}, D_{ij},	Interaction parameters
MW	Molecular mass
NAAD	Normalized average absolute deviations; $(\%AAD)_{generalization}$ / $(\%AAD)_{regression}$
N, NPTS	Number of components
N_{ij}, M_{ij}	Exponents of the conformal combing rule
R	Universal gas constant
RMSE	Root mean square error
SS	Objective function
T	Temperature
Y	Any physical property
Z	Compressibility factor
%AAD	Average absolute percent deviation

Greek Letters

α,β,γ	Correlation scaling exponent
α	Equation-of-state temperature dependence function
ω	Acentric factor

Subscripts and Superscripts

c	Critical state
cal	Calculated
exp	Experimental

b	Normal boiling point
r	Reduced property
∞	Limiting property value
0	Initial property value
L	Liquid
V	Vapor

CHAPTER 1

INTRODUCTION

Fluid phase equilibrium properties (*phase temperature, pressure, liquid and vapor compositions*) are widely used in the development of various chemical processes, such as phase separations. Frequently quoted statistics (Zeck and Wolf, 1992) suggest that in conventional chemical plants as much as 70% of the capital costs and 90% of the operating expenses are associated with phase separations. Therefore, accurate prediction of phase equilibrium properties and the associated phase behavior are essential for proper design, operation and optimization of chemical processes. The complexity of molecular interactions precludes *a priori* knowledge of phase behavior; consequently, viable predictive models must be developed from sound theory, judicious approximations and accurate experimental information. That is, models developed from theory must also be validated against intelligently selected experimental data, and the computational difficulties in implementing the theoretical information must be overcome to develop tractable models (Gasem and Robinson, 1995).

The focus of this study is the phase behavior of asymmetric mixtures, involving supercritical solute gases (such as hydrogen, nitrogen, methane, ethane, carbon monoxide, and carbon dioxide) in various solvents including heavy n-paraffins (C_4 to C_{44}), naphthenes (cyclo-hexane and trans-decalin) and aromatics (benzene, naphthalene, 1-methylnaphthalene, phenanthrene, and pyrene). These mixtures, in which large differences in size exist among the components of the mixture, are encountered in many important industrial processes, including coal processing, enhanced oil recovery, supercritical extraction, and in environmental remediation. Thus, enhanced representation of asymmetric mixtures has considerable economic impact on these industries.

Asymmetric mixtures pose a significant challenge to our current phase behavior models for several reasons:

1. Significant differences in molecular size among the mixture components tax the abilities of the current theories on mixing.
2. The presence of near-critical and supercritical components in such mixtures compromises the accuracy of most equation of state models.
3. Variations in the molecular structures of the supercritical components increase the difficulties in developing generalized models.

OBJECTIVES

The purpose of this study is to address some of the issues outlined above relating to the accurate prediction of the phase behavior of asymmetric mixtures. Specifically, experimental data were collected on systematically-selected systems to delineate the effects of molecular structure and size, as well as temperature, pressure, and composition. The specific objectives in this study were as follows:

1. Measure the solubilities of selected binary systems, as indicated in Table 1, to complement our previous database and to provide critically needed experimental data for model development. A special emphasis was placed on the supercritical gas solutes hydrogen and nitrogen since they have low

Table 1

Binary Vapor-Liquid Phase Equilibrium Data Measured at Oklahoma State University

Solvents	**Solutes**					
	H_2	N_2	CH_4	C_2H_6	CO	CO_2
Paraffin						
n-C_4						X
n-C_6	M[1]	X[2]	X	X	X	X
n-C_{10}	X	M	X	X	X	X
n-C_{12}	M	M	X	X	M	X
n-C_{14}	X		X	X	X	X
n-C_{20}	X	X	X	X	X	X
n-C_{28}	X	X	X	X	X	X
n-C_{36}	X	X	X	X	X	X
n-C_{44}			X	X		X
Naphthene						
Cyclohexane		M	X	X	M	X
Trans-Decalin		M	X	X		X
Aromatic						
Benzene	X	M	X	X	X	X
Naphthalene	X	M	X	X	X	X
1-Methylnaphthalene		M				X
Phenanthrene	X	M	X	X	X	X
Pyrene	X	M	X	X	X	X
Temperature Range	300-435 K					
Pressure Range	5-15 MPa					

1. M signifies systems measured in this study.
2. X signifies systems measured previously at OSU.

critical temperatures and relatively fewer literature data, and, in addition, are of practical importance.

2. Evaluate and develop improved cubic equation-of-state (CEOS) models capable of representing the asymmetric mixtures under study. Particular attention was given to the widely-used Peng-Robinson (PR) and Soave-Redlich-Kwong (SRK) equations of state (EOS). This includes (a) developing accurate correlations for predicting the heavy n-paraffin critical properties and acentric factors, (b) developing an improved temperature-dependence function for the PR EOS to accurately predict vapor pressures of heavy hydrocarbons, and (c) evaluating the merits of an alternate EOS combining rule.
3. Present the modeling results for mixtures in generalized, practical EOS formats suitable for use in process engineering calculations.

ORGANIZATION

Section I of this dissertation is focused on experimental measurements undertaken in this study, and Section II details the EOS model development efforts. References are given in each section.

Chapter 2 outlines the experimental method, procedures and measurements acquired in this study, as well as the results and discussion for each system investigated. Also given in this chapter are PR and SRK binary interaction parameters and Henry's constants generated from the newly acquired data.

Section II consists of Chapters 3-6. It contains the EOS modeling work. Chapter 3 outlines some of the difficulties associated with EOS modeling of asymmetric mixtures. Chapter 4 describes the efforts to update the Asymptotic Behavior Correlation and improve the prediction of heavy n-paraffin critical properties and acentric factors. Chapter 5 presents the evaluation results for the development of a new PR EOS temperature-dependence function. Finally, Chapter 6 provides the details on the alternate EOS combining rule and generalized EOS predictions. Also included in this chapter are EOS binary interaction parameters using the classical and alternate combining rules and their corresponding generalized-parameter correlations.

SECTION I. EXPERIMENTAL STUDIES

CHAPTER 2

HIGH-PRESSURE SOLUBILITIES OF HYDROGEN, NITROGEN AND CARBON MONOXIDE IN SELECTED HYDROCARBONS FROM 323.2 TO 433.2 K AT PRESSURES TO 22.8 MPa

INTRODUCTION

Research to validate any theoretical development requires pertinent, accurate experimental data over an adequate range of operating conditions. Nevertheless, the quantity of data required can be reduced dramatically if the experiments are carefully designed to serve specific, critical roles in the development and testing of the theoretical models and correlations. Such a research program should logically include (a) critical evaluation of existing literature data, (b) identification of viable correlation frameworks that contain a minimum number of input parameters (and those parameters should be amenable to generalization), and (c) an experimental facility able to provide the data for the model and process development efforts (Gasem and Robinson, 1995).

Vapor-liquid equilibrium (VLE) experimental data have been rated as top priorities in phase equilibrium model development, yet the literature data are insufficient for present needs, especially for the asymmetric systems. Therefore, a matrix of binary systems that needed experimental measurements was proposed at Oklahoma State University (OSU) years ago (see, e.g., Gasem and Robinson, 1985a) as shown in Table 1 of Chapter 1. The systems and conditions are selected in such a way as to provide proper experimental data to develop models that can reflect the effects of variations in the solute, the solvent molecular structure/size, and the phase conditions of temperature and pressure. The effects that the selected solutes and solvents intended to reflect are shown in Table 1. On the solute side, the critical temperatures for the selected solutes vary widely. Thus, for a given experimental temperature, a wide range of reduced temperatures exists. Moreover, the solute gases considered reflect a wide range of structural attributes, such as the quantum effect for hydrogen and the quadruple effect of carbon dioxide. Comparison of the phase behavior predictions of a binary mixture comprised of a specific solvent and hydrogen or nitrogen would delineate the impact of the quantum effect on such predictions. As such, these solutes provide a systematic test of the current models over a wide range of operating conditions. On the solvent side, straight chain paraffins were selected to study the effect of molecular size variations on the model predictions. Cyclic compounds (naphthenes and aromatics) were also selected to reflect variations in molecular size and structure.

More than 80 mixtures in Table 1 of Chapter 1 have been measured at OSU. However, the current OSU data combined with literature data are incomplete for model development. Specifically, fewer data exist for mixtures involving gas solutes with low critical temperatures, such as nitrogen; therefore, measurements involving nitrogen and hydrogen were selected to expand the current database. The binary mixtures measured in this study are listed in Table 1 and labeled M. They include the following measurements: hydrogen in hexane and dodecane; carbon monoxide in dodecane and cyclohexane; nitrogen in decane, dodecane, cyclohexane, trans-decalin, benzene, naphthalene,

Table 1

Design of Experimental Measurements

	Studies on Solute Variations					
Solute	H_2	N_2	CH_4	C_2H_6	CO	CO_2
(T_c, K)	(33.2)	(126.2)	(190.4)	(305.4)	(132.9)	(304.2)
H_2		quantum				
N_2			T_r	T_r	structure	
CH_4						T_r
C_2H_6						quadruple

Studies of Solvent Structure and Size Effects

n-Paraffins

Naphthene

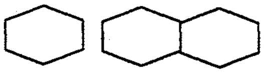

Aromatics

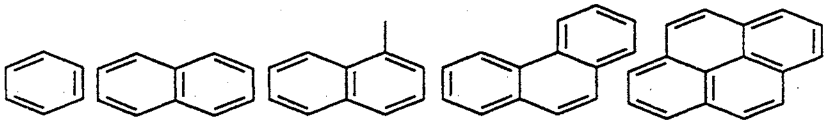

1-methylnaphthalene, phenanthrene and pyrene. These binary data constitute a valuable complement to our previous measurements.

Systems studied in our group (see, e.g., nitrogen + decane by Tong, 1994) were used to verify the accuracy of current measurements. For nitrogen in normal alkanes, there are also literature data for the decane binary (Azarnoosh and McKetta, 1963; Llave and Chung, 1988), which offered further verification. For nitrogen in selected naphthenic and aromatic solvents, there are literature data for nitrogen + cyclohexane (Shibate and Sandler; 1989) at 366.5 K and 410.9 K and for nitrogen + benzene system (Llave and Chung, 1988; Miller and Dodge, 1940) at 373.2 K within our pressure range. de Leeuw, et al. (1989) have reported data for nitrogen in benzene and naphthalene; portions of their experimental conditions overlap ours. No other published data exist for the remaining systems of this study.

The present measurements gave us the opportunity to evaluate the literature data, verify our previous measurements, and expand the experimental database. In addition, the solubility measurements of the selected systems offer a useful basis to develop and test models for predicting the phase behavior of asymmetric mixtures.

EXPERIMENTAL METHOD

The experimental apparatus and procedures have been described by Darwish (Darwish, 1991) and Park (Park, 1994) and are summarized briefly here. A detailed diagram of the facility is shown in Figure 1, and the basis for this experiment is illustrated in Figures 2 and 3. The pressure-volume (p-V) phase diagram of a binary mixture at constant composition is depicted in Figure 2. The region in the circle contains

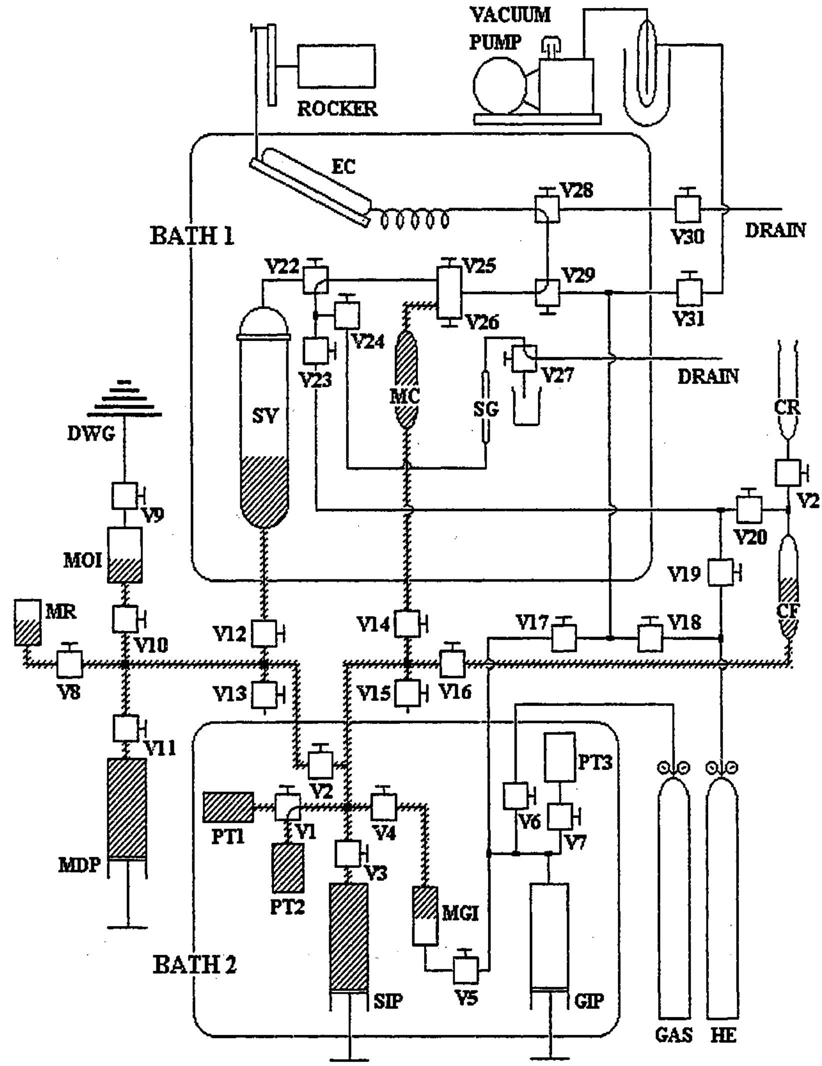

CF	Cleaning Fluid Cylinder	MGI	Mercury-Gas Interface
CR	Cleaning Fluid Reservoir	MC	Mercury Storage Cell
DWG	Dead Weight Gauge	MOI	Mercury-Oil Interface
EC	Equilibrium Cell	MR	Mercury Reservoir
GAS	Solute Gas	PT's	Pressure Transducers
EC	Equilibrium Cell	SG	Sight Glass
GIP	Solute Gas Injection Pump	SIP	Solvent Injection Pump
HE	Helium Gas	SV	Solvent Storage Cell
MDP	Mercury Displacement Pump	V1-V31	Valves

Figure 1. Schematic Diagram of Experimental Apparatus.

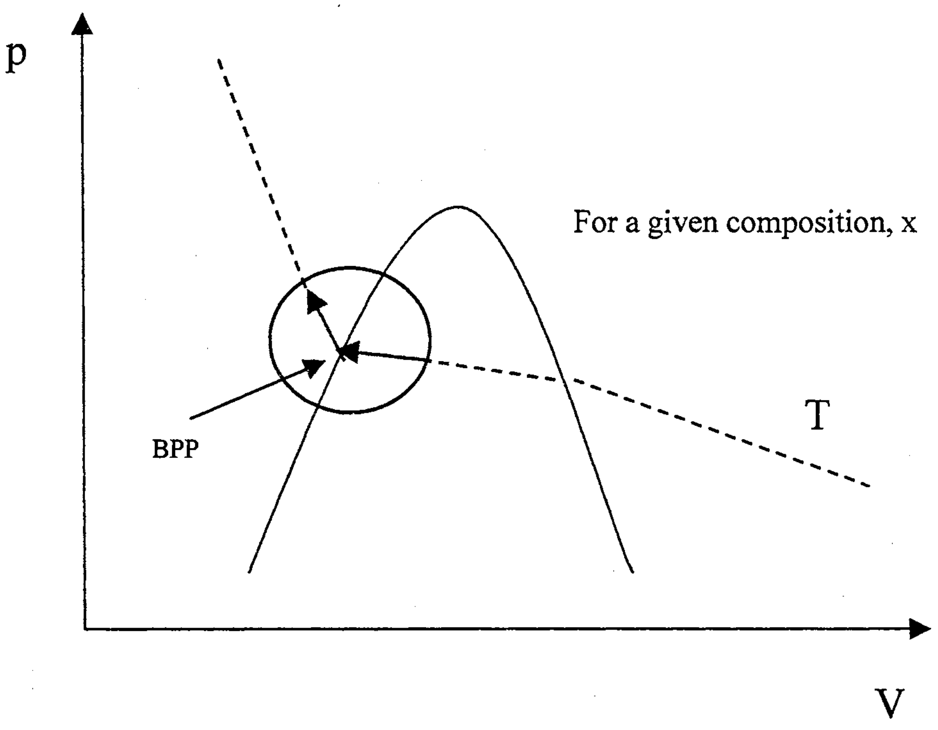

Figure 2. The Concept for the Experimental Method Used in This Study.

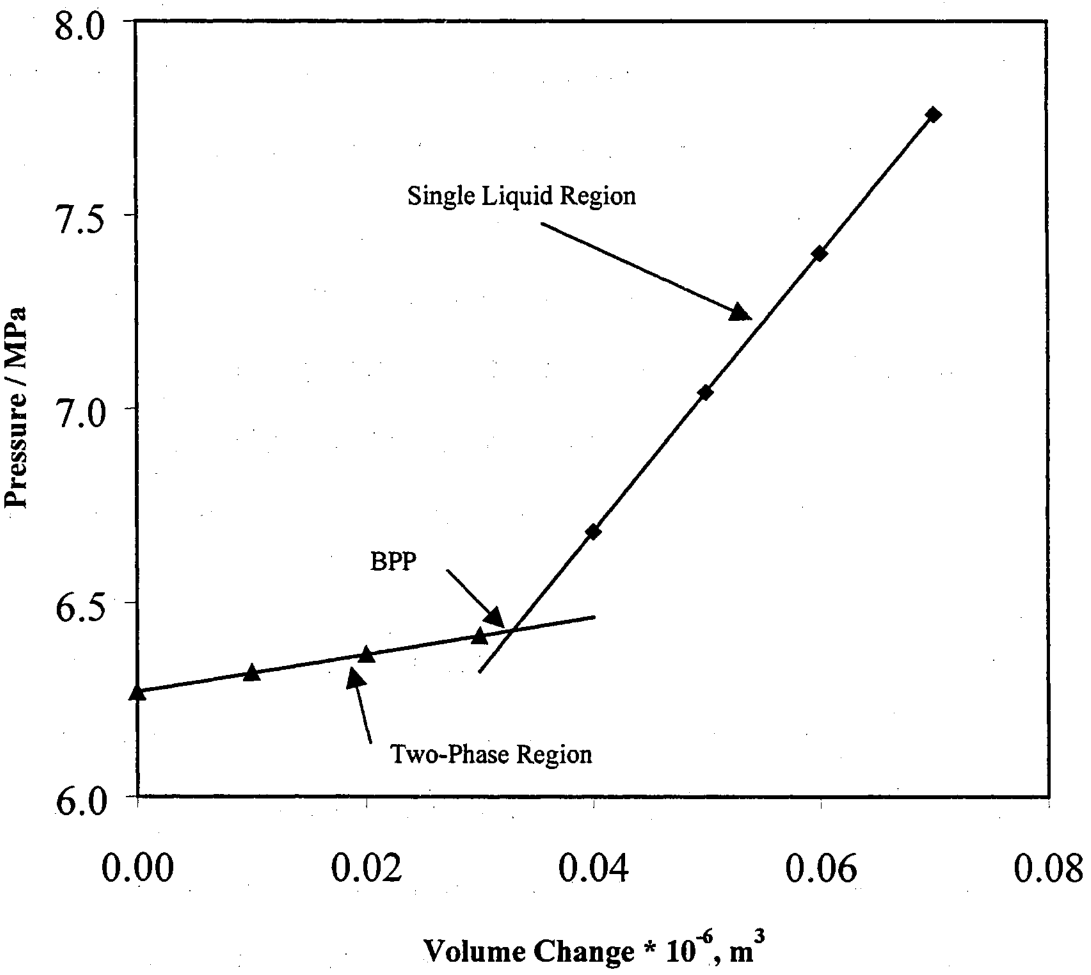

Figure 3. A Sample Pressure-Volume Plot for Bubble Point Determination.

the operational range. As the mixture is compressed from two-phase vapor-liquid region to single liquid phase region, the bubble point 'BPP' is determined by the difference in the compressibility of the mixture in the two regions. A sample pressure-volume plot from experiment is shown in Figure 3. The intersection point 'BPP' by the operation line from the two-phase region and that from the single liquid region is the bubble point we identified.

Phase equilibrium is established in a variable-volume, thermostated, static-type blind cell. Two steel balls are placed in the equilibrium cell, and the cell can be rocked 45 degrees above and below the horizontal position to hasten the establishment of equilibrium. The effective volume of the cell can be varied by the introduction or withdrawal of mercury.

A known amount of degassed liquid solvent is injected volumetrically into the initially evacuated equilibrium cell. A known amount of solute gas is then injected into the rocking cell from a gas-injection pump. After each solute injection, the bubble point pressure of the mixture is determined by sequentially injecting known amounts of mercury into the equilibrium cell to alter the system volume. After each mercury injection, the equilibrium cell is rocked to bring the system to equilibrium, and the pressure is recorded. The bubble point pressure (for the mixture of known composition) is identified graphically from the discontinuity in a pressure vs. total-volume-of-mercury-injected plot (Figure 3) as the mixture passes from the more compressible two-phase state to the less compressible single-liquid-phase state. Additional solute is then added to the cell and the above procedure repeated at the new (higher) solute mole fraction.

Measurement uncertainties are estimated to be 0.1 K in temperature, 0.007 MPa in pressure, and less than 0.001 in composition (mole fraction). However, the estimated uncertainties (ε_{bp}) in the reported bubble point pressures (p_{bp}) at a specified mole fraction range from less than 0.1 MPa for the benzene system to about 0.5 MPa for the phenanthrene system, since $(\varepsilon_{bp})^2 = (\varepsilon_p)^2 + (d[p_{bp}]/dx)^2(\varepsilon_x)^2$; the temperature effect is small enough to be omitted. Thus the total uncertainty in the reported bubble point pressure (at specified mole fraction) depends on both pressure and composition uncertainties and, in addition, the steepness of the bubble point pressure - composition curve. Detailed error analysis is outlined in Darwish (1991), Park (1994) and Tong (1994) and, as such, is not detailed here.

CONSISTENCY TESTS

At the inception of experimental work, two types of consistency tests were performed to ensure the viability of experimental measurements: instrumental and external consistency tests (Gasem, 1986).

1. Instrumental Consistency Test

Instrumental consistency for the temperature and pressure devices was ascertained by frequent calibrations. The RTD temperature sensor with a digital display supplied by Fluke Inc. (Model 2180A) was calibrated after every two system measurements, against the ice point measurement, and against a platinum resistance thermometer (Minco Products, Inc., Model S7929PA1L180C Serial No. 1593.) at 344.3, 377.6, 410.9, and 433.2 K. Typically, the deviations were within 0.1 K, which is within the precision of the sensor. The pressure transducers (Model No. ST5E1890, TJE/743-11) coupled with the digital display (Model No. 450D, GM) supplied by Sensotec Inc. were calibrated against a Dead Weight Gauge (Ruska Instrument Corporation, Model 2400.1) before and after each system run. In addition, vapor pressures of benzene and pentane were regularly measured to verify the accuracy of temperature and pressure combined. Sample vapor pressure values obtained in this work, along with comparable data from the literature, are given in Table 2. The observed differences are within the expected uncertainty of the apparatus.

2. External Consistency Test

External consistency tests were employed to verify the accuracy of the apparatus and procedures by comparing the present experimental measurements to similar measurements from reliable sources. Measurements for two isotherms of nitrogen + decane at 344.3 K and 410.9 K were performed for purposes of comparison with the data of Tong (1994). The consistency of results from these two studies was evaluated by the comparisons shown in Figure 4. Results are given in terms of deviations (δx) of the experimental solubilities (liquid mole fraction of nitrogen) from values predicted by the PR EOS, using temperature independent C_{ij} values determined from the combined data sets; details on EOS data reduction is given later. The difference in the δx values between data sets (not the magnitude of the deviation of either set from the reference EOS model) is of interest in these comparisons, since the difference in δx between data sets is independent of the reference model employed. That is, for two data sets A and B, at a fixed temperature and pressure: $\delta x_A - \delta x_B = [(x_{expt}) - (x_{EOS})]_A - [(x_{expt}) - (x_{EOS})]_B =$

Table 2

Vapor Pressure of Pure Benzene and Pentane

Component	T (K)	Vapor Pressure (MPa)		
		This Work	Literature	Reference
Benzene	410.9	0.439	0.445	Reid, et al., 1987
Pentane	377.6	0.640	0.644	Reid, et al., 1987

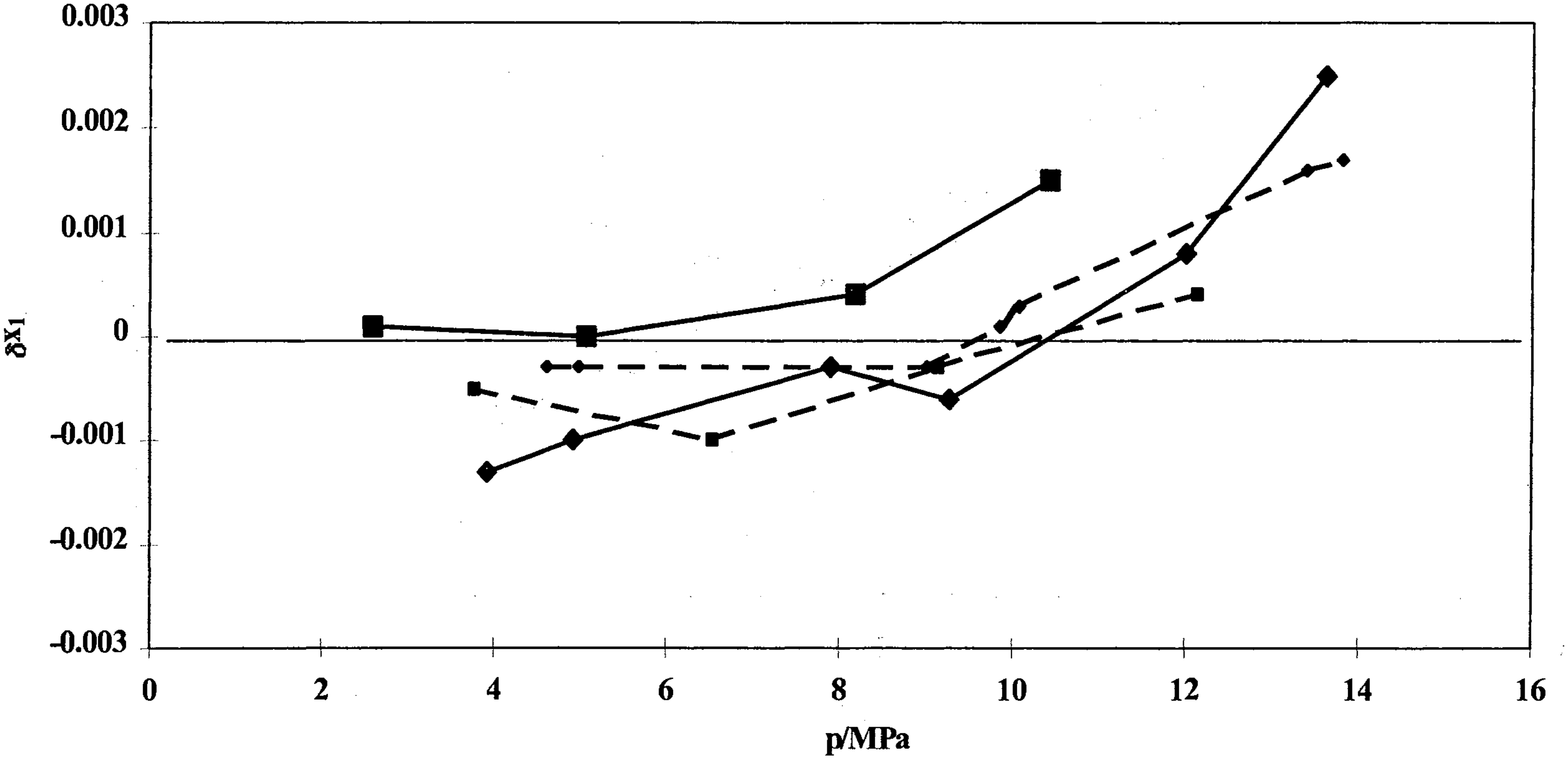

Figure 4. Comparison of Solubility Data for Nitrogen (1) in Decane (2): (◆) Tong, 1994; (■) this work, dashed lines are 344.3 K and solid lines are 410.9 K. In Figures 4-11, δx_1 is the difference between the measured solubility and that predicted by the PR equation.

$(x_{expt})_A$ - $(x_{expt})_B$. This principle is used whenever two data sets are compared. The results for nitrogen + decane are in good agreement; maximum differences in the two data sets are on the order of 0.001 in nitrogen mole fraction.

Following the above confirmations of the viability of experimental apparatus and associated procedures, efforts were directed at measuring the solubility of the targeted binary mixtures.

MATERIALS

All chemicals used in this study are shown in Table 3 along with the suppliers and stated purities. No further purification of the chemicals was attempted.

RESULTS AND DISCUSSION

The measurements in this study cover the temperature range from 323.2 to 433.2 K and pressures to 22.8 MPa. The solute liquid composition range for the data acquired extends from 0.01 to 0.16 in mole fraction. A typical graphical representation of the experimental data is given in Figure 5 for the carbon monoxide + n-dodecane system. Following a brief description of the EOS models employed to correlate the experimental data, detailed presentation and discussion are given for the systems studied.

The Soave-Redlich-Kwong (SRK) EOS (Soave, 1972) and Peng-Robinson (PR) EOS (Peng and Robinson, 1976) were used to correlate the experimental data. The SRK EOS is:

Table 3

Suppliers and Stated Purities of the Chemicals Used in this Work

Chemical Names	Supplier	Purity (mol %)
Hydrogen	Union Carbide Corporation	99.995
Carbon Monoxide	Matheson Gas Products	99.99
Nitrogen	Sooner Airgas, Inc.	99.995
Cyclohexane	Aldrich Chemical Company	99.9+
n-decane	Aldrich Chemical Company	99+
n-dodecane	Aldrich Chemical Company	99+
Benzene	Aldrich Chemical Company	99.9+
Trans-declin	Aldrich Chemical Company	99+
Naphthalene	Aldrich Chemical Company	99+
1-methylnaphthalene	Aldrich Chemical Company	95+
Phenanthrene	Aldrich Chemical Company	98
Pyrene	Aldrich Chemical Company	98

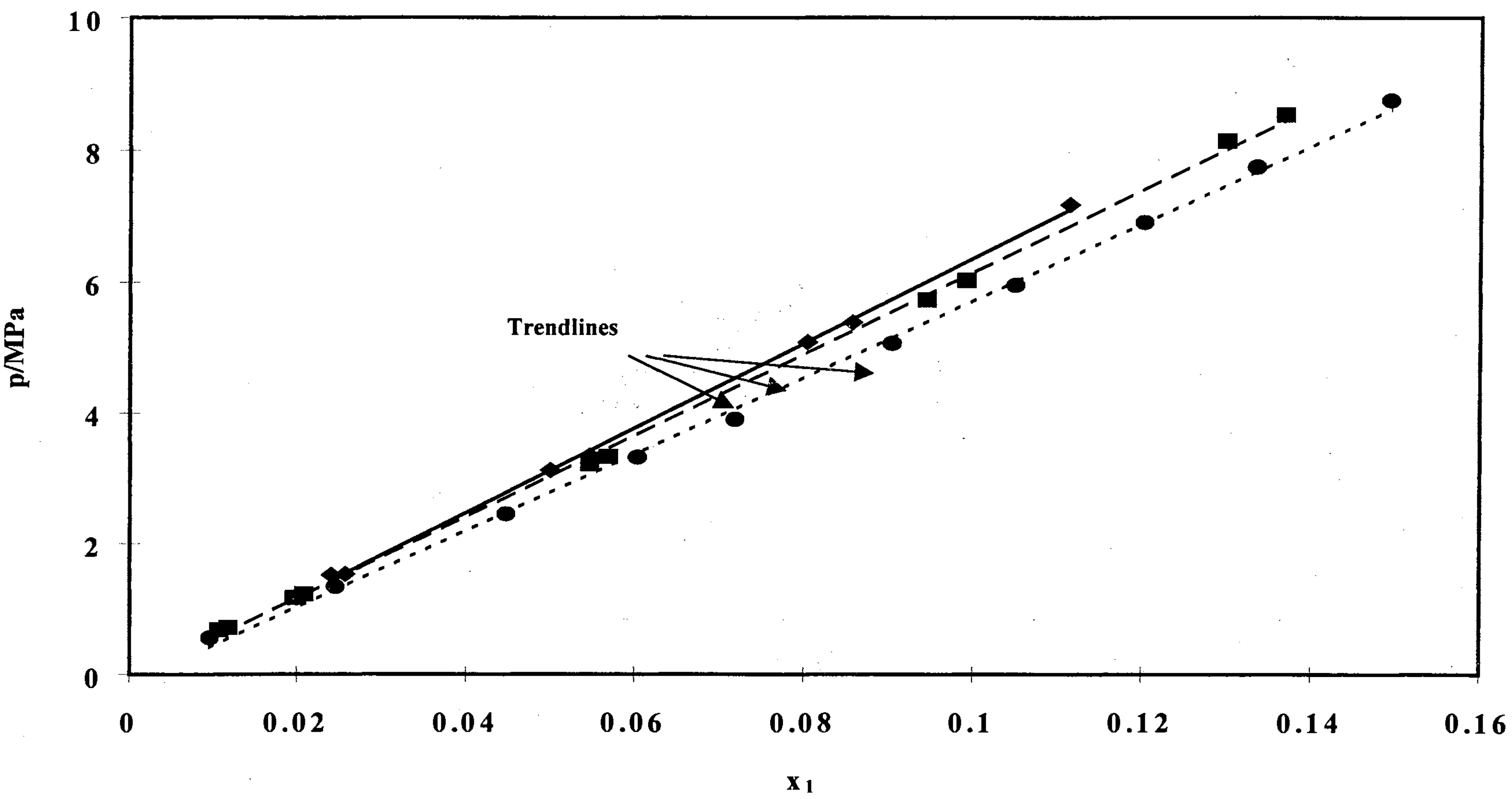

Figure 5. Solubility of Carbon Monoxide (1) in n-Dodecane (2) at (◆) 344.3 K, (■) 377.6 K, (●) 410.9 K.

$$p = \frac{RT}{v - b} - \frac{a}{v(v + b)} \tag{1}$$

where

$$a = a_c \alpha(T) \tag{2}$$

$$b = 0.08664RT_c/P_c \tag{3}$$

and

$$a_c = 0.42748R^2T_c^2/p_c \tag{4}$$

$$\alpha(T)^{1/2} = 1 + k(1 - T_r^{1/2}) \tag{5}$$

$$k = 0.480 + 1.574\omega - 0.176\omega^2 \tag{6}$$

Similarly, the PR EOS is as follows:

$$p = \frac{RT}{v - b} - \frac{a}{v(v + b) + b(v - b)} \tag{7}$$

where

$$a = a_c \alpha(T) \tag{8}$$

$$b = 0.0778RT_c/P_c \tag{9}$$

and

$$a_c = 0.45724R^2T_c^2/p_c \tag{10}$$

$$\alpha(T)^{1/2} = 1 + k(1 - T_r^{1/2}) \tag{11}$$

$$k = 0.37464 + 1.54226\omega - 0.26992\omega^2 \tag{12}$$

where p is the pressure, R is the gas constant, T is the temperature, a and b are EOS constants, v is the molar volume, T_c is the critical temperature, p_c is the critical pressure,

T_r is the reduced temperature, $\alpha(T)$ expresses the temperature dependence in the parameter 'a', and ω is the acentric factor.

To apply the SRK and PR EOS to mixtures, the values of a and b were determined using the mixing rules (Gasem et al., 1989):

$$a = \sum_{i}^{N}\sum_{j}^{N} z_i z_j (1 - C_{ij})(a_i a_j)^{1/2} \tag{13}$$

$$b = 0.5\sum_{i}^{N}\sum_{j}^{N} z_i z_j (1 + D_{ij})(b_i + b_j) \tag{14}$$

where z_k represents the mole fraction of component "k" in a mixture, and N is the number of components in mixture. The input parameters for the pure components (acentric factors, critical temperatures and critical pressures) required by the CEOS are presented in Table 4.

In Eqs. 13 and 14, the summations are over all chemical species, and C_{ij} and D_{ij} are empirical interaction parameters characterizing the binary interactions between components "i" and "j". Interaction parameter values were determined by fitting the experimental data to minimize the objective function, SS, which represents the sum of squared relative deviations in predicted bubble point pressures, i.e.:

$$SS = \sum_{i}^{n} \left(\frac{p_{calc} - p_{exp}}{p_{exp}}\right)_i^2 \tag{15}$$

where n is the number of data points, p_{calc} is the calculated pressure, and p_{exp} is the experimental pressure. Further details of the data reduction technique are given by Gasem (Gasem et al., 1985; Gasem, 1986).

Table 4

The Critical Properties and Acentric Factors Used in the Cubic Equation-of-State Evaluations

Component	p_c / MPa	T_c / K	ω	Reference
Nitrogen	3.39	126.2	0.039	Reid et al. (1987)
Hydrogen	1.30	33.2	-0.218	Reid et al. (1987)
Carbon Monoxide	3.50	132.9	0.066	Reid et al. (1987)
Hexane	3.00	507.3	0.303	Reid et al. (1987)
Decane	2.12	617.7	0.489	Reid et al. (1987)
Dodecane	1.82	658.2	0.575	Reid et al. (1987)
Cyclohexane	4.07	553.5	0.212	Reid et al. (1987)
trans-Decalin	3.14	687.1	0.270	Reid et al. (1987)
Benzene	4.89	562.2	0.212	Reid et al. (1987)
Naphthalene	4.05	748.4	0.302	API Monograph Series (1978)
1-Methylnaphthalene	3.60	772.0	0.310	Reid et al. (1987)
Phenanthrene	3.30	873.2	0.540	API Monograph Series (1979a)
Pyrene	2.60	938.2	0.830[a]	API Monograph Series (1979b)

[a] Turek, 1988

1. Nitrogen in Selected Naphthenic and Aromatic Hydrocarbons

Solubilities of nitrogen in cyclohexane, *trans*-Decalin, benzene, naphthalene, 1-methylnaphthalene, phenanthrene, and pyrene at temperatures from 344.3 K to 433.2 K at pressures up to 22.8 MPa were measured. The experimental data are presented in Table 5. A trend of increasing nitrogen solubility with increasing temperature and pressure is observed for each of the solvents studied.

Since a single interaction parameter (C_{ij}) represents the data for the present systems adequately, addition of a second parameter (D_{ij}) was not necessary (i.e., $D_{ij} = 0$ was employed). Using the optimized value of the interaction parameter, C_{ij}, the solubilities at specified pressures were calculated. Results of the EOS representations of the solubilities are shown in Table 6. In general, the absolute average percent deviations in the calculated bubble point pressures range from about 0.5% for the naphthalene system to 3.0% for the pyrene system. The PR EOS is capable of describing the data with RMSE deviations less than 0.002 in mole fraction when one interaction parameter, C_{ij}, is regressed for each binary system. When a separate value of C_{ij} is used for each isotherm of a given system, representation of the data improves to about 0.001 in mole fraction.

The nitrogen systems show a relatively weak temperature dependence of C_{ij}, which is consistent with our previous studies of mixtures involving the solutes methane, ethane, and CO_2 (Anderson et al., 1986; Darwish, 1991; Darwish et al., 1993; Gasem et al., 1989; Gasem and Robinson, 1985; Park et al., 1995; Srivatsan et al., 1995).

Table 5

Solubility of Nitrogen in Naphthenic and Aromatic Hydrocarbons

x_1	p / MPa		x_1	p / MPa
		Cyclohexane		
		366.5 K		
0.0168	2.08		0.0655	7.59
0.0292	3.46		0.0749	8.72
0.0400	4.68		0.0898	10.49
0.0500	5.80		0.0999	11.71
		410.9 K		
0.0187	2.16		0.0768	7.66
0.0349	3.51		0.0950	9.17
0.0497	5.08		0.1174	11.62
0.0650	6.34		0.1240	12.13
		***Trans*-Decalin**		
		344.3 K		
0.0292	4.15		0.0704	10.44
0.0426	6.05		0.0758	11.48
0.0592	8.65		0.0942	14.57
		377.6 K		
0.0310	3.93		0.0746	10.10
0.0452	5.99		0.0897	12.21
0.0599	7.86		0.1016	14.15
		410.9 K		
0.0313	3.74		0.0748	9.07
0.0482	5.75		0.0901	11.12
0.0598	7.19		0.1105	13.85

Table 5

Solubility of Nitrogen in Naphthenic and Aromatic Hydrocarbons - *continued*

x_1	p / MPa		x_1	p / MPa
		Benzene		
		373.2 K		
0.0200	3.38		0.0624	10.43
0.0290	4.86		0.0750	12.57
0.0360	5.99		0.0888	15.09
0.0494	8.21		0.0929	15.81
		410.9 K		
0.0211	3.24		0.0788	11.00
0.0346	4.86		0.0832	11.56
0.0500	7.09		0.1035	14.44
0.0598	8.34			
		Naphthalene		
		377.6 K		
0.0250	6.96		0.0442	12.95
0.0307	8.73		0.0529	15.95
0.0401	11.59		0.0571	17.51
		410.9 K		
0.0257	6.22		0.0552	14.09
0.0350	8.87		0.0628	16.27
0.0460	11.62		0.0713	18.82
		1-Methylnaphthalene		
		344.3 K		
0.0206	7.22		0.0431	16.00
0.0255	9.25		0.0527	20.91
0.0387	14.63		0.0547	21.45
		377.6 K		
0.0189	5.16		0.0535	15.49
0.0335	9.44		0.0552	16.25
0.0399	11.33		0.0706	21.13
		410.9 K		
0.0203	4.96		0.0502	12.61
0.0296	7.18		0.0620	15.80
0.0449	11.08		0.0762	20.06

Table 5

Solubility of Nitrogen in Naphthenic and Aromatic Hydrocarbons - *continued*

x_1	p / MPa	x_1	p / MPa
Phenanthrene			
383.2 K			
0.0222	10.47	0.0337	16.12
0.0241	11.45	0.0411	19.85
0.0300	14.33	0.0431	20.82
410.9 K			
0.0254	10.44	0.0452	18.60
0.0298	12.47	0.0491	20.35
0.0404	16.74	0.0517	21.40
Pyrene			
433.2 K			
0.0178	7.59	0.0354	15.48
0.0256	11.09	0.0492	21.90
0.0310	13.50	0.0512	22.88

Table 6

SRK and PR Equation-of-State Representations of the Solubility of Nitrogen in Naphthenic and Aromatic Hydrocarbons

T/K	SRK Parameters (PR Parameters) C_{12}	Deviation in Predicted Solute Mole Fraction RMSE	Deviation in Predicted Solute Mole Fraction |MAX|	SRK Henry's Const (PR Henry's Const) MPa
		Cyclohexane		
366.5	0.186	0.0016	0.0030	105.6
	(0.184)	(0.0014)	(0.0029)	(105.8)
410.9	0.170	0.0014	0.0022	85.0
	(0.161)	(0.0013)	(0.0021)	(85.4)
366.5 and 410.9	0.180	0.0020	0.0050	85.9
	(0.176)	(0.0019)	(0.0047)	(87.2)
		***trans*-Decalin**		
344.3	0.242	0.0006	0.0012	131.2
	(0.242)	(0.0006)	(0.0012)	(131.0)
377.6	0.240	0.0008	0.0012	119.9
	(0.235)	(0.0008)	(0.0012)	(120.2)
410.9	0.248	0.0010	0.0022	109.7
	(0.234)	(0.0010)	(0.0021)	(110.3)
344.3, 377.6 and 410.9	0.243	0.0011	0.0029	108.9
	(0.238)	(0.0010)	(0.0027)	(110.9)
		Benzene		
373.2	0.194	0.0013	0.0022	148.8
	(0.196)	(0.0011)	(0.0021)	(148.9)
410.9	0.189	0.0010	0.0021	121.1
	(0.184)	(0.0010)	(0.0020)	(121.6)
373.2 and 410.9	0.192	0.0015	0.0034	121.6
	(0.192)	(0.0013)	(0.0033)	(123.1)
		Naphthalene		
377.6	0.284	0.0002	0.0002	257.9
	(0.288)	(0.0002)	(0.0002)	(257.4)
410.9	0.286	0.0007	0.0011	225.2
	(0.285)	(0.0007)	(0.0011)	(225.8)
377.6 and 410.9	0.285	0.0006	0.0012	224.8
	(0.287)	(0.0006)	(0.0012)	(226.5)

Table 6

SRK and PR Equation-of-State Representations of the Solubility of Nitrogen in Naphthenic and Aromatic Hydrocarbons - *continued*

T/K	SRK Parameters (PR Parameters) C_{12}	Deviation in Predicted Solute Mole Fraction RMSE	Deviation in Predicted Solute Mole Fraction |MAX|	SRK Henry's Const (PR Henry's Const) MPa
		1-Methylnaphthalene		
344.3	0.406	0.0009	0.0015	312.3*
	(0.398)	(0.0008)	(0.0013)	(310.4)
377.6	0.366	0.0012	0.0025	248.1
	(0.357)	(0.0011)	(0.0023)	(247.8)
410.9	0.385	0.0009	0.0017	220.7
	(0.365)	(0.0009)	(0.0016)	(221.4)
344.3, 377.6 and 410.9	0.388	0.0021	0.0032	221.7
	(0.376)	(0.0021)	(0.0031)	(225.5)
		Phenanthrene		
383.2	0.403	0.0008	0.0016	408.6*
	(0.405)	(0.0009)	(0.0015)	(406.5)
410.9	0.405	0.0014	0.0018	353.0
	(0.401)	(0.0013)	(0.0018)	(352.6)
383.2 and 410.9	0.404	0.0010	0.0020	408.9
	(0.403)	(0.0011)	(0.0020)	(403.8)
		Pyrene		
433.2	0.505	0.0012	0.0021	**
	(0.496)	(0.0011)	(0.0018)	**

* Vapor pressure equations used for 1-methylnaphthalene, phenanthrene are out of the temperature range for some low temperatures.

** Valid vapor pressure equation was not available.

Our data for nitrogen + cyclohexane are compared with the previous measurements of Shibate and Sandler (1989) at 366.5 K and 410.9 K in Figure 6. Considerable disagreement exists between our data and those of Shibate and Sandler at both temperatures, with differences approaching 0.01 in mole fraction.

Comparisons of the present data for nitrogen + benzene at 373 K with those of Llave and Chung (1988), Miller and Dodge (1940) and de Leeuw et al. (1989) are shown in Figure 7. The solubility values for the PR EOS are calculated using values of the interaction parameter C_{ij} regressed from our data at each temperature of interest. The figure shows good agreement between our data and those of Miller and Dodge, with differences on the order of 0.002 mole fraction, while agreement with the data of Llave and Chung is less satisfactory. The data of de Leeuw et al. are in excellent agreement with ours. Comparison of our data at 411 K with those of de Leeuw et al. appears in Figure 8; agreement is within about 0.003 mole fraction.

Figure 9 contains a comparison of our data for nitrogen + naphthalene at 377 and 411 K with those of de Leeuw et al. Differences in the data sets are on the order of 0.004 in their common range of pressures. No literature data on the solubilities for the other systems are available for comparison.

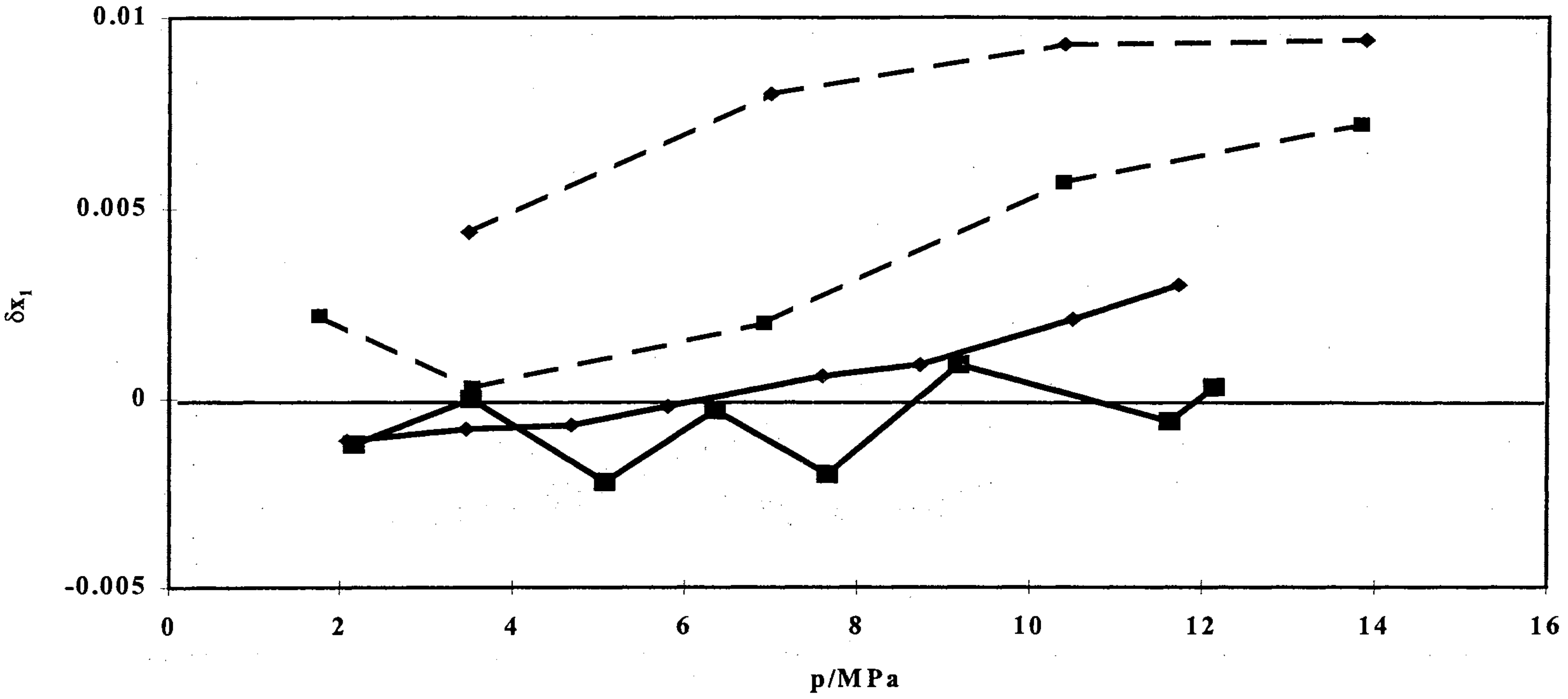

Figure 6. Comparison of Solubility Data for Nitrogen (1) in Cyclohexane (2): solid lines are this work, dashed lines are Shibate and Sandler. (◆) 366.5 K, (■) 410.9 K.

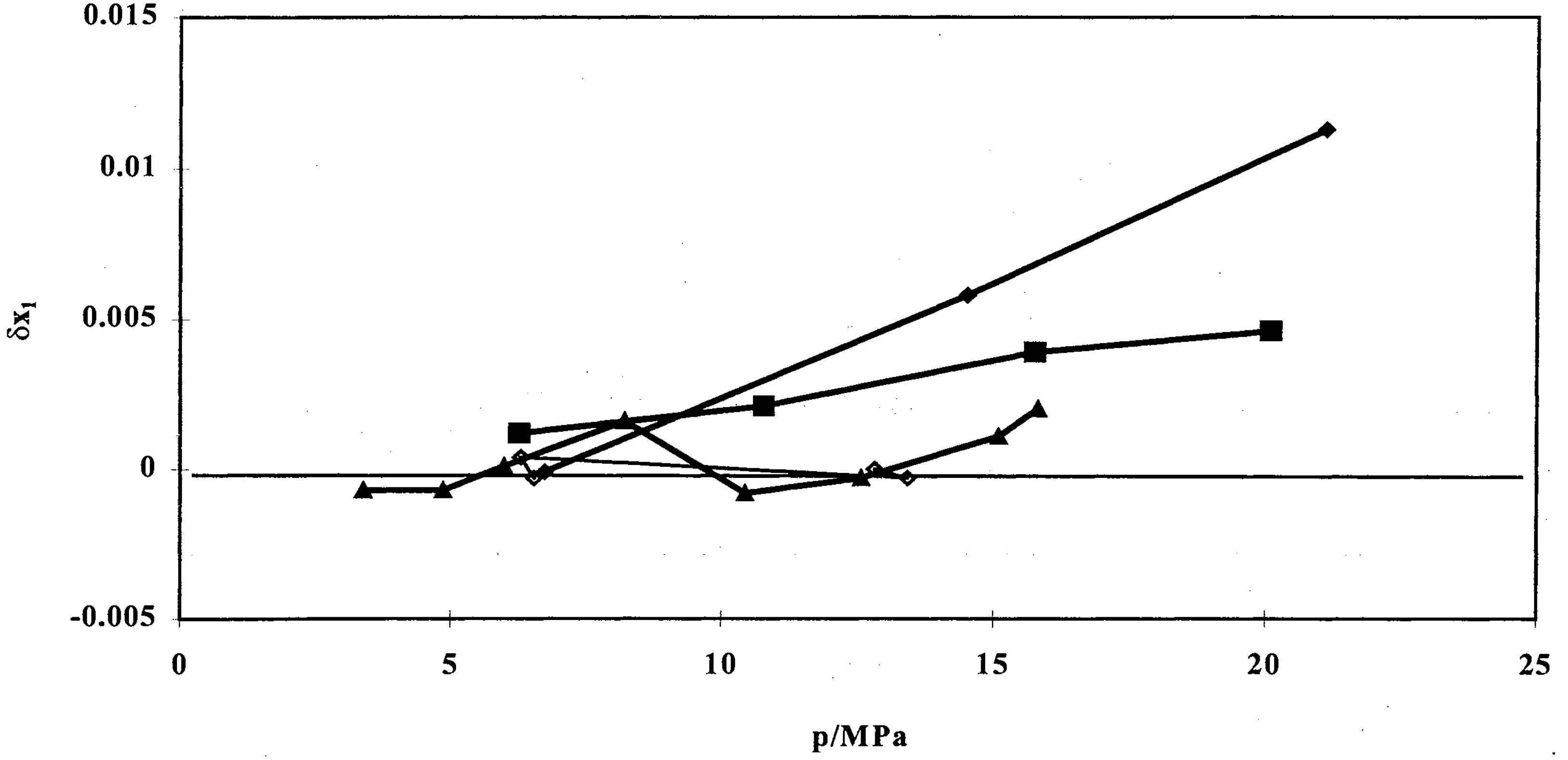

Figure 7. Comparison of Solubility Data for Nitrogen (1) in Benzene (2) at 373.2 K: (◆) Llave, (■) Miller, (▲) this Work, (◇) de Leeuw. (The data of de Leeuw are at temperatures in the interval from 369.8 to 378.8 K.)

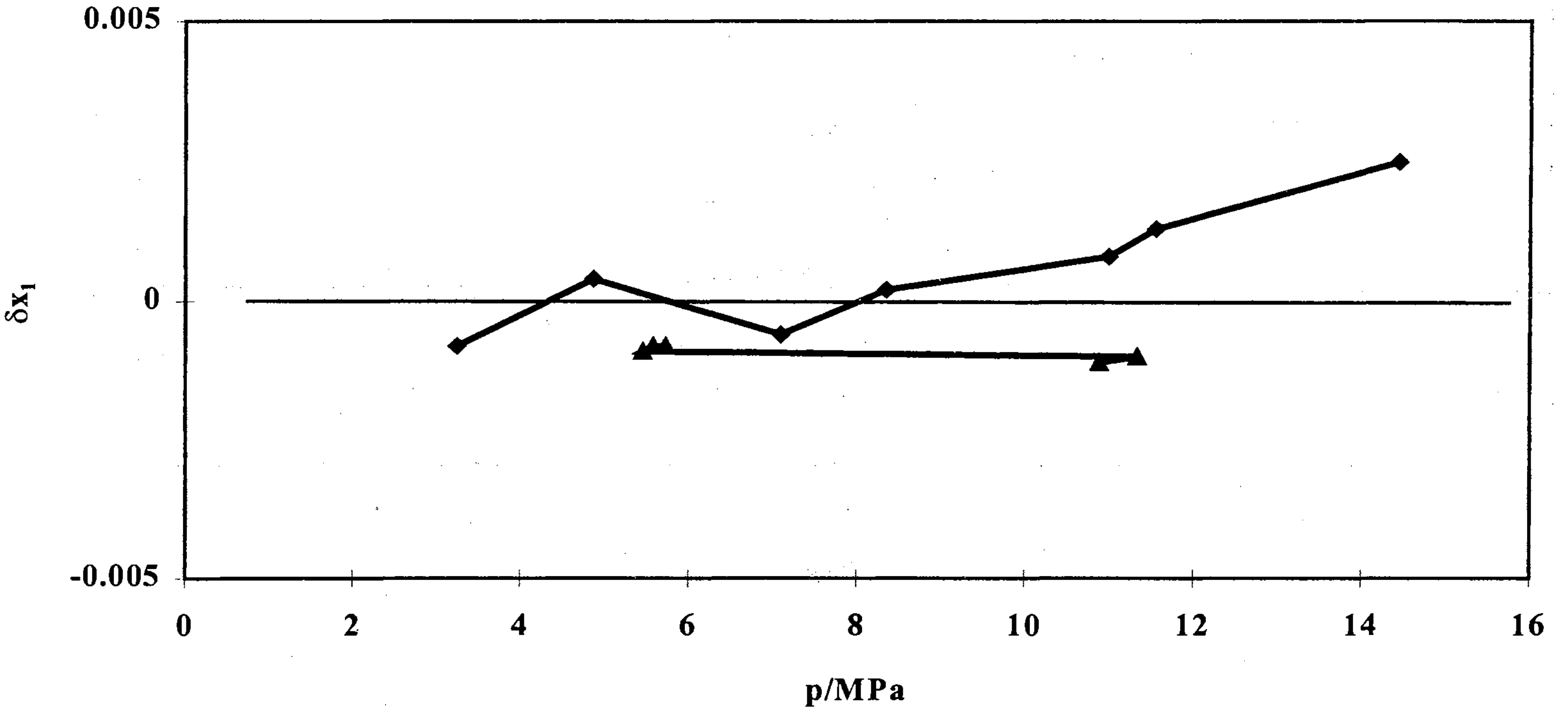

Figure 8. Comparison of Solubility Data for Nitrogen (1) in Benzene (2): (◆) this work at 410.9 K, (▲) de Leeuw. (The data of de Leeuw are at temperatures in the interval from 404.6 to 423.0 K.)

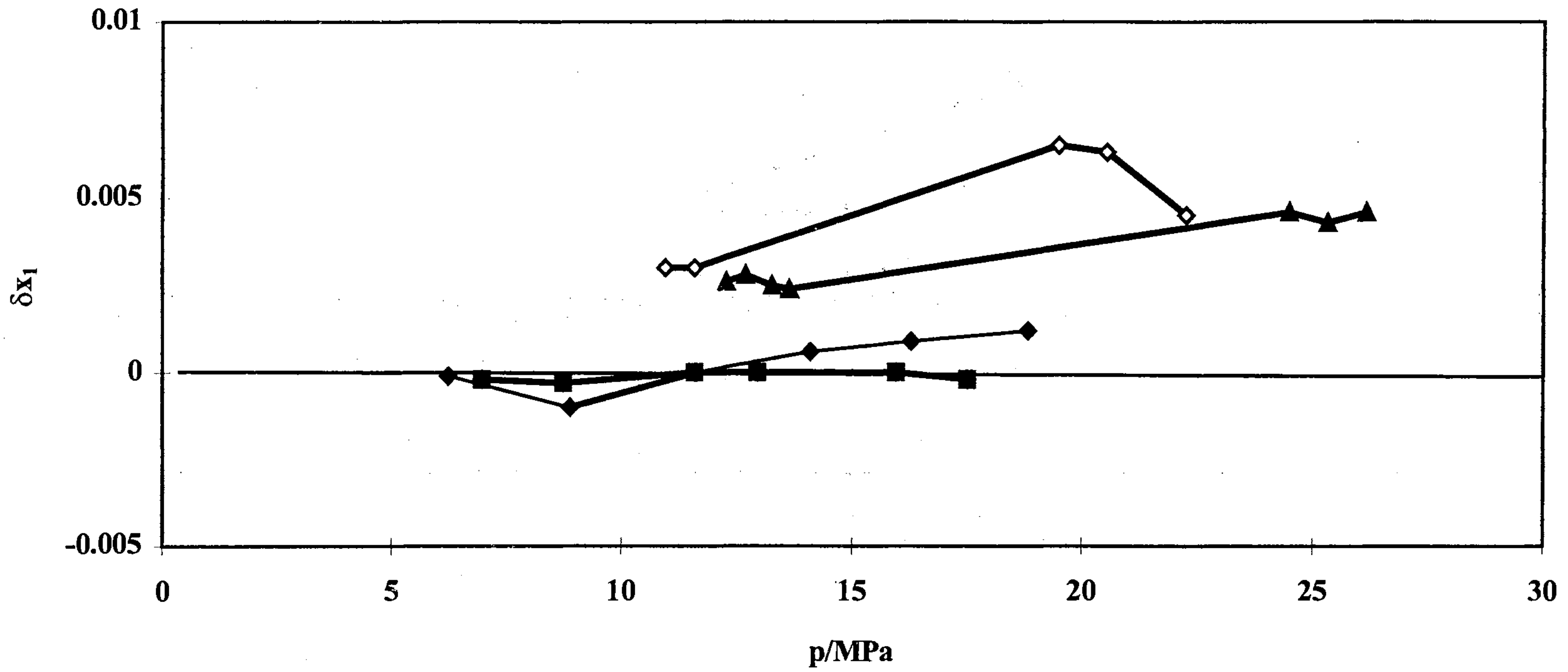

Figure 9. Comparison of Solubility Data for Nitrogen (1) in Naphthalene (2): (■) this work at 377.6 K, (◆) this work at 410.9 K, (▲) de Leeuw at temperatures in the range from of 372.0 to 387.2 K, (◇) de Leeuw at temperatures in the range from 406.1 to 422.1 K.

2. Hydrogen, Nitrogen and Carbon Monoxide in Dodecane

The experimental measurements for the solubilities of hydrogen, nitrogen and carbon monoxide in dodecane are reported in Table 7. Equation-of-state representations of the experimental data are illustrated for carbon monoxide in dodecane in Figure 10. In this figure, the data are shown in terms of the deviation, δx_1, in the solubility (liquid mole fraction) predicted by the PR EOS from the measured value, i.e., $\delta x_1 = x_1(\text{PR}) - x_1(\text{expt'l.})$. The solubility values for the PR EOS are calculated using a separate interaction parameter, C_{ij}, regressed from the data at each isotherm of our measurements.

Details of the EOS representations of the solubilities are shown in Table 8. In general, the SRK EOS and PR EOS are capable of describing the data with RMSE within 0.002 in mole fraction when one interaction parameter, C_{ij}, is used for each isotherm. When a single interaction parameter is regressed for a given system for the complete temperature range, the RMSE are within 0.003. If two interaction parameters, C_{ij} and D_{ij}, are used for each isotherm, the quality of the predictions improves, resulting in RMSE less than 0.001 in mole fraction; however, the interaction parameters are erratic in their temperature dependence, indicating a high correlation between the parameters C_{ij} and D_{ij}. For that reason, and because a single interaction parameter represents the data adequately, no results for two interaction parameters are presented here.

Table 7

Solubility of Hydrogen, Nitrogen and Carbon Monoxide in Dodecane

x_1	p / MPa		x_1	p / MPa
		Hydrogen		
		344.3 K		
0.0297	3.36		0.0703	8.26
0.0302	3.37		0.0802	9.38
0.0505	5.80		0.0900	10.79
0.0506	5.81		0.1010	12.00
		377.6 K		
0.0144	1.42		0.0804	8.43
0.0355	3.56		0.0904	9.55
0.0550	5.59		0.1000	10.64
0.0707	7.39		0.1204	13.24
		410.9 K		
0.0209	1.77		0.0803	7.13
0.0348	2.92		0.0956	8.55
0.0500	4.31		0.1108	10.14
0.0652	5.62		0.1252	11.54
		Nitrogen		
		344.3 K		
0.0314	2.30		0.0804	6.30
0.0422	3.15		0.0915	7.27
0.0559	4.23		0.1046	8.45
0.0675	5.22		0.1165	9.55
		377.6 K		
0.0195	1.41		0.0801	5.90
0.0350	2.43		0.0950	6.97
0.0493	3.53		0.1101	8.27
0.0651	4.65		0.1242	9.42
		410.9 K		
0.0202	1.29		0.0801	5.31
0.0354	2.31		0.0955	6.48
0.0498	3.21		0.1100	7.43
0.0649	4.32		0.1251	8.66

Table 7

Solubility of Hydrogen, Nitrogen and Carbon Monoxide in Dodecane - *continued*

x_1	p / MPa	x_1	p / MPa
Carbon Monoxide			
344.3 K			
0.0240	1.52	0.0804	5.08
0.0256	1.53	0.0857	5.39
0.0500	3.12	0.1113	7.18
0.0546	3.35	0.1150	7.87
377.6 K			
0.0113	0.69	0.0945	5.73
0.0118	0.71	0.0992	6.03
0.0197	1.17	0.1300	8.14
0.0208	1.23	0.1368	8.54
0.0568	3.34		
410.9 K			
0.0245	1.34	0.1049	5.95
0.0447	2.47	0.1202	6.91
0.0603	3.32	0.1335	7.75
0.0718	3.91	0.1493	8.75
0.0904	5.07		

Table 8

SRK and PR Equation-of-State Representations of the Solubility of Hydrogen, Nitrogen and Carbon Monoxide in Dodecane

T/K	SRK Parameters (PR Parameters) C_{12}	Deviation in Predicted Solute Mole Fraction		SRK Henry's Const (PR Henry's Const) MPa
		RMSE	|MAX|	
		Hydrogen		
344.3	0.3723	0.0012	0.0030	105.3
	(0.3567)	(0.0011)	(0.0027)	(106.1)
377.6	0.4569	0.0010	0.0020	93.5
	(0.4002)	(0.0008)	(0.0013)	(94.6)
410.9	0.4688	0.0011	0.0026	79.3
	(0.3863)	(0.0006)	(0.0011)	(80.3)
344.3, 377.6 and 410.9	0.4194	0.0021	0.0063	
	(0.3775)	(0.0014)	(0.0047)	
		Nitrogen		
344.3	0.2162	0.0002	0.0004	70.8
	(0.2095)	(0.0002)	(0.0003)	(70.9)
377.6	0.2252	0.0008	0.0015	66.5
	(0.2086)	(0.0007)	(0.0012)	(66.8)
410.9	0.2352	0.0010	0.0021	61.2
	(0.2049)	(0.0008)	(0.0023)	(61.6)
344.3, 377.6 and 410.9	0.2226	0.0008	0.0016	
	(0.2082)	(0.0008)	(0.0023)	

Table 8

SRK and PR Equation-of-State Representations of the Solubility of Hydrogen, Nitrogen and Carbon Monoxide in Dodecane - *continued*

T/K	SRK Parameters (PR Parameters) C_{12}	Deviation in Predicted Solute Mole Fraction RMSE	|MAX|	SRK Henry's Const (PR Henry's Const) MPa
		Carbon Monoxide		
344.3	0.1061	0.0016	0.0031	58.9
	(0.1120)	(0.0016)	(0.0032)	(58.9)
377.6	0.1009	0.0018	0.0041	56.6
	(0.1004)	(0.0017)	(0.0037)	(56.8)
410.9	0.0711	0.0008	0.0015	51.8
	(0.0671)	(0.0006)	(0.0012)	(52.2)
344.3, 377.6	0.0965	0.0022	0.0052	
and 410.9	(0.0965)	(0.0027)	(0.0063)	

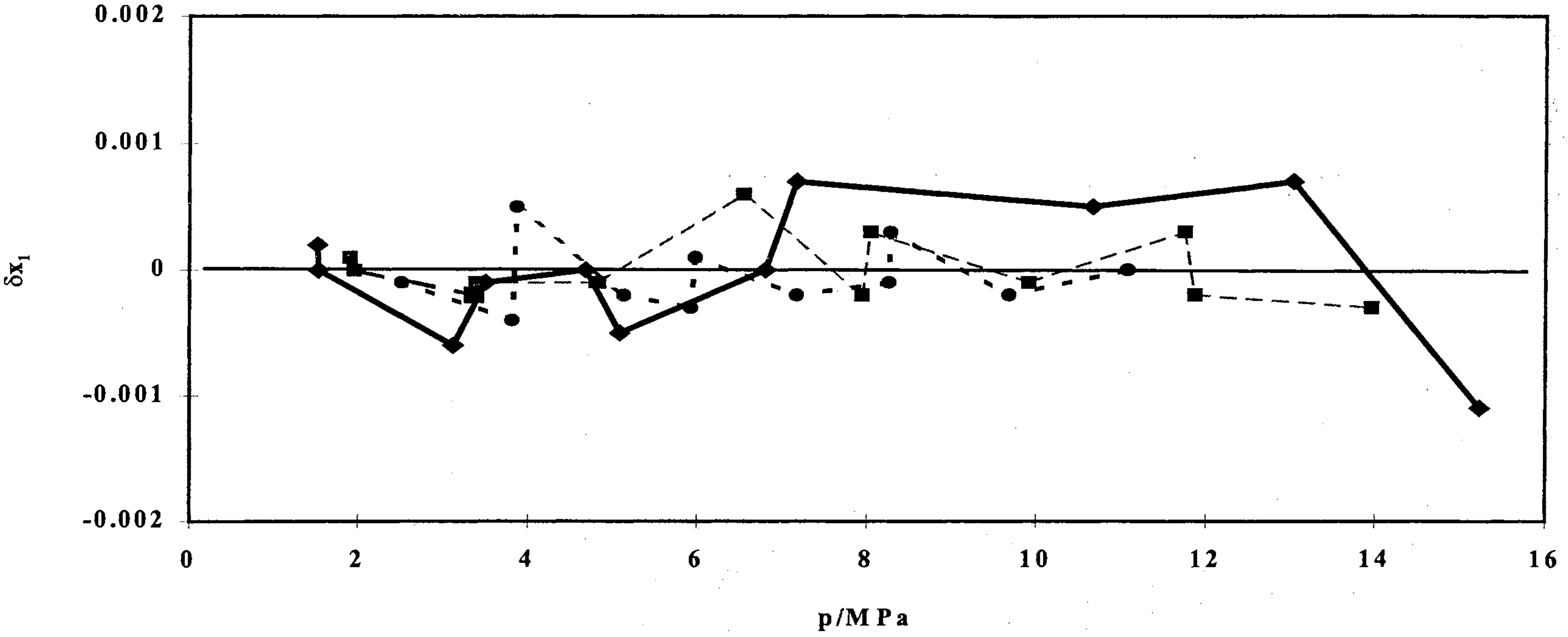

Figure 10. PR EOS Representation of Carbon Monoxide (1) in Dodecane (2) at (◆) 344.3 K, (■) 377.6 K, (●) 410.9 K.

3. Hydrogen in n-Hexane and Carbon Monoxide in Cyclohexane

The experimental measurements are reported in Tables 9 and 10. EOS representations of the experimental data are illustrated for hydrogen in n-hexane in Figure 11. The solubility values for the PR EOS were calculated using a separate interaction parameter, C_{ij}, regressed from the data at each isotherm of our measurements. The C_{ij} values were optimized to minimize the root-mean-square errors in the calculated bubble-point pressures at fixed temperature and liquid mole fraction.

Our data for hydrogen +n-hexane are compared with the previous measurements of Nicholes et al (1957) at 344 K, 377 K and 411 K in Figure 11. Some disagreement exists between our data and those of Nicholes at 344 K, while at 377 K and 410 K, good agreement is achieved, within 0.002 in mole fraction.

Details of the EOS representations of the solubilities are shown in Tables 11 and 12. In general, the SRK EOS and PR EOS are capable of describing the data with RMSE within 0.002 in mole fraction when one interaction parameter, C_{ij}, is used for each isotherm. When a single interaction parameter is regressed for a given system for the complete temperature range, the RMSE are within 0.005. If two interaction parameters, C_{ij} and D_{ij}, are used for each isotherm, the quality of the predictions improves, resulting in RMSE less than 0.001 in mole fraction; however, the interaction parameters are erratic in their temperature dependence, indicating a high correlation between the parameters C_{ij} and D_{ij}. For that reason, and because a single interaction parameter represents the data adequately, no results for two interaction parameters are presented here.

Table 9

Solubility of Hydrogen in n-Hexane

x_1	p / MPa	x_1	p / MPa
344.3 K			
0.0105	1.24	0.0289	3.36
0.0107	1.29	0.0352	4.11
0.0136	1.65	0.0408	4.69
0.0197	2.30	0.0420	4.93
0.0226	2.67	0.0612	7.07
0.0286	3.36	0.0727	8.70
377.6 K			
0.0122	1.38	0.0912	9.31
0.0394	3.93	0.1037	10.65
0.0554	5.46	0.1131	11.71
0.0628	6.24	0.1288	13.48
0.0680	6.84	0.1430	15.11
0.0763	7.71		
410.9 K			
0.0179	1.97	0.0854	7.52
0.0302	2.95	0.0920	8.09
0.0408	3.78	0.0979	8.61
0.0520	4.70	0.1169	10.32
0.0678	6.00	0.1204	11.08
0.0814	7.18		

Table 10

Solubility of Carbon Monoxide in Cyclohexane

x_1	p / MPa		x_1	p / MPa
		344.3 K		
0.0166	1.59		0.0712	6.73
0.0173	1.68		0.0910	8.67
0.0367	3.50		0.1088	10.66
0.0368	3.45		0.1316	13.03
0.0489	4.68		0.1321	12.83
0.0708	6.81		0.1543	15.22
		377.6 K		
0.0200	1.90		0.0898	7.94
0.0209	1.95		0.0901	8.04
0.0376	3.37		0.1110	9.90
0.0376	3.39		0.1320	11.74
0.0539	4.80		0.1321	11.86
0.0544	4.83		0.1544	13.96
0.0732	6.55			
		410.9 K		
0.019	1.98		0.087	7.18
0.027	2.51		0.100	8.26
0.044	3.86		0.100	8.28
0.044	3.81		0.118	9.68
0.061	5.13		0.135	11.07
0.071	5.92		0.135	11.08
0.071	5.98			

Table 11

SRK and PR Equation-of-State Representations of the Solubility of Hydrogen in n-Hexane

T/K	SRK Parameters (PR Parameters) C_{12}	Deviation in Predicted Solute Mole Fraction RMSE	|MAX|	SRK Henry's Const (PR Henry's Const) MPa
344.3	0.4501	0.0007	0.0019	107.1
	(0.3948)	(0.0006)	(0.0017)	(107.6)
377.6	0.5124	0.0013	0.0034	86.1
	(0.4294)	(0.0007)	(0.0020)	(87.6)
410.9	0.7117	0.0012	0.0031	71.7
	(0.5419)	(0.0011)	(0.0022)	(72.9)
344.3, 377.6	0.5128	0.0046	0.0131	84.3
and 410.9	(0.4321)	(0.0038)	(0.0121)	(84.6)

Table 12

SRK and PR Equation-of-State Representations of the Solubility of Carbon Monoxide in Cyclohexane

T/K	SRK Parameters (PR Parameters) C_{12}	Deviation in Predicted Solute Mole Fraction RMSE	|MAX|	SRK Henry's Const (PR Henry's Const) MPa
344.3	0.0442	0.0018	0.0046	87.7
	(0.0640)	(0.0018)	(0.0045)	(87.6)
377.6	0.0330	0.0014	0.0031	84.4
	(0.0505)	(0.0012)	(0.0027)	(80.5)
410.9	0.0341	0.0015	0.0032	72.6
	(0.0469)	(0.0014)	(0.0029)	(72.9)
344.3, 377.6	0.0387	0.0025	0.0064	83.2
and 410.9	(0.0560)	(0.0019)	(0.0047)	(83.5)

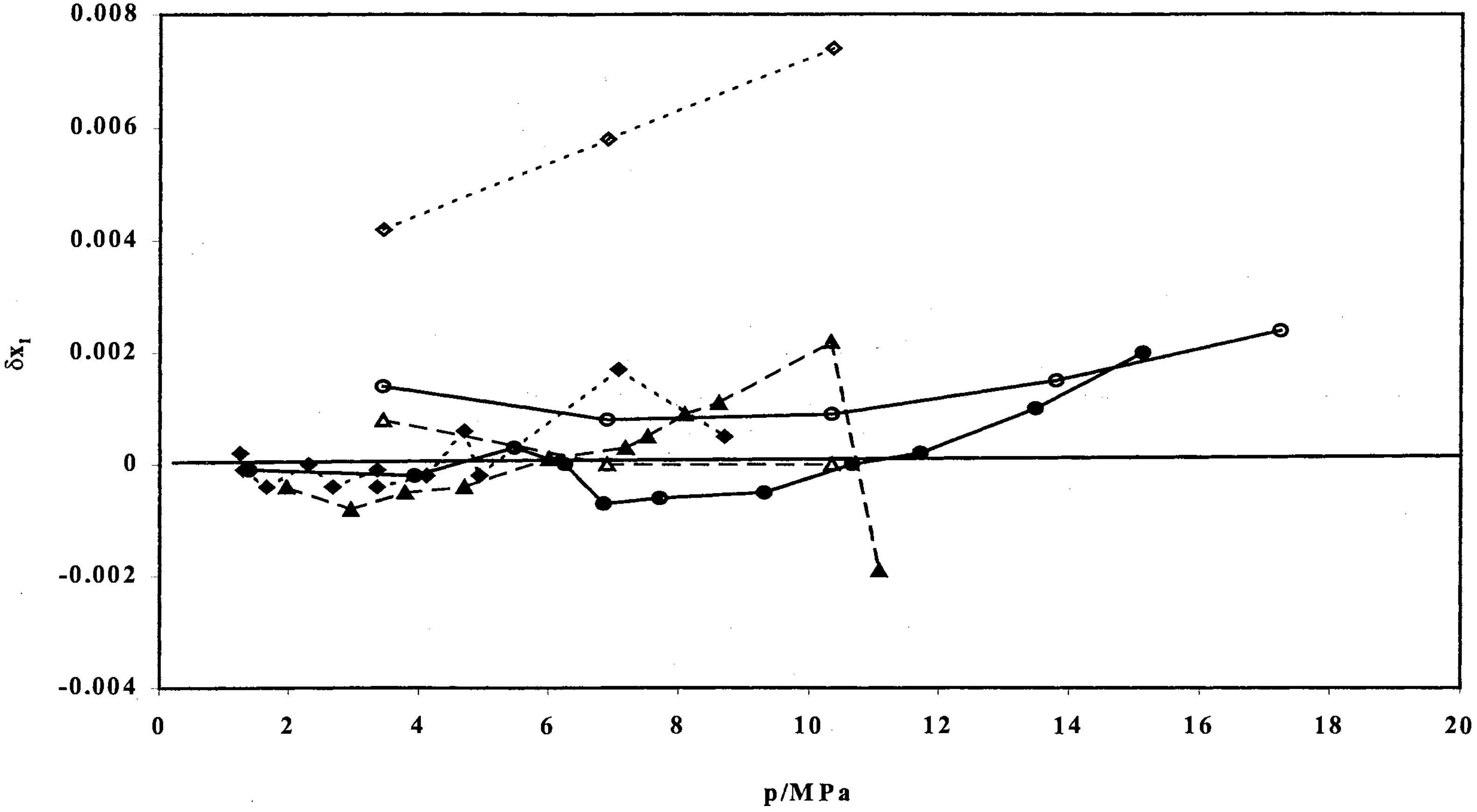

Figure 11. Comparison of Solubility Data for Hydrogen (1) in n-Hexane (2) at (◇) 344.3 K, (O) 377.6 K, (△) 410.9 K. Solid symbols are this study, and open symbols are Nicoles (1957).

HENRY'S CONSTANTS

By definition, Henry's constant of solute (1) in a hydrocarbon solvent (2) is given as:

$$H_{1,2} = \lim_{x_1 \to 0}(\hat{f}_1 / x_1) = \lim_{x_1 \to 0}(\hat{\varphi}_1 p) \qquad (16)$$

where $\hat{f}_1$, x_1, $\hat{\varphi}_1$ are the fugacity, liquid mole fraction, and fugacity coefficient, respectively for the solute. Estimates for Henry's constant were obtained for the present data using SRK and PR equations of state in accordance with the above definition, using a regressed interaction parameter per isotherm, $C_{ij}(T)$. As shown in Tables 6-11, the SRK EOS produces slightly lower $H_{1,2}$ values (~ 1% lower) than those obtained from the PR EOS.

SUMMARY

Measurements are reported for the solubilities of hydrogen, nitrogen and carbon monoxide in dodecane from 344.3 K to 410.9 K at pressures up to 13.2 MPa; of hydrogen in n-hexane and carbon monoxide in cyclohexane from 344.3 K to 410.9 K at pressures up to 15.1 MPa; and of nitrogen in cyclohexane, *trans*-Decalin, benzene, naphthalene, 1-methylnaphthalene, phenanthrene, and pyrene from 344.3 K to 433.2 K at pressures up to 22.8 MPa. Thorough evaluations indicate that the present data are both precise and in general agreement with existing literature measurements. Interaction parameters for both the SRK and the PR EOS were determined for the systems studied, and the CEOS represent the data adequately. In general, the SRK and the PR EOS are capable of describing the data with RMSE within 0.001 in mole fraction, when two interaction parameters are used for each isotherm. Moreover, the SRK and PR EOS are comparable in representing the mixtures studied.

REFERENCES

1. Anderson, J. M.; Barrick, M. W.; Robinson, Jr., R. L. Solubilities of Carbon Dioxide in Cyclohexane and trans-Decalin at Pressures to 10.7 MPa and Temperatures from 323 to 423 K. *J. Chem. Eng. Data,* **1986,** *31*, 172-175.

2. API Monograph Series; *Anthracene and Phenanthrene*; Monograph No. 708; American Petroleum Institute: Washington, DC, **1979a.**

3. API Monograph Series; *Four-Ring Condensed Aromatic Compounds*; Monograph No. 709; American Petroleum Institute: Washington, DC, **1979b.**

4. API Monograph Series; *Naphthalene*; Monograph No. 707; American Petroleum Institute: Washington, DC, **1978.**

5. Azarnoosh, A.; McKetta, J. J. Nitrogen-n-Decane System in the Two-Phase Region. *J. Chem. Eng. Data,* **1963,** *8*, 494-496.

6. Darwish, N. A. *Binary Vapor-Liquid Phase Equilibrium for Methane in Selected Heavy Normal Paraffins, Naphthenes, and Aromatics*. Ph.D. Dissertation, Oklahoma State University, Stillwater, OK, **1991.**

7. Darwish, N. A.; Fathikalajahi, J.; Gasem, K. A. M.; Robinson, Jr., R. L. Solubility of Methane in Heavy Normal Paraffins at Temperatures from 323 to 423 K and Pressures to 10.7 MPa. *J. Chem. Eng. Data,* **1993,** *38*, 44-48.

8. de Leeuw, V. V.; Poot, W.; de Loos, T. W.; de Swaan Arons, J. High Pressure Phase Equilibria of the Binary Systems N_2 + benzene, N_2 + p-xylene, and N_2 + naphthalene. *Fluid Phase Equilib.,* **1989,** *49*, 75-101.

9. Gasem, K. A. M. *Binary Vapor-Liquid Phase Equilibrium for Carbon Dioxide + Heavy Normal Paraffins*. Ph.D. Dissertation, Oklahoma State University, Stillwater, OK, **1986.**

10. Gasem, K. A. M.; Bufkin, B. A.; Raff, A. M.; Robinson, Jr., R. L. Solubilities of Ethane in Heavy Normal Paraffins at Pressures to 7.8 MPa and Temperatures from 348 to 423 K. *J. Chem. Eng. Data,* **1989,** *34*, 187-191.

11. Gasem, K. A. M.; Robinson, R. L. Jr., Predictions of CO_2 Solubility in Heavy Normal Paraffins Using Generalized-Parameters Cubic Equations of State, Paper Presented at National AIChE meeting, Houston, Texas, **1985a.**

12. Gasem, K. A. M.; Robinson, R. L., Jr. *Phase Behavior of Light Gases in Hydrocarbon and Aqueous Solvents*. DOE Proposal, **1995.**

13. Gasem, K. A. M.; Robinson, Jr., R. L. Solubilities of Carbon Dioxide in Heavy Normal Paraffins (C_{20}-C_{44}) at Pressures to 9.6 MPa and Temperatures from 323 to 423 K. *J. Chem. Eng. Data,* **1985**, *30,* 53-56.

14. Llave, F. M.; Chung, T. H. Vapor-Liquid Equilibria of Nitrogen-Hydrogen Systems at Elevated Pressures. *J. Chem. Eng. Data,* **1988**, *33*, 123-128.

15. Miller, P.; Dodge, B. F. The System Benzene-Nitrogen Liquid-Vapor Phase Equilibria at Elevated Pressures. *Ind. Eng. Chem.*, **1940**, 32(3), 434-438.

16. Nichols, W. B.; Reamer, H. H.; and Sage, B. H.. Volumetric and Phase Behavior in the Hydrogen-n-Hexane System. *AIChE J.*, **1957**, *3*, 262-267.

17. Park, J. *Binary Vapor-Liquid Equilibrium Measurements for Selected Asymmetric Mixtures and Equation of State Development.* Ph.D. Dissertation, Oklahoma State University, Stillwater, OK., 1994.

18. Park, J.; Robinson, Jr., R. L.; Gasem, K. A. M. Solubilities of Hydrogen in Heavy Normal Paraffins at Temperatures from 323.2 to 423.2 K and Pressures to 17.4 MPa. *J. Chem. Eng. Data,* **1995**, *40*, 241-244.

19. Park, J.; Robinson, Jr., R. L.; Gasem, K. A. M. Solubilities of Hydrogen in Aromatic Hydrocarbons from 323 to 433 K and Pressures to 21.7 MPa. *J. Chem. Eng. Data,* **1995**, *40,* 70-73.

20. Park, J.; Robinson, R. L., Jr.; Gasem, K. A. M. Solubilities of Hydrogen in Aromatic Hydrocarbons from 323 to 433 K and Pressures to 21.7 MPa. *J. Chem. Eng. Data,* **1996**, *41,* 70-73.

21. Peng, D. Y.; Robinson, D. B. A New Two-Constant Equation of State. *Ind. Eng. Chem. Fundam.*, **1976**, *15*(1), 59-64.

22. Reid, R. C.; Prausnitz, J. M.; Poling, B. E. *The Properties of Gases & Liquids*, 4th ed.; McGraw-Hill: **1987**.

23. Rossini, F.D.; Pitzer, K.S.; Arnett, R.L.; Braun, R.M.; Pimentel, G.C. *Selected Values of Physical and Thermodynamic Properties of Hydrocarbons and Related Compounds*. Carnegie Press. Pittsburgh, PA. **1952**.

24. Shibate, S. K.; Sandler, S. L. High-Pressure Vapor-Liquid Equilibria of Mixtures of Nitrogen, Carbon Dioxide and Cyclohexane. *J. Chem. Eng. Data,* **1989**, 34, 419-424.

25. Soave, G. Equilibrium Constants from a Modified Redlich-Kwong Equation of State. *Chem. Eng. Sci.,* **1972**, *27*, 1197-1203.

26. Srivatsan, S.; Yi, X.; Robinson, Jr., R. L.; Gasem, K. A. M. Solubilities of Carbon Monoxide in Heavy Normal Paraffins at Temperatures from 311 to 423 K and Pressures to 10.2 MPa. *J. Chem. Eng. Data,* **1995**, *40*, 237-240.

27. Tong, J. *Solubility Data for Nitrogen in n-Paraffins and Equation-of-State Methods to Describe Light Gas Solubilities in Hydrocarbons*. M.S. Thesis, Oklahoma State University, Stillwater, OK, **1994**.

28. Turek, E. A., Amoco Production Co., Tulsa, OK, personal communication, **1988**.

29. Zeck, S.; Wolf, D. *Requirements of Thermodynamic Data in Chemical Industry.* Paper presented at the Sixth International Conference for Fluid Properties and Phase Equilibria for Processing and Design, Cortina, Italy, July, **1992**.

SECTION II. DEVELOPMENT OF CUBIC EQUATIONS OF STATE

CHAPTER 3

INTRODUCTION

Although experiments can provide accurate data at specific phase conditions, such data are generally limited and do not meet the industrial needs for process design and development. To describe the phase behavior of a system, accurate analytic models are needed to provide the required property predictions within a reasonable range of conditions. Therefore, aside from the ability to correlate existing experimental data, the true measure of any correlation framework is the ability to provide predictions for (a) systems or conditions for which there are no data, and (b) properties not included in the data reductions (Gasem and Robinson, 1995). Equations of state (EOS) have the potential to meet these criteria for modeling in chemical engineering applications and, therefore, current modeling efforts focus on EOS development. In particular, we attempt to enhance the predictive capability of the classical cubic EOS (CEOS).

CEOS are developed based on the semi-empirical van der Waals EOS, which qualitatively describes molecules that are similar in size and nature. Property calculations of these equations are relatively simple and accurate; therefore, CEOS are widely used in industry. Previous studies (Gasem et al., 1993) have shown that CEOS are capable of predicting the equilibrium properties of asymmetric mixtures, once accurate binary interaction parameters are available. The most often used cubic EOSs are the Soave-

Redlich-Kwong (SRK) (Soave, 1972) and Peng-Robinson (PR) (Peng and Robinson, 1976) equations, described in Chapter 2. Solubility data are normally adequate for evaluation of model parameters, if interest is restricted to predict only equilibrium phase compositions (Gasem and Robinson, 1995).

One advantage of CEOS, such as SRK, is that they do not require pure-fluid adjustable parameters to be regressed from experimental data. Instead, CEOSs require accurate critical properties and the acentric factor for each of the components involved. For this reason, numerous efforts have been expended to measure such properties (Ambrose and Tsonopoulos, 1995). However, reliable experimental data for critical properties are limited to the relatively light compounds, because using conventional techniques, n-paraffins above octadecane thermally decompose before reaching the critical point (Gasem, 1985; Teja, 1990); consequently, several correlations have been proposed to represent the available experimental data precisely and to provide extrapolations for the properties of the heavier compounds. The accuracy of these extrapolations for the heavy compounds is questionable.

The temperature dependence function 'α' in the cubic EOS attractive term 'a' has a large influence on the accuracy of the pure substance vapor pressure calculations (Soave, 1972). Correlations for the temperature dependence used in both SRK and PR were developed based on limited experimental critical properties and vapor pressure (see, e.g., Soave, 1972; Peng and Robinson, 1976). Newly acquired experimental critical properties and vapor pressures for heavier compounds provide an excellent opportunity to test and improve the CEOS vapor pressure predictions, which are essential to the phase equilibrium calculation.

For mixtures, adjustable binary interaction parameters, C_{ij} and D_{ij}, are often needed to describe the systems precisely; this is especially true for highly asymmetric systems. Due to the asymmetric nature of the molecular interactions involved in the mixture and limited knowledge on such systems, no existing theory can predict these parameters well enough. Therefore, those parameters are regressed from experimental data to precisely represent the phase behavior. Moreover, correlations for generalized EOS interaction parameters are developed to facilitate phase behavior predictions of similar systems lacking experimental data.

Concurrent with our experimental program, an integrated model development effort was pursued to provide accurate predictions for phase equilibrium properties of selected asymmetric mixtures. Chapters 4-6 present the EOS modeling work addressing the three specific topics outlined above. Chapter 4 describes the efforts to update the Asymptotic Behavior Correlation and improve the prediction of heavy n-paraffin critical properties and acentric factors. Chapter 5 presents the evaluation results for the development of a new PR EOS temperature-dependence function. Finally, Chapter 6 includes details on alternate EOS combining rule and generalized EOS predictions. Also included in this chapter are the EOS binary interaction parameters using the classical and alternate combining rules and their corresponding generalized-parameter correlations.

CHAPTER 4

UPDATED ABC MODEL FOR PREDICTING HEAVY N-PARAFFIN PHYSICAL PROPERTIES

ABSTRACT

Critical properties and acentric factors are essential ingredients in the use of equation-of-state models. Limited experimental data for such properties, especially for heavy hydrocarbons, necessitate the use of property correlations based on data for lighter hydrocarbons. Poor estimates of the critical properties and the acentric factors translate to erroneous phase behavior predictions and often to computational failure of equations of state.

Recent experimental measurements extend the available data on the critical properties of n-paraffins up to n-C_{36}; therefore, we have undertaken this study to examine a number of existing correlations for predicting n-paraffin physical properties. Careful evaluation of the quality and the extrapolation capability of the correlations considered indicates that the Asymptotic Behavior Correlation (ABC) is well suited for the task; accordingly, we have updated the ABC correlations using the recent experimental data. The accuracy with which the updated ABC correlations represent the available experimental critical temperature, critical pressure, acentric factor, critical compressibility, and normal boiling point temperature is 0.2%, 0.8%, 0.4%, 0.6%, and 0.1%, respectively.

INTRODUCTION

Cubic equations of state (CEOS), such as Soave-Redlich-Kwong (SRK) (Soave, 1972) and Peng-Robinson (PR) (Peng and Robinson, 1976) are widely used by the hydrocarbon industry to perform phase equilibrium calculations. Pure-fluid critical properties and acentric factors have significant influence on the phase behavior predictions of CEOS (Teja, et al., 1990). Riazi, et al. (1998) showed that sizeable errors in the predicted thermophysical properties could result from small errors in the critical properties and acentric factor.

Experimental measurements are the most reliable method for determining these physical properties; however, the available experimental data have been limited to light hydrocarbons. This limitation exists because, using conventional techniques, n-paraffins above octadecane decompose thermally before reaching the critical point (Teja, et al., 1990); consequently, numerous correlations have been developed based on available experimental data, relying on extrapolation to predict the critical properties and acentric factor of the heavy compounds. Some of these correlations require the molecular structure of the hydrocarbon and others employ normal boiling point and specific gravity data.

In this study, we focus our attention on n-paraffins, for which the carbon number correlates directly with molecular size. Several investigators have reviewed correlations utilizing the carbon number (see, e.g., Teja, et al., 1990; Simmrock, et al., 1986; Constantinou, et al., 1995). Similar to other hydrocarbons, most published correlations for n-paraffin critical properties and acentric factors were developed based on limited experimental data involving n-C_{18} and lighter n-paraffins; therefore, property estimates for the heavier n-paraffins are extrapolations that require careful examination.

We have selected several promising correlations in the open literature to examine their extrapolation capabilities for the properties of interest. As indicated by Figures 1-5, large differences exist among the extrapolated property values generated from various correlations. Consequently, we have directed our efforts to updating the ABC correlation to provide more accurate correlations for the critical temperature, pressure, volume, and compressibility; the acentric factor; and the normal boiling point of n-paraffins extending to C_{100}, using newly published data on critical properties and vapor pressure. Specifically, we have relied on recent measurements for the critical temperatures and pressures extending to C_{36} by Nikitin, et al. (1994, 1997) and vapor pressures to C_{28} by Morgan and Kobayashi (1994).

MODEL DEVELOPMENT

Previous studies (see, e.g., Kreglewski and Zwolinski, 1966; Gasem, 1986; Gasem, et al., 1993; Marano and Holder, 1997) have established that several of the n-paraffin physical properties are asymptotic in nature; that is, a limiting value for the physical property is reached asymptotically at very large carbon number. Moreover, proper representation of a property limiting behavior is a prerequisite for reliable extrapolations. Marano and Holder (1997) estimated the limiting values of the critical temperature, critical pressure and critical compressibility based on the Lattice-Fluid theory of Kurata and Isida (1955) and Flory theory of Flory et al. (1964). Both theories predict asymptotic limiting values for the critical temperature and critical pressure;

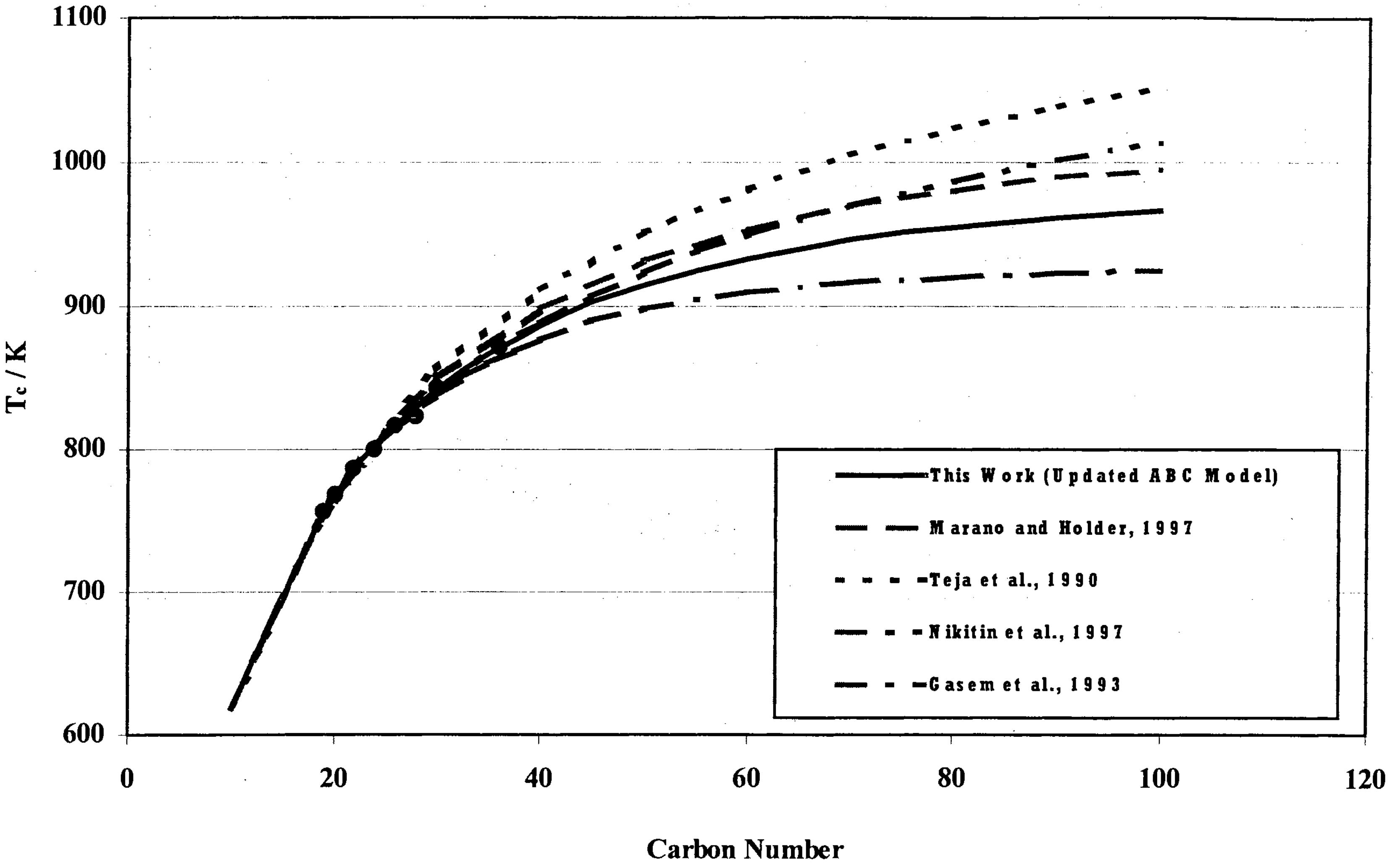

Figure 1. Critical Temperature Predictions for n-Paraffins.

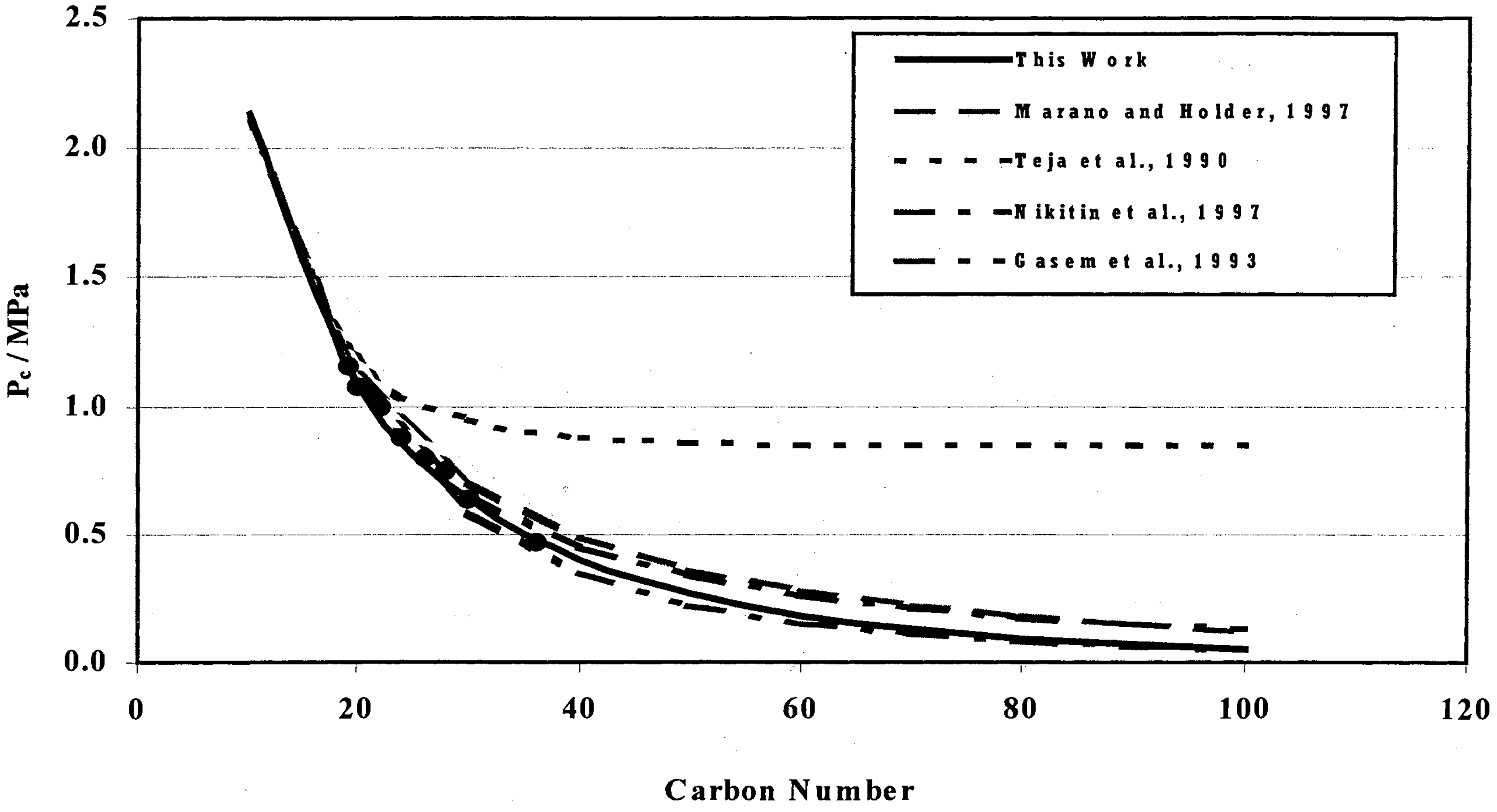

Figure 2. Critical Pressure Predictions for n-Paraffins.

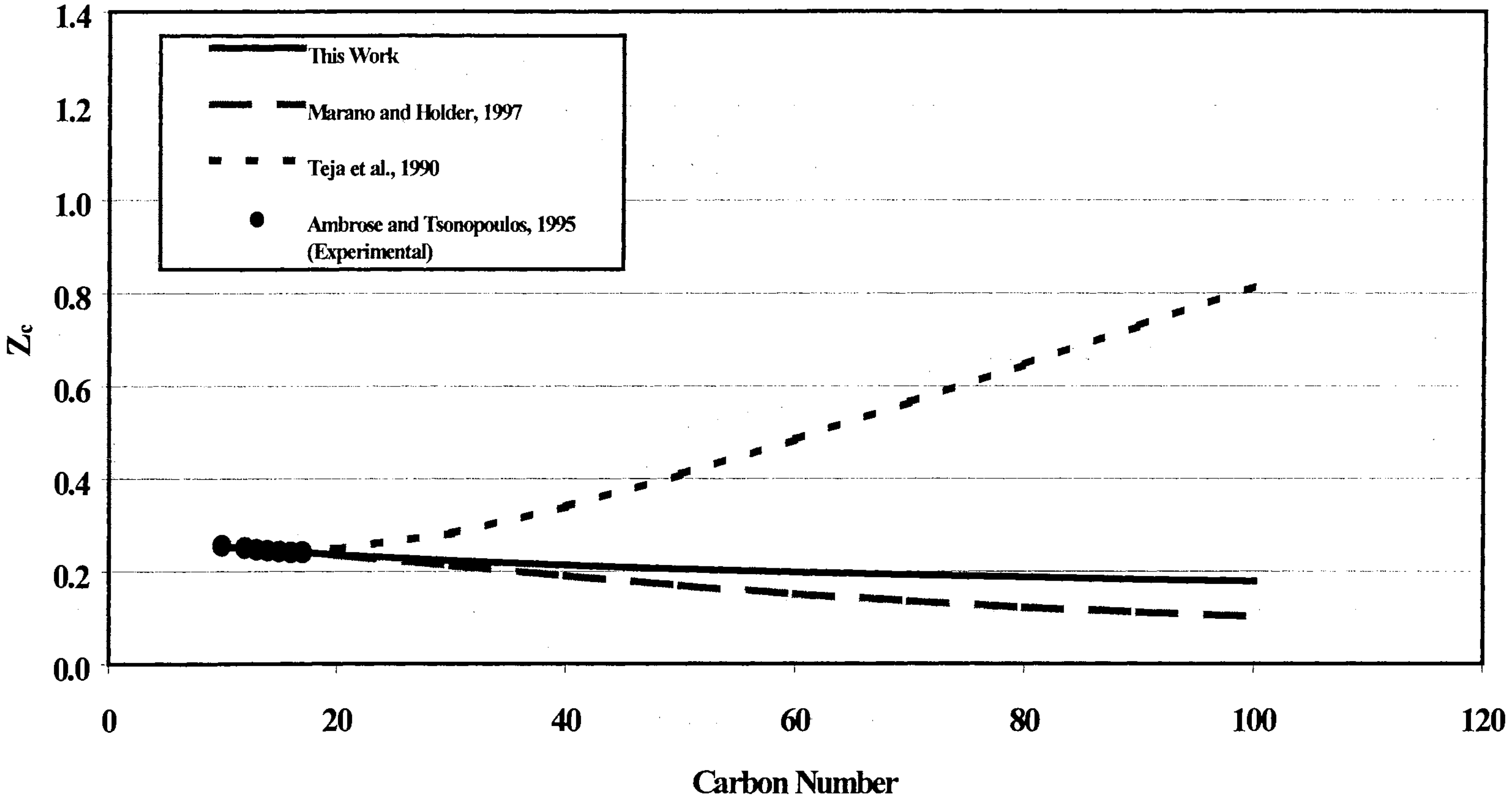

Figure 3. Critical Compressibility Predictions for n-Paraffins.

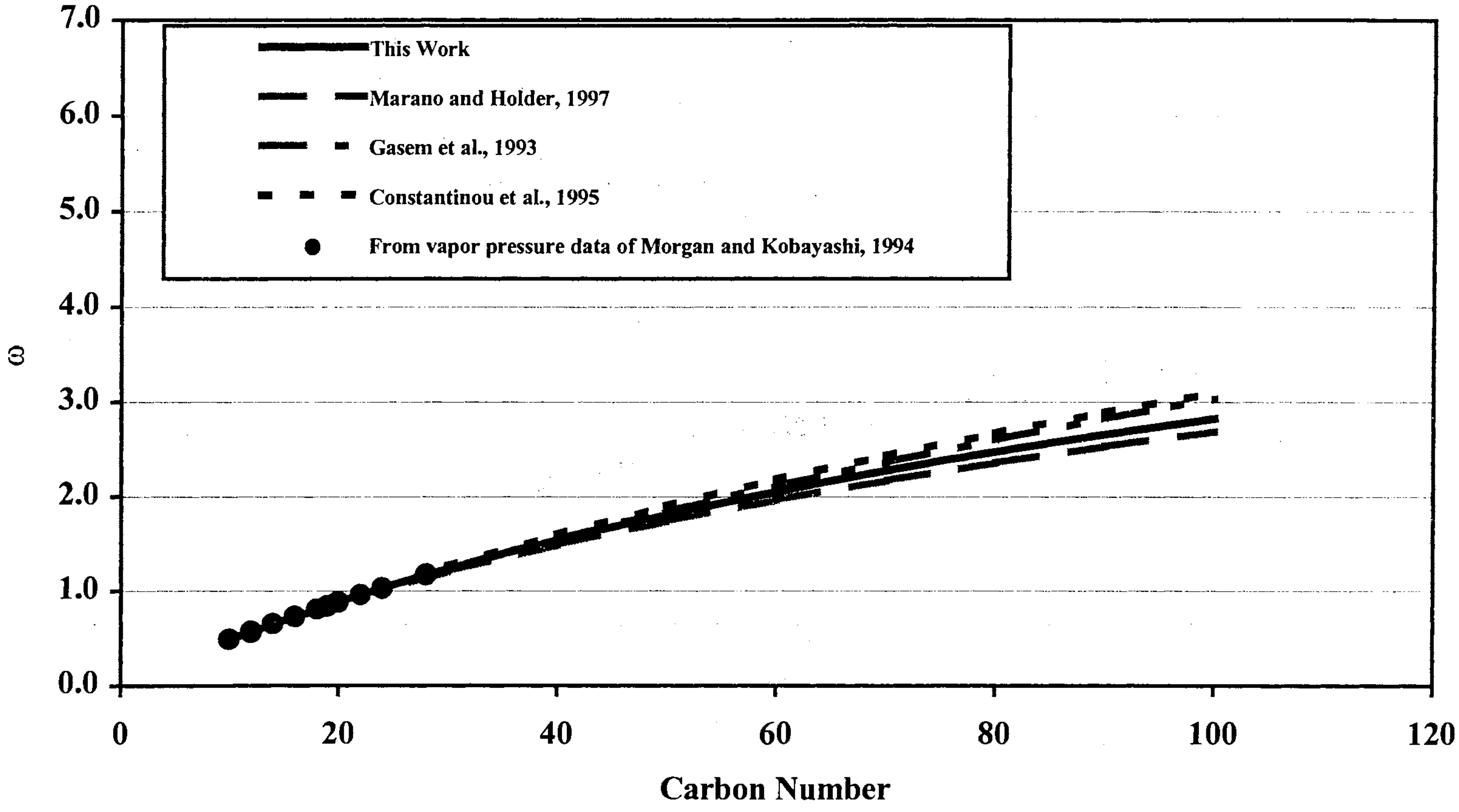

Figure 4. Acentric Factor Predictions for n-Paraffins.

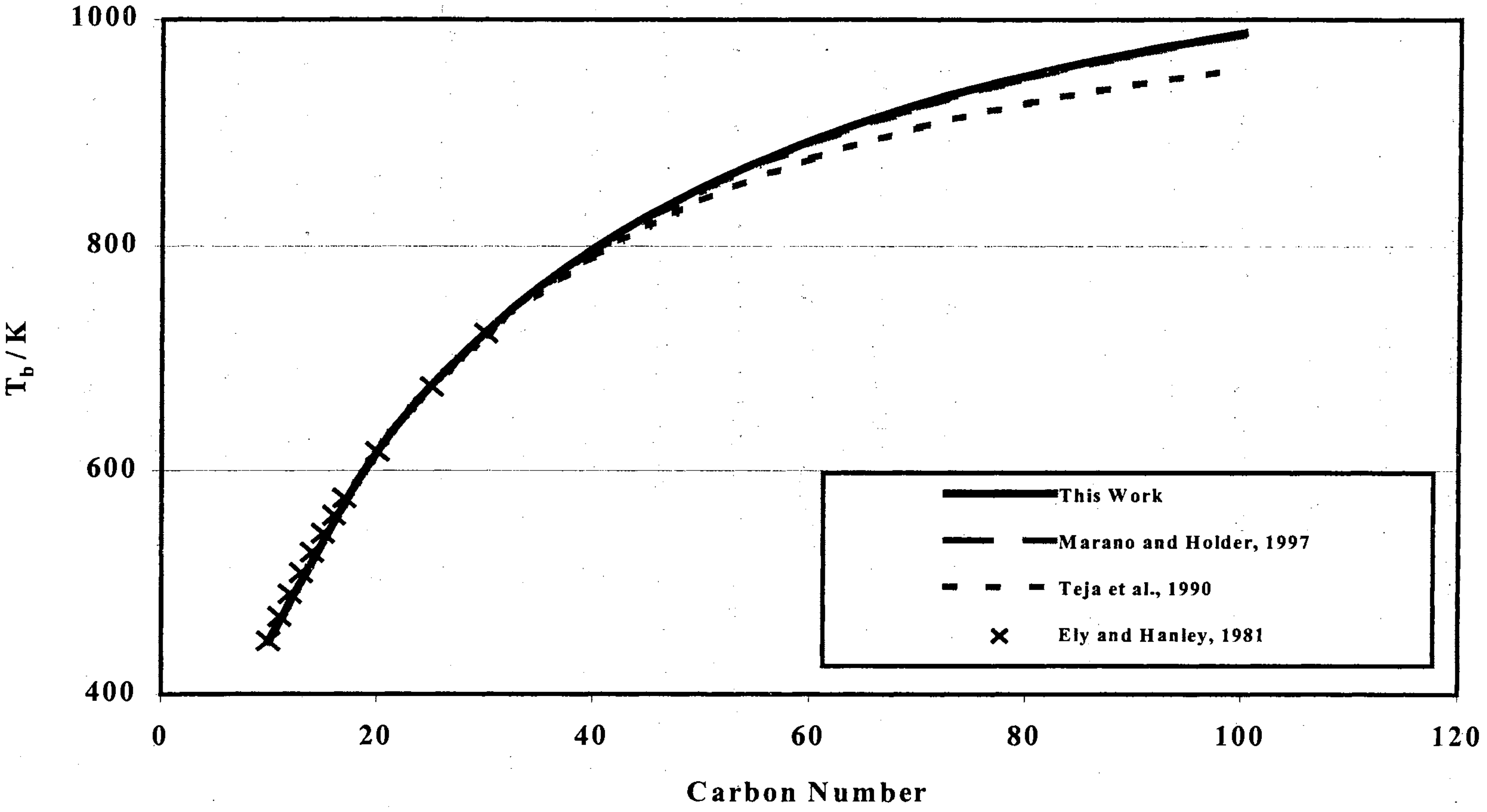

Figure 5. Normal Boiling Point Temperature Predictions for n-Paraffins.

however, the limiting value for the critical pressure from Flory theory is finite while the Lattice-Fluid theory projects a zero value. Similarly, the Lattice-Fluid theory (Marano and Holder, 1997) suggests an asymptotic behavior for the critical compressibility. An asymptotic behavior for the normal boiling point has also been suggested by Kreglewski and Zwolinski (1966).

In the early 1980's, Gasem and Robinson developed the Asymptotic Behavior Correlation (ABC) to predict the physical properties of n-paraffins (Gasem, 1986). In its simplest form, the ABC model is given as

$$Y = [Y_\infty^\alpha - (Y_\infty^\alpha - Y_0^\alpha)\exp(-\alpha\beta(CN - 1)]^{1/\alpha} \tag{1}$$

where Y is the selected properties, CN is the carbon number, Y_0 and Y_∞ are the initial value and the limiting value as CN goes to infinity, and α, β are scaling coefficients. Physical properties (Gasem, et al., 1993) as well as saturation properties (Shaver, et al., 1991) have been successfully correlated using variations of this function. For a given property, this growth-type model is designed to precisely interpolate between the initial value and the limiting value of the property. It has the capability of representing a diversity of functional shapes beyond the asymptotic curve, including exponential, sigmoid, logarithmic, and linear. More recently, Marano and Holder (1997) extended the use of the ABC framework to correlating the physical properties of a wide set of hydrocarbon homologous series.

In this study, we introduce an exponent (γ) on the carbon number to give the model more flexibility, or

$$Y = [Y_\infty^\alpha - (Y_\infty^\alpha - Y_0^\alpha)\exp(-\alpha\beta(CN^\gamma - CN_0^\gamma))]^{1/\alpha} \tag{2}$$

Properties of propane are used to represent the initial property values in the above equation (CN_0=3) to avoid trend irregularity exhibited by the critical properties of methane and ethane. In the ABC correlations, we have sought to meet the following criteria: (1) precise representation of the available experimental data; (2) appropriate limiting behavior; (3) reasonable extrapolation at high carbon numbers; and (4) an internally-consistent set of physical properties, which may serve effectively as reducing coordinates and input data for EOS models.

DATABASE EMPLOYED

Ambrose and Tsonopoulos (1995) have evaluated available experimental critical temperatures and critical pressures of n-paraffins up to C_{24}, and critical volumes and critical compressibilities up to C_{18}. In addition, they have presented estimated uncertainties for their recommended values. In this study, we use Ambrose and Tsonopoulos's values for paraffins up to C_{24} and those of Nikitin (1997) for the n-paraffins from C_{25} to C_{36}. To generate a consistent set of physical properties, the critical volumes are calculated from the critical temperatures, pressures and compressibilities predicted by the ABC correlations.

Accurate vapor pressures are necessary for acentric factor calculations, since by definition:

$$\omega = -\log(p_r)_{T_r=0.7} - 1 \tag{3}$$

We find the data of Morgan and Kobayashi (1994) to be most accurate in comparison with the existing data for the heavy n-paraffins (C_{10} to C_{28}). Accordingly, we use the vapor pressure data to determine the acentric factors of these compounds aided by the Wagner equation (Ambrose, 1986) and our ABC correlations for the critical properties. These calculated acentric factors combined with the acentric factors from Reid et al. (1987) for the light hydrocarbons form our database for acentric factors. Finally, the normal boiling point data from the National Institute of Science and Technology (Ely and Hanley, 1981) are used to develop the normal boiling point correlation of n-paraffins.

We have considered several weighting strategies when regressing the model parameters; nevertheless, minimizing the sum of squared relative deviations in each property is found to be representative of the quality of the data considered. Therefore, the objective function is chosen as follows:

$$SS = \sum_{i}^{n} \left(\frac{Y_{exp} - Y_{calc}}{Y_{cal}} \right)_i^2 \tag{4}$$

where n is the number of data points, Y_{calc} is the calculated property, and Y_{exp} is the experimental property. The Chauvenets' criterion by Young (1962) was applied to discard data points displaying excessive deviations, and a second regression was then performed. Specifically, the critical temperature measurement for C_{28} was discarded and similarly, we discarded the critical pressure measurements for C_{18} and C_{28}. Inspection of the data points rejected by Chauvenets' criterion showed that these points did not yield typical random deviations. Detailed procedures for data reduction are given by Gasem (1986).

RESULTS AND DISCUSSION

The ABC model is particularly useful when the limiting property values are available. Although we have all the initial property values (Y_0), the limiting property values (Y_∞) are lacking, and as such require careful examination. The literature estimates of the limiting value for the critical temperature extend from 926 to 1120 K (Teja, et al, 1990; Gasem, et al., 1993; Marano and Holder, 1997; Kudcgadker, et al., 1986; Tsonopoulos, 1987.) and for the critical pressure is approximately zero (Gasem, et al., 1993; Marano and Holder, 1997; Kudcgadker, et al., 1986; Tsonopoulos, 1987.) The Lattice-Fluid theory (Kurata and Isida, 1955) suggests a limiting value of 1/3 for the critical compressibility, which is clearly very high in light of the available experimental data. To assess the impact of erroneous limiting value for the critical compressibility, we have evaluated four different limiting values: 0.2, 0.15, 0.1 and 0.0. Our results indicate that the predicted values for the critical compressibility (up to n-C_{100}) are insensitive to the limiting value. Subsequently, we have used 0.15 as the limiting value for the critical compressibility. A super-linear ($CN^{3/2}$) relationship for critical volume has been suggested by Marano and Holder (1997) based on the Lattice-Fluid theory. In this study, to develop an internally consistent set of physical properties, the critical volume is calculated directly from the critical temperature, pressure and compressibility.

There is no clear guidance on the limiting value of the acentric factor; however, since the acentric factor characterizes the non-sphericity of the molecule, and since molecules may fold as they grow larger in size, it is plausible that the acentric factor limiting behavior is asymptotic. The limiting value for the acentric factor is regressed from the available data. The ABC acentric factor extrapolations show reasonable agreement with values calculated directly from vapor pressure correlations (Kreglewski and Zwolinski, 1966) and the critical property correlations from this study. Specifically, we observe a deviation within 1% at C_{100}. Although some polynomials (Hoshino, et al., 1982) can be used to represent the existing acentric factor data with the same precision, their extrapolations are not reliable (Gasem, 1986). Finally, following Kreglewski and Zwolinski (1966), we have adopted 1078 K as the limiting value for the normal boiling point.

Table 1 presents the summary of the results obtained for the various properties using the ABC model. Absolute average deviations (AAD) of 0.2%, 0.8%, 0.4%, 0.6%, and 0.1% are obtained for the critical temperature, critical pressure, critical compressibility, acentric factor, and normal boiling point, respectively. In general, the precision of the present correlations is in direct proportion to the quality of data used.

Figures 1-5 present the n-paraffin property predictions of the models considered. Inspection of Figures 1-5 reveals the general agreement of the various models in representing the properties of lighter hydrocarbons; however, significant variations exist for the property extrapolations beyond C_{20}. Also shown is the impact the limiting property value on the extrapolated predictions when the ABC model is employed.

Detailed comparisons of the predictions obtained from the various models are shown in Figures 6-9. The original model parameters are used for all the literature correlations. The reason for so doing is to examine their extrapolations in light of the new data and to illustrate the need for updated correlations. All previous correlations

Table 1

Summary of the Results for n-Paraffin Property Predictions Using the Updated ABC Model

	Critical Temperature	**Critical Pressure**	**Critical Compressibility**	**Acentric Factor**	**Normal Boiling Point Temperature**
Y_∞	.9818E+03	0^+	.1500E+00	.5492E+01	.1078E+04
Y_0	.3701E+03	.4244E+01	.2770E+00	.1515E+00	.2311E+03
α	.1276E+01	.1000E+01	.1000E+01	.6851E+00	.1000E+01
β	.1435E+00	.3757E+00	.1416E+00	.6859E-01	.1150E+00
γ	.6667E+00	.5684E+00	.5000E+00	.6667E+00	.6667E+00
RMSE	1.42 K	0.018 MPa	0.0012	0.0037	0.32 K
%ADD	0.16	0.84	0.42	0.58	0.05

yield poor predictions for the heavy n-paraffins. This is to be expected since all these correlations were based on experimental measurements of lighter n-paraffins.

In closing, while the updated ABC model successfully incorporates the new data for the heavier n-paraffins, a need exists for better theory and carefully designed molecular simulations to resolve the dilemmas of the limiting behavior of the property of interest.

SUMMARY

New experimental measurements for the critical properties and the vapor pressures of heavy n-paraffins have been assembled and evaluated. The current physical property correlations give poor predictions for the heavy n-paraffins. The ABC correlation has been updated, after carefully examining the limiting behavior of each property, to describe the properties. The updated ABC model provides precise representations for the properties considered and offers improved predictions for the heavier n-paraffins.

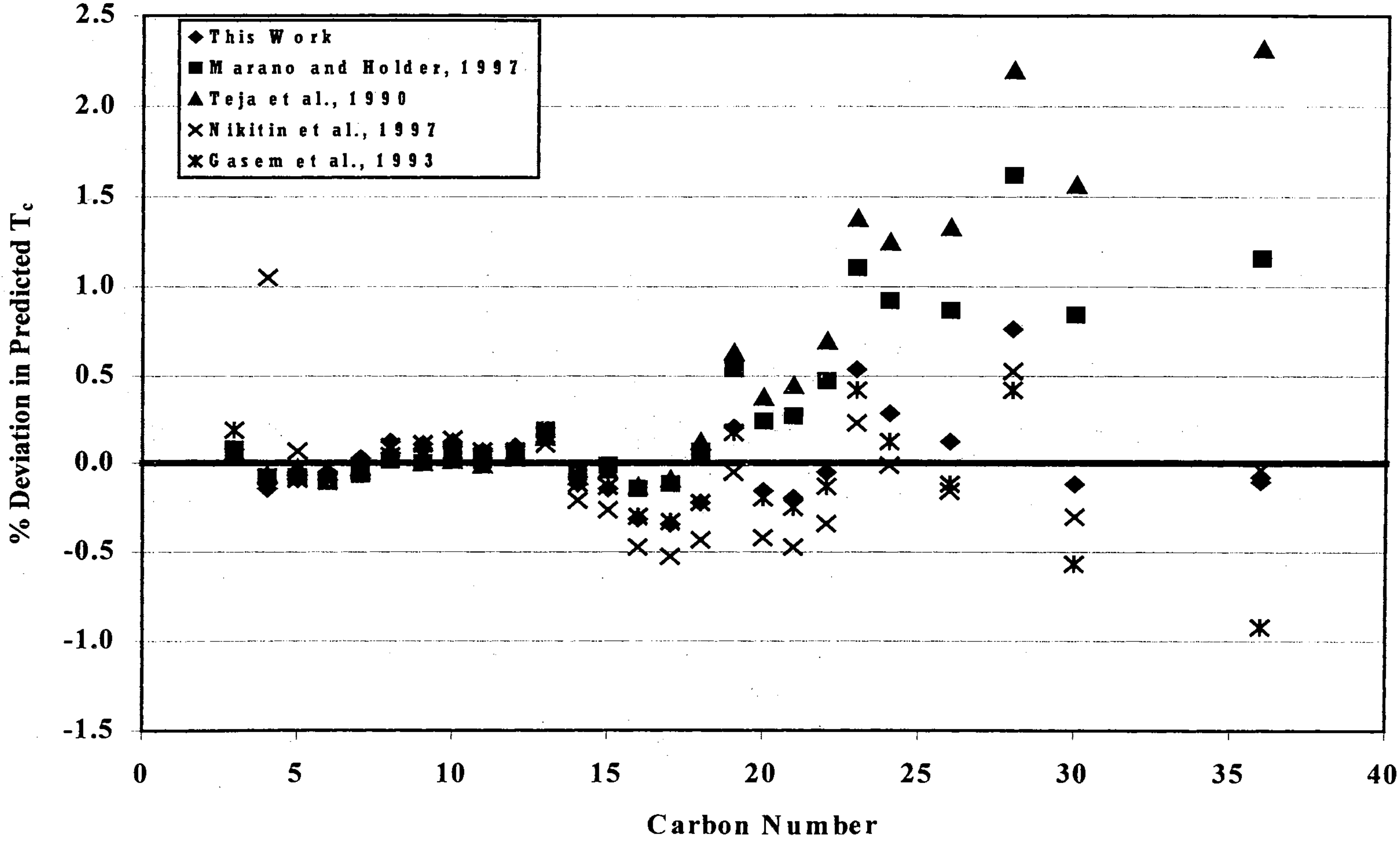

Figure 6. Comparison of the Critical Temperature Predictions of n-Paraffins.

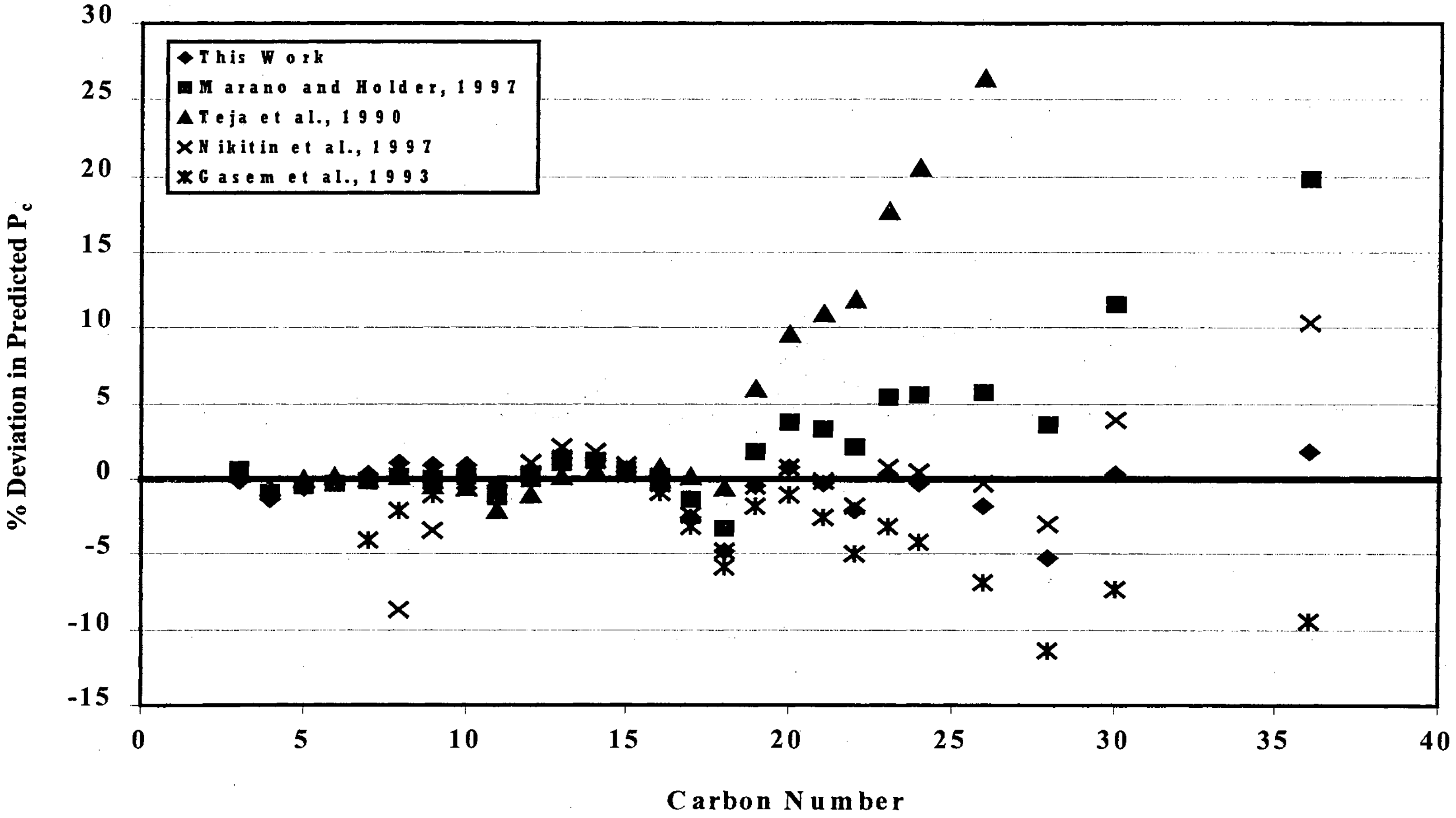

Figure 7. Comparison of the Critical Pressure Predictions of n-Paraffins.

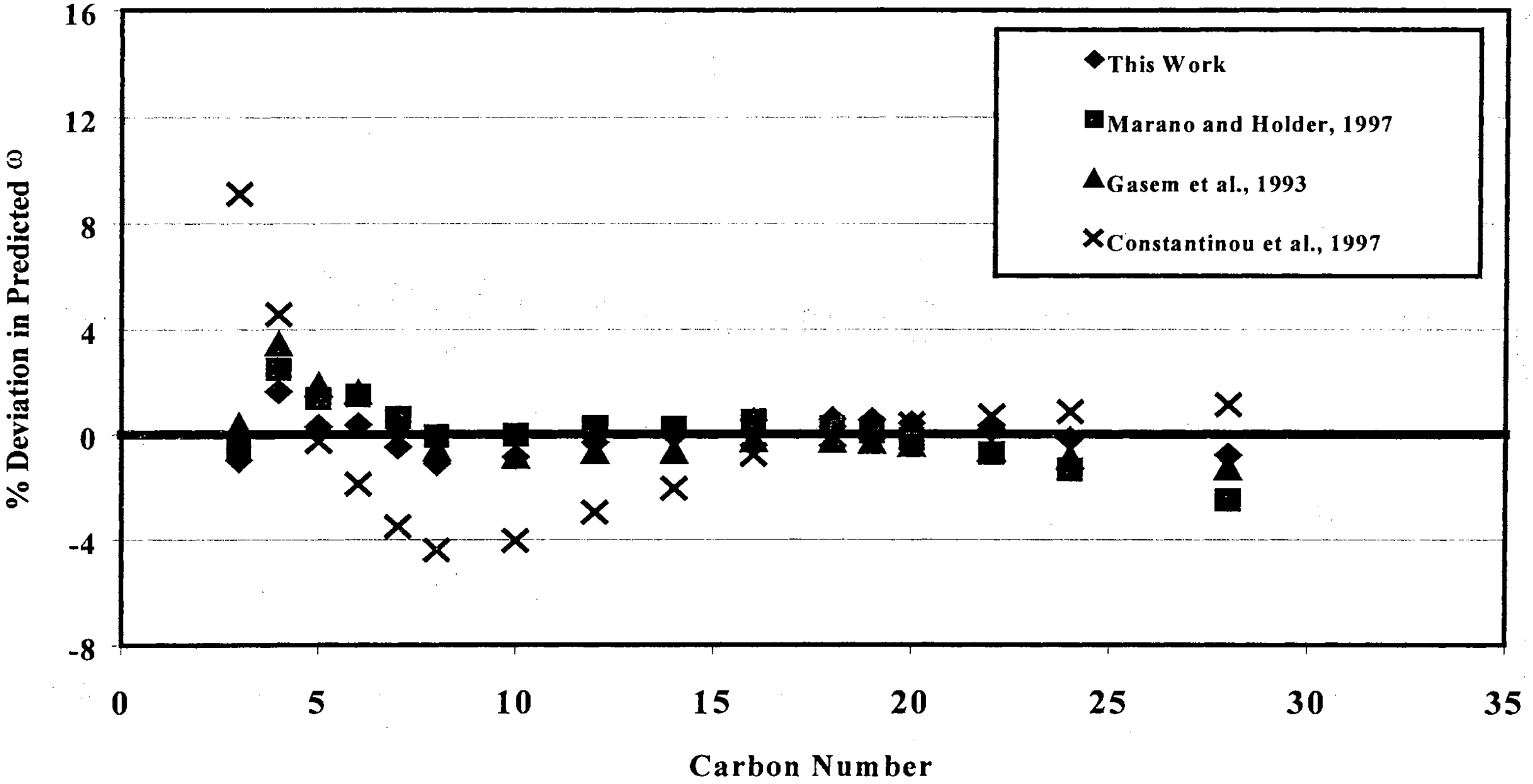

Figure 8. Comparison of the Acentric Factor Predictions of n-Paraffins.

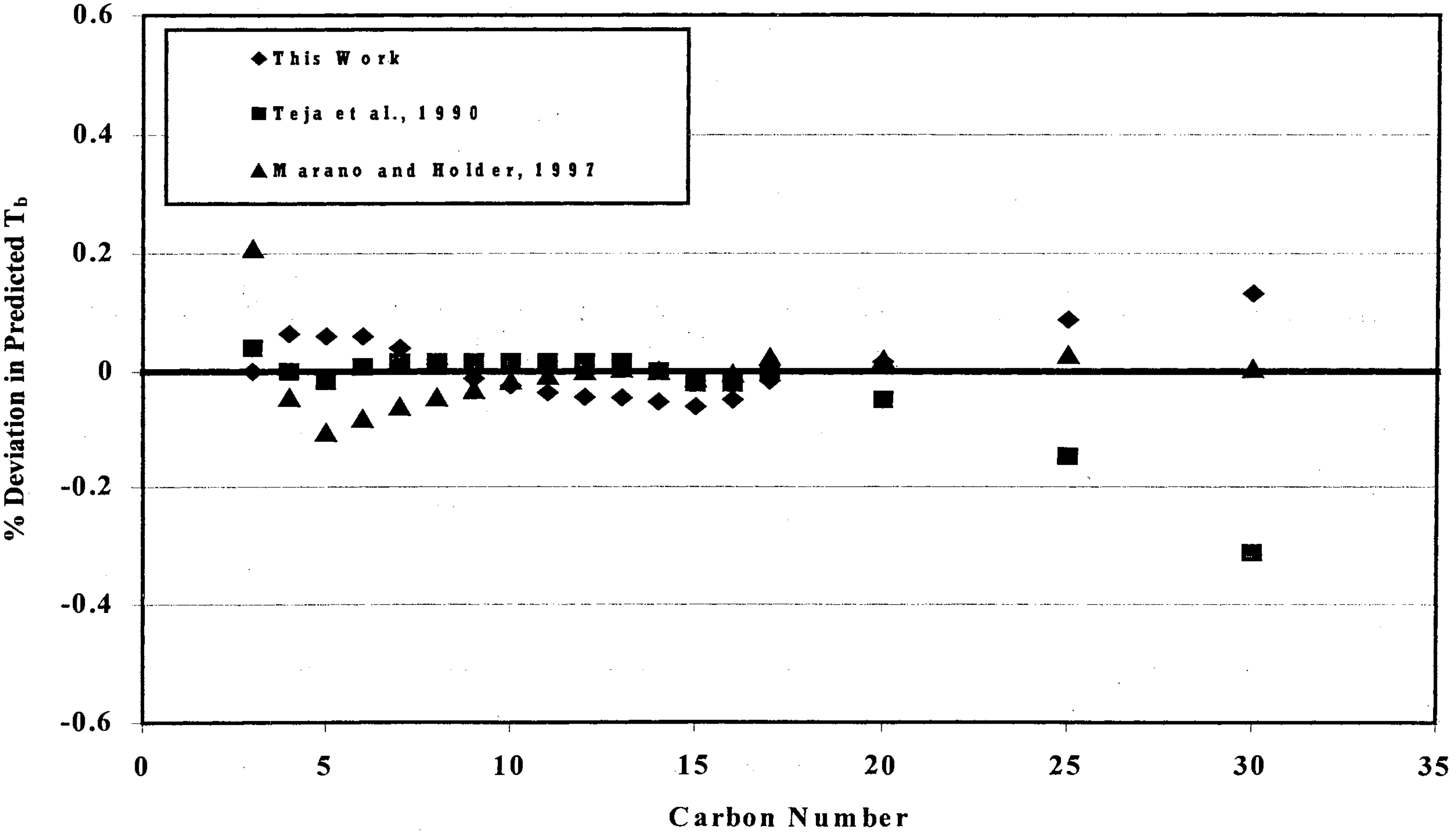

Figure 9. Comparison of Normal Boiling Point Temperature Predictions for n-Paraffins.

CHAPTER 5

MODIFYING THE TEMPERATURE DEPENDENCE OF THE PENG-ROBINSON EQUATION OF STATE

ABSTRACT

A number of modifications have been suggested for the temperature dependence of the Peng-Robinson equation of state (PR EOS) through the α function of the attraction law constant. In most cases, the work was motivated by the need to improve vapor pressure predictions of heavy hydrocarbons. While marginal improvements have been realized, most successful α function modifications suffered from (a) limited experimental pvT and equilibrium measurements for heavy hydrocarbons, and (b) reliance on the use of switching functions below and above the critical temperature.

In this work, we proposed a new temperature dependence α function for the PR EOS. This new function is developed based on pure-component vapor pressures of different molecular species, including heavy hydrocarbons. The modified PR EOS α function leads to improved vapor pressure predictions (about 1% absolute average percentage deviations) for the systems considered (28 pure fluids encompassing over 1100 measurements). In addition, the new PR EOS α function has been found to be more accurate for *a priori* predictions (AAD of 13.9 %) of the bubble point pressure, where interaction parameters are set to zero, and comparable to the original α function in representing 48 binary asymmetric mixtures involving diverse molecular species (AAD of 3%, using paraffin-dependent interaction parameters).

INTRODUCTION

Cubic equations of state (CEOS) have been applied successfully by the hydrocarbon industry to describe the thermodynamic properties of pure fluids and mixtures. Although more theoretically-based equations of state, such as the Simplified-perturbed-hard-chain theory (SPHCT) EOS (Kim et al., 1986; Shaver et al., 1993), the simplified-statistical-associating-fluid theory (SAFT) EOS (Chapmen et al., 1990) and the modified Park-Gasem-Robinson (MPGR) EOS (Row, 1998), have been proposed and developed in recent years, the simplicity and wide applications of CEOS have justified continued efforts to develop such equations.

Although the CEOS has been successfully used to correlate equilibrium properties, invariably empirical binary interaction parameters are required to obtain precise representation of the experimental data. Attempts to generalize the interaction parameters, even for a set of binaries within a homologous series, often are not successful. Inaccuracy of the PR EOS representations of the pure component equililibrium properties is a contributing factor to the observed scatter in the interaction parameters of highly related binaries (e.g., binaries originating from the same homologous series). That is, sufficiently accurate pure-fluid vapor pressure predictions are a prerequisite for accurate mixture phase equilibrium calculations using EOS (Soave, 1972).

Since the introduction of the Redlich-Kwong (1949) EOS, a sizeable portion of the efforts to improve the precision of CEOS has been concentrated on modifying the temperature dependence of the model parameters through the α function of the attraction law constant. A partial list of the literature α functions for the CEOS is shown in Table 1.

Table 1

Temperature Dependence of α Function

$1/\sqrt{T}$	Redlich-Kwong (1949)
$T_r + (1.57 + 1.62\omega)(1 - T_r)$	Wilson (1966)
$[1 + (c_1 + c_2\omega + c_3\omega^2)(1 - T_r^{0.5})]^2$	Soave (1972)
$1 + (1 - T_r)(M + N/T_r)$	Soave (1979)
$\left[1 + c_1\left(1 - \sqrt{T_r}\right) + c_2\left(1/T_r - 1\right)\right]^2$	Harmens and Knapp (1980)
$\left[1 + c_1\ \ln(T_r) + c_2\left(1 - \ln T_r\right)^2\right]^2 \qquad (T_r > 1)$	Harmens and Knapp (1980)
$\exp\left[c_1\left(1 - T_r^n\right)\right]$	Heyen (1980)
$\left[1 + c_1\left(1 - \sqrt{T_r}\right) + c_2\left(1 - T_r\right)\left(0.7 - T_r\right)\right]^2$	Mathias (1983)
$[1 + m(1 - T_r^{0.5})]^2$, $m = c_1 + c_2\omega + c_3\omega^2$, $T_r<1$ $\exp\left[c_1\left(1 - T_r^d\right)\right]$, $d=1+m/2$, $c=1-1/d$, $T_r>1$	Boston and Mathias (1983)
$\left[1 + c_1\tau + c_2\tau^2 + c_3\tau^3\right]^2$ where $\tau = 1 - \sqrt{T_r}$	Mathias and Copeman (1983)
$[1 + k(1 - T_r^{0.5})]^2$ $k = c_1 + c_2\omega + c_3\omega^2 + c_4\omega^3 + k_1(1 - T_r^{1/2})(0.7 - T_r)$	Stryjek-Vera (1986)
$10^{\left[c_1\left(a_o + a_1T_r + a_2T_r^2\right)\left(1 - T_r\right)\right]}$	Yu and Lu (1987)
$1 + c_1\left(1 - \sqrt{T_r}\right) + c_2\left(1 - T_r\right)$	Carrier et al. (1988)
$\left[1 + c_1\tau + c_2\tau^2 + c_3\tau^3\right]$ where $\tau = 1 - T_r^{2/3}$	Androulakis et al. (1989)
$\exp\left[c_1\left(1 - T_r\right) + c_2\left(1 - \sqrt{T_r}\right)^2\right]$	Melhem et al. (1989)
$T_r^{c_3(c_2 - 1)}\ \exp\left[c_1\left(1 - T_r^{c_2c_3}\right)\right]$	Twu et al. (1991)
$1 + c_1(1 - T_r) + c_2(1 - T_r)^2$	Soave (1993)
$T_r^{A_1}\ \exp\left[B_1\left(1 - T_r^{C_1}\right)\right] + \omega(T_r^{A_2}\ \exp\left[B_2\left(1 - T_r^{C2}\right)\right]$ $- T_r^{A_1}\ \exp\left[B_1\left(1 - T_r^{C_1}\right)\right])$	Twu et al. (1995)

Most of the developments for the α functions were to improve the vapor pressure predictions of the high-boiling and polar components (Flöter et al., 1998). Many proposed α functions used either high order polynomials of the acentric factor (e.g., Stryjek and Vera, 1986; Boukouvalas et al., 1994; Danesh et al., 1995) or temperature (e.g., Mathias and Copeman, 1983; Schwartzentruber et al., 1990; Flöter et al., 1998) to correlate vapor pressures more precisely. Interestingly, most proposed α functions produce an erroneous temperature limiting behavior, including the original Soave α function. Specifically, most functions do not yield a finite and positive limiting α value as the temperature becomes infinitely large, as is asserted by several studies (Sandler, 1985; Melham, 1989; Twu et al., 1991).

Another source of difficulty for many proposed α functions is their inability to produce accurate representation of supercritical behavior based on subcritical model parameter generalizations (Boston and Mathias, 1980; Mathias, 1983; Melham et al., 1989, Twu, 1995.) This situation is commonly encountered when the PR EOS is used in vapor-liquid equilibrium (VLE) calculations involving supercritical components. To overcome this problem, many researchers introduced switching functions (e.g., Boston and Mathias, 1980; Twu et al., 1995, Danesh et al., 1995) or component-specific parameters (e.g., Melham et al., 1989; Twu et al., 1991; Flöter, et al., 1998); however, an α function employing component-specific parameters or switching functions is less desirable than a simple generalized α function with comparable capabilities.

Some researchers have developed α functions using pure-component supercritical data directly. For example, Rijkers (1991) developed an α function using pvT data of methane and Flöter et al. (1998) using fugacity of methane; however, neither have generalized their results, perhaps because the VLE calculations generally are not sensitive to the accuracy of the pvT predictions. Other researchers, such as Twu et al. (1995), have proposed a pure-component switching α function for the supercritical region, based on mixture phase equilibrium data. Although this strategy is effective in addressing the mixtures involved, accurate representation of pure-component behavior is a sound basis for the successful description of multicomponent mixtures (Soave, 1972; Vidal, 1983; Flöter, et al., 1998). Therefore, we have avoided the temptation to develop a pure-component α function based on mixture data, since such efforts invariably make the α function dependent on the type of mixtures used to derive its parameters.

Beyond selecting the proper functional form for the EOS temperature dependence, previous α functions suffered the consequences of limited vapor pressure data for the heavy hydrocarbons and uncertain estimates for their critical properties. Specifically, the critical properties and vapor pressure data were not available for compounds heavier than C_{10}, when the SRK and PR EOS were developed. Expectedly, when dealing with heavy components, the extrapolation of α function predictions beyond the temperature and acentric factor ranges within which the model constants were generated is a contributing factor to the poor accuracy of these equations.

In this study, we use recent vapor pressure data for heavy n-paraffins (Morgan and Kobayashi, 1997) and improved critical property estimates (Gao et al., 1999a) to develop a new PR α function, which meets the following criteria:

(1) An appropriate temperature limiting behavior for the function

(2) Model parameters based solely on pure-component properties

(3) Improved predictions for the pure-fluid vapor pressures of simple, normal and slightly-polar fluids, including heavy hydrocarbons, and

(4) Comparable or superior mixture equilibrium property predictions to those of the original PR EOS without using switching functions.

MODEL DEVELOPMENT

In this study, we focus our attention on improving the PR EOS predictions. The PR EOS yields better liquid density predictions than the Soave-Redlich-Kwong (Soave, 1972) EOS; however, it is less accurate in predicting the vapor pressures of the heavy hydrocarbons (Twu et al., 1995). The original PR EOS is given as

$$p = \frac{RT}{v - b} - \frac{a}{v(v + b) + b(v - b)} \tag{1}$$

where

$$a = a_c\alpha(T) \tag{2}$$

$$b = 0.0778RT_c/P_c \tag{3}$$

and

$$a_c = 0.45724R^2T_c^2/p_c \tag{4}$$

$$\alpha(T)^{1/2} = 1 + k(1 - T_r^{1/2}) \tag{5}$$

$$k = 0.37464 + 1.54226\omega - 0.26992\omega^2 \tag{6}$$

where p is the pressure, R is the gas constant, T is the temperature, a and b are EOS constants, v is the molar volume, T_c is the critical temperature, p_c is the critical pressure, T_r is the reduced temperature, $\alpha(T)$ expresses the temperature dependence in the parameter a, and ω is the acentric factor.

Many attempts have been made to improve the PR EOS vapor pressure predictions by modifying the original α function or proposing new ones. As pointed by

Twu et al. (1995), the α function dependence on the acentric factor for the PR EOS is a linear function rather than a higher order polynomial; therefore, higher order polynomials do not improve the phase behavior predictions; on the contrary, in many cases, they worsen such predictions.

To explore α(T) behavior, we present in Figures 1-3 experimental α values generated by solving the equal-fugacity equilibrium equation at the corresponding experimental temperatures and pressures. Figure 1 illustrates the linear acentric factor dependence of the α function for n-paraffins extending to C_{28}. Similarly, Figures 2-3 indicate that relatively simple temperature dependence functions are adequate for correlating the vapor pressure data. Figure 2 shows that log(α) varies essentially in a linear fashion with T_r in the subcritical region. This explains the tendency to use logarithmic-type α functions in the literature, as shown in Table 1. Similarly, Figure 3 shows that $\alpha^{0.5}$ varies linearly with $(1-T_r^{0.5})$ in the subcritical region, as was concluded by Soave (1972).

Previous studies have clearly demonstrated the success of logarithmic-type and Soave-type α functions in representing the pure-fluid vapor pressures well (e.g., Soave, 1972; Twu et al., 1995). During this study, we have also found that many temperature functions can be used to represent the vapor pressure accurately; however, other considerations are equally important in evaluating a successful α function, including (a) the ability to adequately represent the fluid supercritical behavior, while maintaining the appropriate temperature dependence over the full temperature range; (b) improved equilibrium predictions for systems involving subcritical components, to capitalize on the more accurate pure behavior limits; and (c) derivative properties free of cross-over

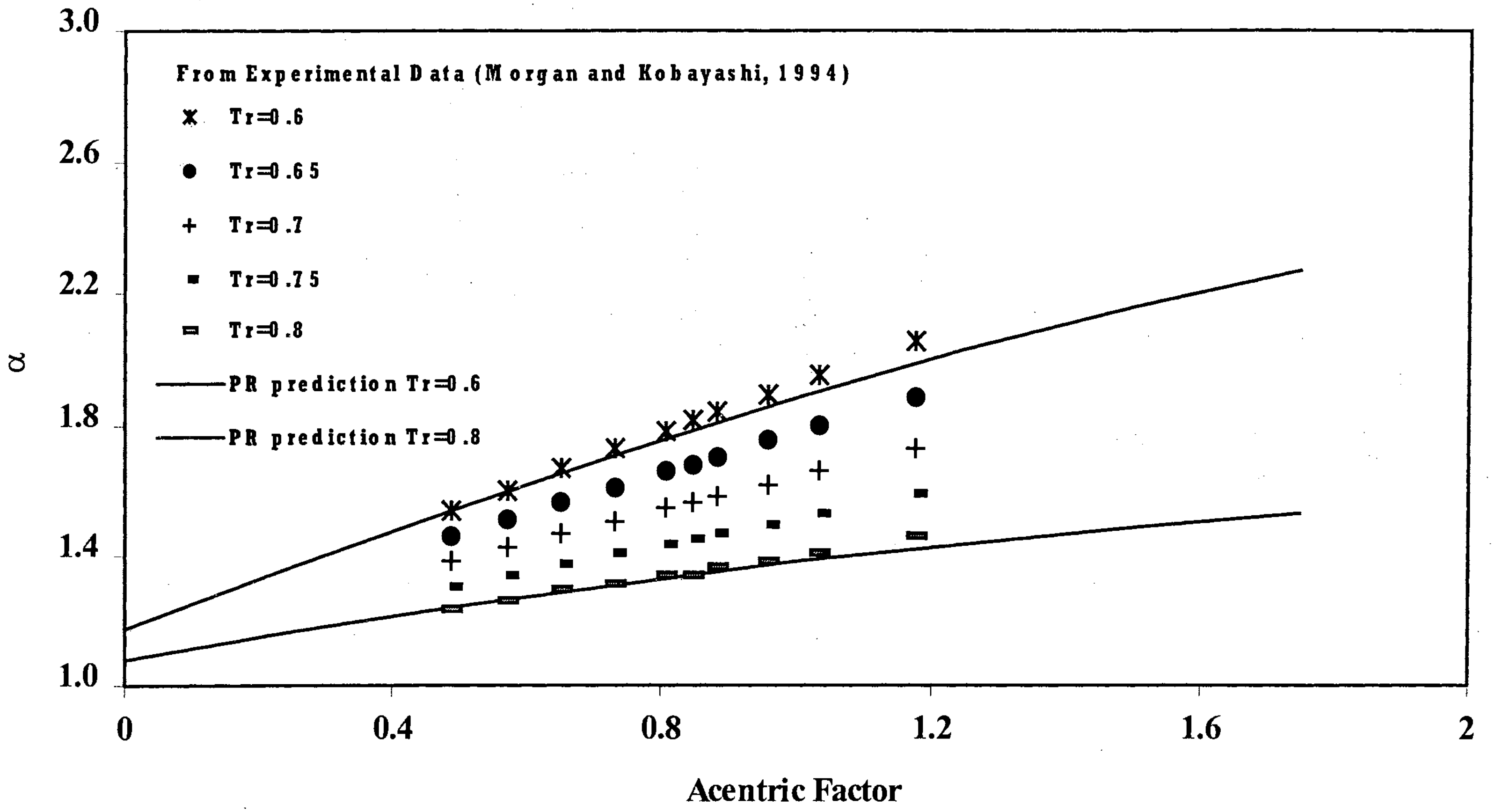

Figure 1. Variations of n-Paraffin α Values with Acentric Factor and Temperature.

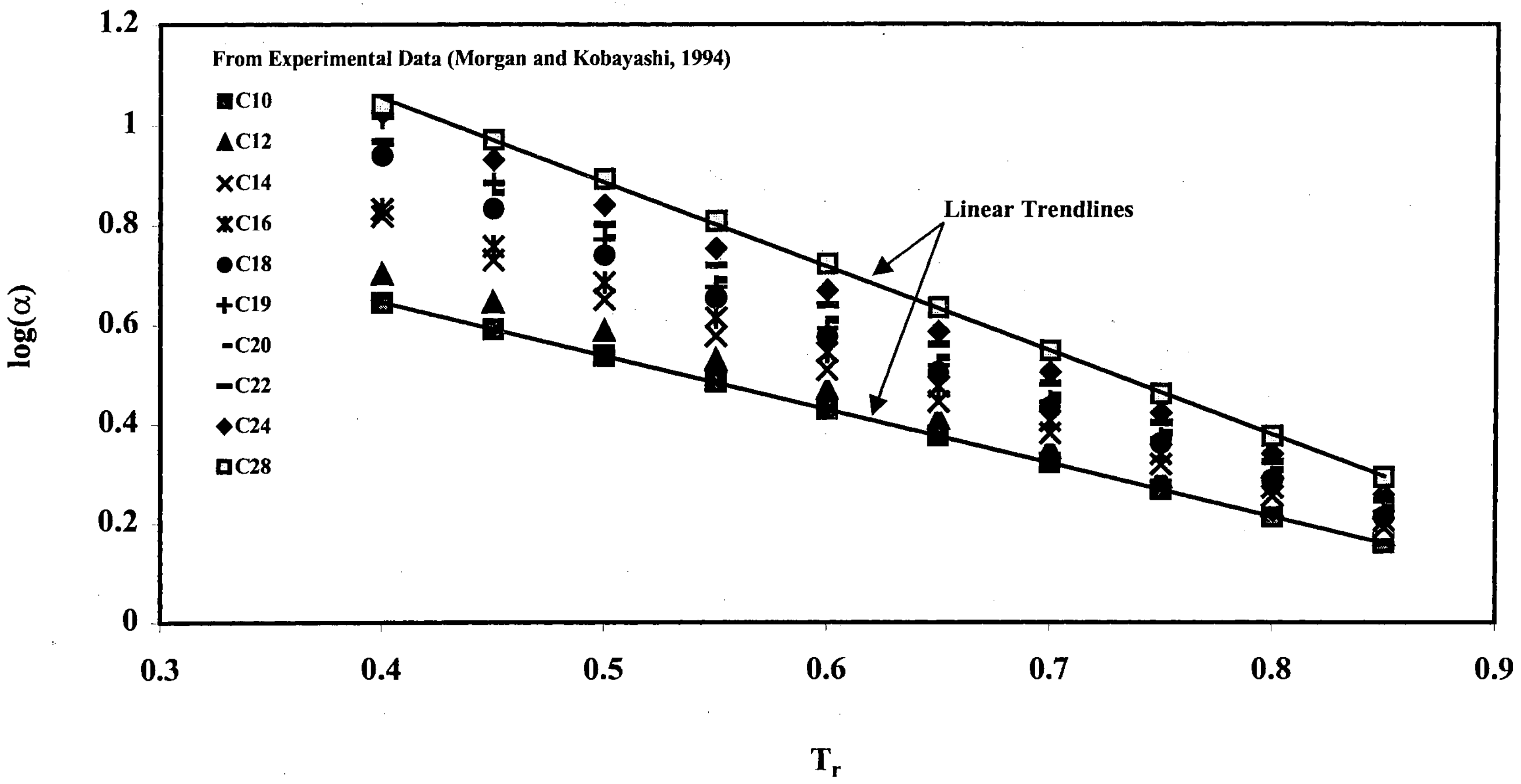

Figure 2. Logarithm-Type Temperature Dependence for n-Paraffin α Function.

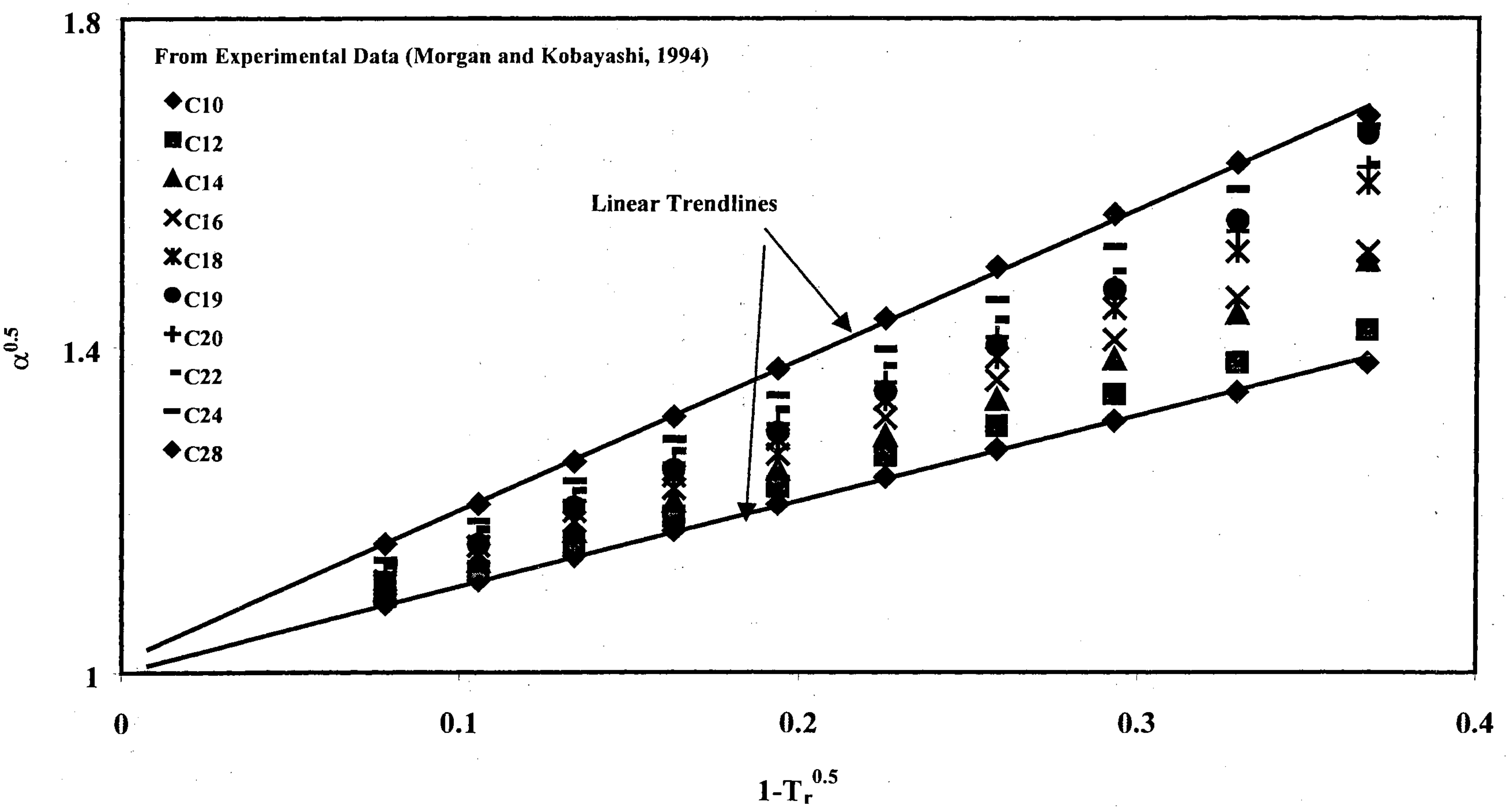

Figure 3. Soave-Type Temperature Dependence for n-Paraffin α Function.

anomalies (Trebble and Bishnoi, 1986). In this work, we only explore the quality of EOS predictions for mixtures involving supercritical components.

Table 2 presents three α functions we have selected for evaluation, based on the above analysis. The first model is the Soave-type α function, where Case 1 is used to examine the original PR EOS α function, and Case 1R is used to evaluate the function performance after re-determining the model parameters. Although the temperature limiting behavior of the Soave-type α function is not correct, we felt it necessary to examine its capability in light of the new data for the heavy n-paraffins; and more so, since it is one of the two major types of temperature-dependence functions in the literature. The second model (Twu's 1995 model) represents a more recent logarithmic-type function. In Case 2R, we evaluate Twu's α function after re-determining its parameters, and in Case 2S we employ Twu's second model, which incorporates a switching function. In this case, the α function is equipped with two sets of model parameters, one set for pure-component subcritical region and the other for the supercritical region. Model 3 is the proposed model in this study. It is a variation of the logarithmic-type α function suggested first by Heyen (1980) and developed further by Twu et al. (1991, 1995).

DATABASE USED

The pure-fluid physical properties employed in this study to evaluate the proposed α functions are given in Table 3. The critical properties and acentric factor for n-paraffins decane and above are given by Gao et al. (1999a), the rest of the data are from Reids, et al. (1987). Also given in Table 3 are the reduced temperature ranges for the experimental

Table 2

Model Evaluation of Selected α Functions

Model No.	α Model	Notes
1, 1R	$(1+(A+B\omega+C\omega^2)(1-T_r^D))^{1/E}$	i
2, 2R, 2S	$T_r^A \exp(B(1-T_r^C)) + \omega(T_r^D \exp(E(1-T_r^F)) - T_r^A \exp(B(1-T_r^C)))$	ii
3	$\exp((A+BT_r)(1-T_r^{C+D\omega+E\omega^2}))$	iii

i. Original α in PR EOS: Case 1 uses the original model parameters
Case 1R uses regressed model parameters

ii. Twu et al. (1995): Case 2 uses Twu's model parameters
Case 2R regressed model parameters
Case 2S uses two different sets of model parameters
(for $T_r > 1$ and $T_r < 1$)

iii. Proposed in this study

Table 3

Pure-Fluid Physical Properties Used in Evaluating α Functions

Name	T_c	P_c	ω	T_b	Z_c	MW	T_r
Methane	190.56	45.99	0.0113	111.63	0.2838	16.04	0.476 - 1.0
Ethane	305.33	48.71	0.1004	184.55	0.2822	30.07	0.360 - 1.0
Propane	369.82	42.47	0.1542	231.05	0.2785	44.10	0.449 - 1.0
Argon	150.80	48.74	-0.0040	87.30	0.2912	39.95	0.556 – 1.0
Nitrogen	126.20	33.90	0.0390	77.35	0.2876	28.01	0.500 – 1.0
Benzene	562.16	48.98	0.2120	353.24	0.2714	78.11	0.496 - 1.0
Carbon Dioxide	304.21	73.83	0.2251	194.60	0.2756	44.01	0.712 - 1.0
Water	647.14	220.50	0.3290	373.15	0.2295	18.02	0.438 - 1.0
Fluorine	144.30	52.18	0.0480	85.00	0.2879	38.00	0.371 - 1.0
n-Butane	425.16	37.96	0.2004	272.65	0.2754	58.12	0.329 - 1.0
Ammonia	405.60	112.77	0.2500	239.70	0.2425	17.03	0.482 - 1.0
Acetone	508.10	47.01	0.3090	329.40	0.2326	58.08	0.510 - 1.0
Oxygen	154.58	50.43	0.0240	90.18	0.2865	32.00	0.352 - 1.0
Hydrogen	32.98	12.93	-0.2200	20.28	0.3018	2.02	0.423 - 1.0
Methanol	512.60	80.96	0.5590	337.80	0.2242	32.04	0.562 - 1.0
Ethanol	516.20	63.83	0.6350	351.50	0.2484	46.07	0.567 – 1.0
Ethylene	282.40	50.36	0.0850	169.40	0.2767	28.05	0.368 - 1.0
n-Decane	618.59	21.30	0.4885	447.32	0.2543	142.29	0.522 - 1.0
n-Dodecane	658.66	18.32	0.5746	489.50	0.2494	170.34	0.536 - 1.0
n-Tetradecane	692.17	15.92	0.6572	526.70	0.2450	198.39	0.539 - 1.0
n-Hexadecane	720.67	13.94	0.7368	560.00	0.2408	226.45	0.545 - 1.0
n-Octadecane	745.25	12.29	0.8137	589.50	0.2368	254.50	0.554 - 1.0
n-Nonadecane	756.32	11.57	0.8513	603.10	0.2349	268.53	0.559 - 1.0
n-Eicosane	766.66	10.91	0.8883	617.00	0.2331	282.56	0.565 - 1.0
n-Docosane	785.48	9.73	0.9608	640.20	0.2295	310.61	0.577 - 1.0
n-Tetracosane	802.12	8.71	1.0313	662.40	0.2261	338.85	0.565 - 1.0
n-Octacosane	830.31	7.05	1.1672	701.90	0.2197	395.13	0.582 - 1.0

vapor pressures. The vapor pressure measurements for the light compounds extend from the triple point to critical point temperature. For n-C_{10} through n-C_{28}, we use the precise data of Morgan and Kobayachi (1995), along with the critical point. The rest of the data, which encompass a variety of molecular species (including simple, normal, and polar fluids) have been fully documented by Shaver et al. (1991). The objective function used is:

$$SS = \sum_{i}^{n} \left(\frac{p_{calc} - p_{exp}}{p_{exp}} \right)_i^2 \tag{7}$$

where p_{exp} and p_{cal} are the experimental and calculated vapor pressure, respectively.

RESULTS AND DISCUSSION

The new α function was evaluated using pure-component vapor pressures only. The behavior of the proposed α function with respect to the acentric factor and temperature are shown in Figures 4-6, respectively. The figures indicate that, for the various species, the limiting value of α at large temperatures is finite, i.e., α is bounded and of asymptotic diminishing value. In comparison, the Soave-type α value for hydrogen does not abide by this theoretical limiting behavior.

Pure-Fluid Predictions

The summary results for the PR EOS vapor pressure predictions using the various α functions are given Tables 4-5. The original PR EOS α function (Case 1) represents

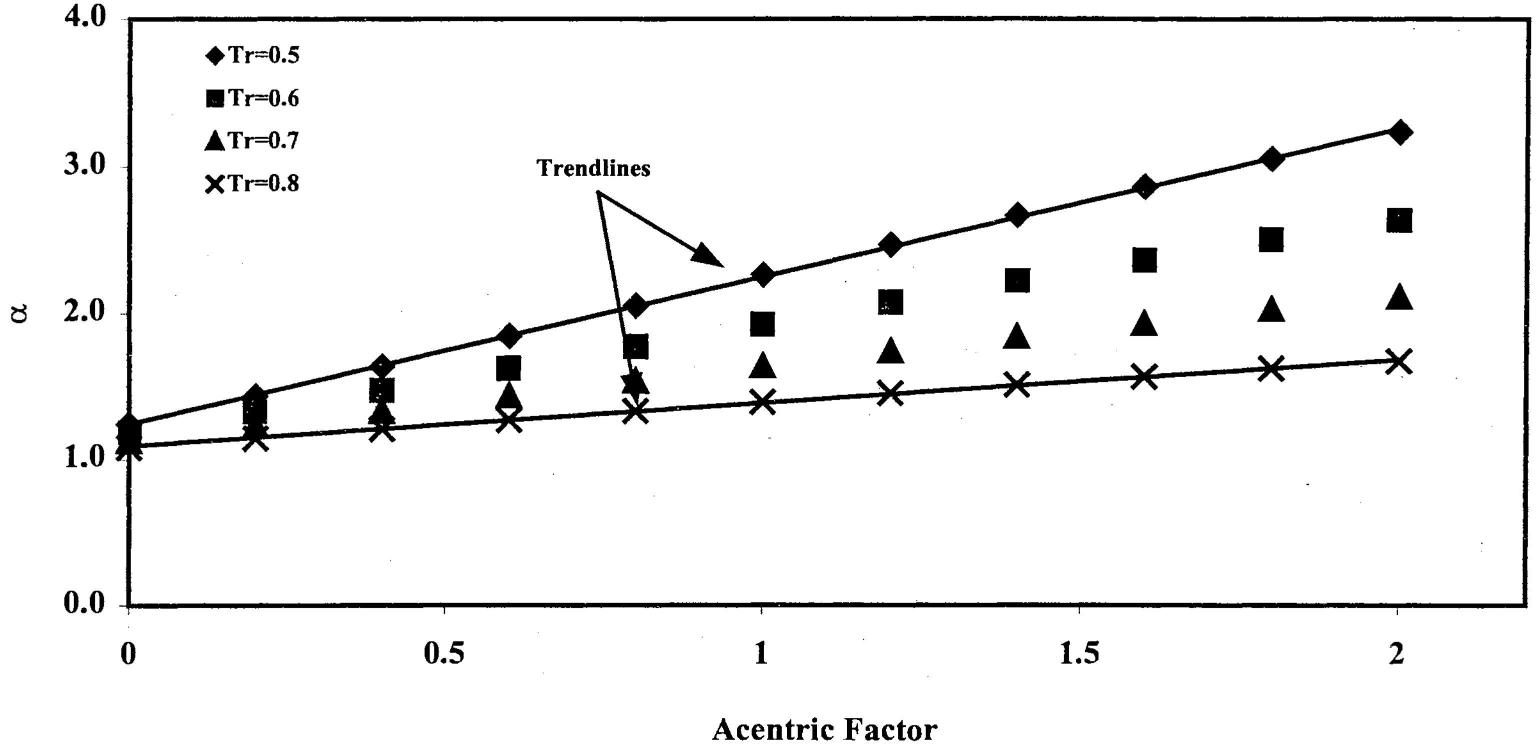

Figure 4. Variations of New α Model with Acentric Factor and Reduced Temperature.

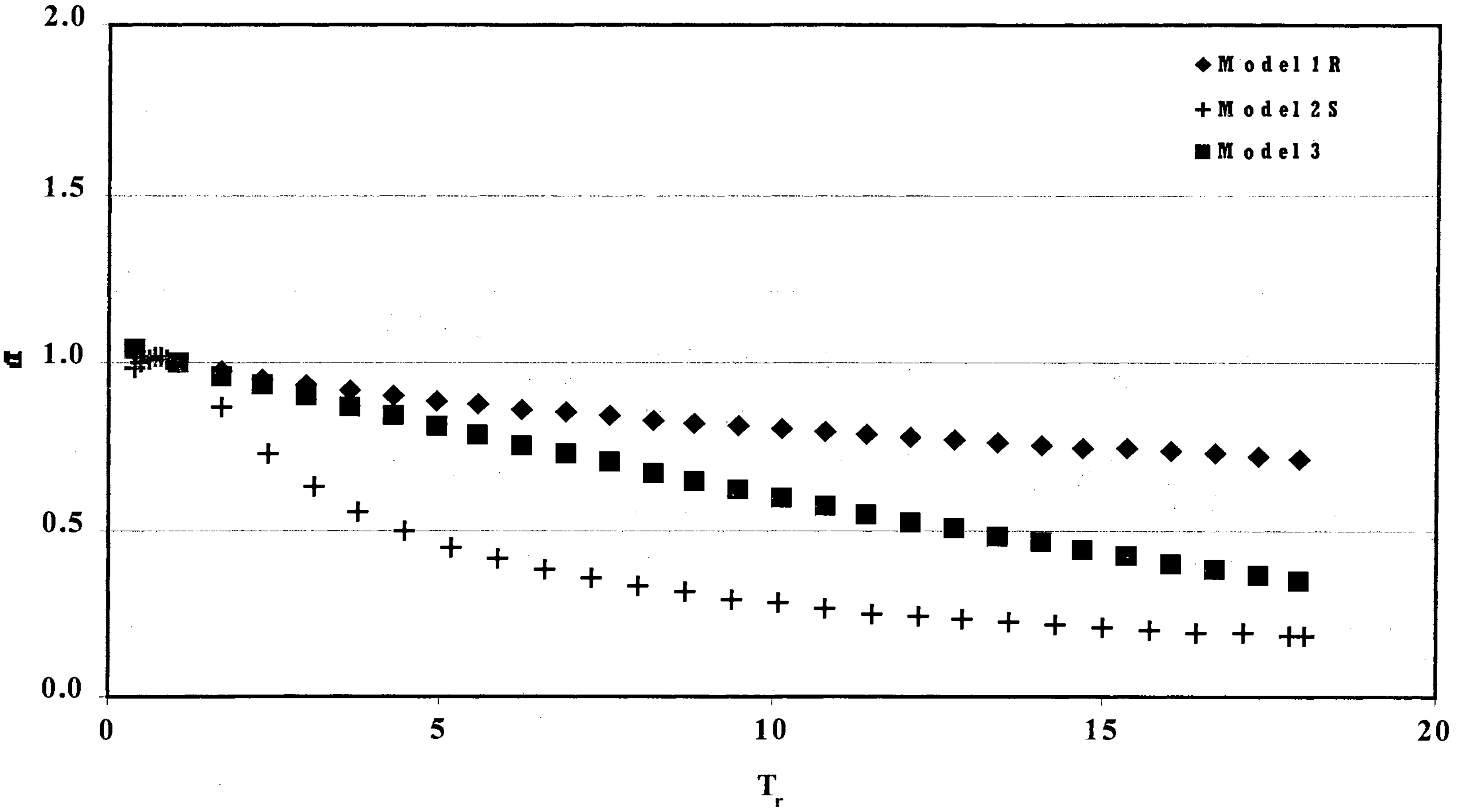

Figure 5. Comparisons of the Limiting Behavior for Various α Models for Hydrogen.

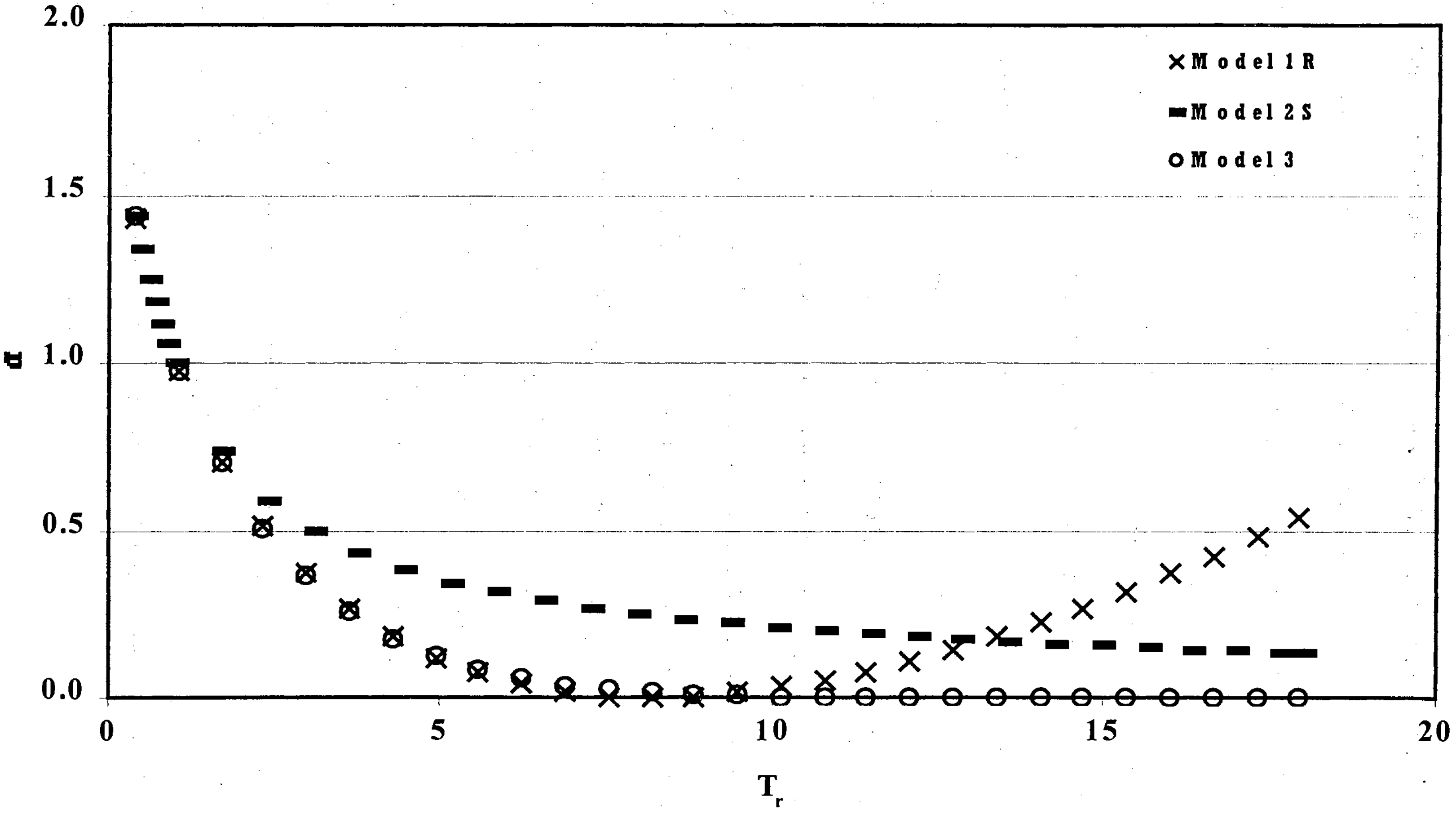

Figure 6. Comparisons of the Limiting Behavior for Various α Models for Ethane.

Table 4

PR EOS Vapor Pressure Predictions Using Various α Functions

Name	%AAD For Each Model					NPTS
	1	1R	2	2R	3	
Methane	1.90	1.27	1.55	1.23	1.35	105
Ethane	0.56	0.86	0.38	0.60	0.53	117
Propane	0.76	0.79	0.37	0.43	0.41	51
Argon	0.89	0.71	0.64	0.25	0.31	54
Nitrogen	0.38	1.29	0.52	0.38	0.54	63
Benzene	1.80	1.73	0.94	1.04	1.61	42
Carbon Dioxide	0.38	0.68	0.16	0.22	0.21	56
Water	2.40	2.68	4.61	3.67	3.59	38
Fluorine	3.05	0.87	2.07	0.91	0.68	123
n-Butane	2.88	1.83	2.29	1.48	0.75	78
Ammonia	0.17	1.44	1.40	1.01	0.85	23
Acetone	1.48	3.35	2.72	2.26	1.72	47
Oxygen	1.65	1.41	0.92	1.27	1.90	21
n-Decane	4.34	2.40	2.17	0.95	0.80	34
Hydrogen	4.67	5.62	4.07	2.56	6.41	21
Methanol	2.57	3.14	3.28	2.68	3.03	19
Ethanol	1.79	2.33	1.14	1.00	0.92	26
Ethylene	6.07	3.52	3.33	2.15	2.52	60
n-Decane	1.75	1.42	1.12	0.74	0.76	16
n-Dodecane	2.73	1.37	0.92	0.66	0.73	14
n-Tetradecane	4.11	1.23	0.85	0.62	0.70	16
n-Hexadecane	6.61	1.74	0.67	0.97	0.46	21
n-Octadecane	9.49	2.22	1.22	1.27	1.06	17
n-Nonadecane	10.05	2.44	1.59	1.17	1.37	17
n-Eicosane	12.57	1.31	0.64	1.38	0.59	17
n-Docosane	17.42	0.69	0.45	1.66	0.36	13
n-Tetracosane	24.69	1.38	0.87	2.91	0.67	14
n-Octacosane	33.00	3.02	0.98	2.72	0.57	15
Overall Results	3.73	1.65	1.52	1.19	1.13	1138
RMSE, bar	0.284	0.204	0.353	0.264	0.282	1138
BIAS, bar	0.073	0.022	0.067	0.070	0.078	1138

Table 5

Model Parameters for α Functions Evaluated in This Study

	Parameters					
Model	A	B	C	D	E	F
1	0.374640	1.54230	-0.26992	0.5	0.5	
1R	0.386590	1.50226	-0.16870	0.5	0.5	
2	-0.171813	0.125283	1.77634	-0.607352	0.511614	2.20517
2R	-0.207176	0.092099	1.94800	-0.502297	0.603486	2.09626
3	2.00	0.836	0.134	0.508	-0.0467	

the vapor pressures of the light components well (deviations within 2%); however, the predictions become increasingly worse for the heavy hydrocarbons (deviations over 30%). In comparison, the results for Case 1R show significant improvement in the distribution of the errors (overall AAD of 1.6%), and more importantly, the vapor pressures of heavy hydrocarbons are represented well. Twu's original model (Model 2) exhibits good overall accuracy (ADD of 1.5%) and good representation for the heavy hydrocarbons. Updating the model parameters (Model 2R) enhances the vapor pressure predictions and yields an overall 1.2% AAD. The proposed model (Model 3) gives, on average, comparable results to Model 2; however, Model 3 produces more accurate vapor pressure predictions for the heavy hydrocarbons.

Mixture Predictions

The above evaluations of the α functions are based on vapor pressure data only. However, when the equations of state are used in VLE calculation, some components may be in the supercritical region. Our studies show that the results of the VLE calculation are sensitive to the temperature dependence of the α function in the supercritical region, which causes many proposed α functions to fail. Thus, one of the required characteristics of a viable α function is accurate representation of equilibrium (solubility) data involving supercritical components, using "reasonable" binary interaction parameters. By "reasonable", we mean that the regressed interaction parameters should be small in value and exhibit uniformly the least possible variation with molecular size and temperature.

Table 6 presents the case studies used to evaluate the quality of the mixture predictions for the α functions considered. Case 1 examines the raw predictive capability of PR EOS, based solely on pure-fluid property input, and Cases 2 and 3 explore the quality of EOS representation of binary mixtures involving supercritical components, using binary interaction parameters. Specifically, in Case 2, we employ paraffin-specific parameters, C_{ij}(CN); and in Case 3, we employ temperature-specific parameters, C_{ij}(CN, T). The binary systems selected for this study are listed in Table 7. The database contains six solutes involving 48 systems and totaling 1154 points. Also given in Table 7 is the reduced temperature range for the various supercritical components, which extends from T_r of 0.9 for the near-critical ethane to T_r of 12.8 for hydrogen. All data are utilized as isothermal p-x measurements, i.e., the bubble point pressure as a function of solute liquid mole fraction, or, alternatively, the solubility of the solute as a function of pressure. We intentionally limited the upper pressure to 90% of the critical pressure, as EOS are inherently inaccurate near the critical point of a mixture. Full documentation of these systems is given by Gao et al. (1999c).

To apply the PR EOS to mixtures, the values of a and b were determined using the mixing rules:

$$a = \sum_{i}^{N}\sum_{j}^{N} z_i z_j (1 - C_{ij})(a_i a_j)^{1/2} \tag{8}$$

$$b = 0.5\sum_{i}^{N}\sum_{j}^{N} z_i z_j (b_i + b_j) \tag{9}$$

Table 6

Case Studies Employed to Evaluate Cubic Equation-of-State Predictions Using C_{ij}

Case	Description
1. $C_{ij}=0$	The simple quadratic mixing rule is used, without any interaction parameters
2. $C_{ij}(CN)$	A single value of C_{ij} is determined for each binary system
3. $C_{ij}(CN, T)$	A separate value of C_{ij} is used for each temperature in a system

Table 7

The Database of Binary Systems Used in This Study

Solvent	Temperature Range, K	Pressure Range, MPa	Solute Mole Fraction Range	NPTS
		Hydrogen [T_r= 9.8 – 12.8]		
n-C_4	327.65 - 394.25	2.778 - 16.847	0.0190 - 0.1930	48
n-C_5	323.15	0.347 - 20.680	0.0016 - 0.1460	11
n-C_6	344.26 - 411.11	1.238 - 24.132	0.0105 - 0.2150	46
n-C_7	424.15 - 498.85	2.420 - 38.714	0.0230 - 0.5370	22
n-C_{10}	344.26 - 423.15	3.710 - 17.390	0.0367 - 0.1288	17
n-C_{20}	323.15 - 423.15	2.230 - 12.910	0.0273 - 0.1289	22
n-C_{28}	348.15 - 423.15	2.860 - 13.100	0.0452 - 0.1572	19
n-C_{36}	373.15 - 423.15	3.560 - 16.750	0.0677 - 0.2271	12
		Nitrogen [T_r= 1.9 - 3.5]		
n-C_4	250.00 - 399.82	0.777 - 15.785	0.0040 - 0.2742	53
n-C_5	277.43 - 377.59	0.250 - 20.781	0.0022 - 0.3390	38
n-C_8	322.00 - 344.30	3.227 - 35.039	0.0430 - 0.3470	10
n-C_9	322.00 - 344.30	3.723 - 34.736	0.0480 - 0.3320	12
n-C_{10}	344.26 - 410.93	3.910 - 16.040	0.0556 - 0.1967	21
n-C_{20}	323.20 - 423.20	3.830 - 17.230	0.0610 - 0.2121	20
n-C_{28}	348.20 - 423.20	4.300 - 16.470	0.0726 - 0.2578	19
n-C_{36}	373.20 - 423.20	5.280 - 17.990	0.1054 - 0.2970	12

Table 7

The Database of Binary Systems Used in This Study - *continued*

Solvent	Temperature Range, K	Pressure Range, MPa	Solute Mole Fraction Range	NPTS
		Carbon Monoxide [T_r= 2.0 – 3.1]		
C_3	273.15 - 323.15	1.379 - 13.790	0.0230 - 0.3840	20
n-C_6	323.15 - 423.15	1.179 - 8.687	0.0099 - 0.1466	18
n-C_8	463.15 - 533.15	0.669 - 6.569	0.0027 - 0.1570	42
n-C_{10}	310.93 - 377.59	2.227 - 10.004	0.0385 - 0.1400	17
n-C_{20}	323.15 - 423.15	1.991 - 8.384	0.0403 - 0.1614	20
n-C_{28}	348.15 - 423.15	1.903 - 8.412	0.0463 - 0.1853	26
n-C_{36}	373.15 - 423.15	1.800 - 8.956	0.0494 - 0.2099	12
		Carbon Dioxide [T_r= 0.9 – 1.6]		
n-C_5	273.41	0.2690 - 2.6680	0.0451 - 0.7012	7
n-C_6	303.15 - 393.15	0.8620 - 7.6200	0.0284 - 0.8435	29
n-C_7	310.65 - 477.21	0.1860 - 8.6940	0.0220 - 0.9290	44
n-C_{10}	310.93 - 377.59	0.6890 - 8.6180	0.0730 - 0.6000	17
n-C_{20}	323.15 - 373.15	0.6200 - 6.7570	0.0730 - 0.5010	23
n-C_{28}	348.15 - 423.15	0.8070 - 9.6040	0.0700 - 0.6170	28
n-C_{36}	373.15 - 423.15	0.5240 - 6.0090	0.0620 - 0.4590	17

Table 7

The Database of Binary Systems Used in This Study - *continued*

Solvent	Temperature Range, K	Pressure Range, MPa	Solute Mole Fraction Range	NPTS
		Methane [T_r= 1.5 – 2.2]		
n-C_4	277.59 - 377.59	1.379 - 10.342	0.0256 - 0.4513	11
n-C_5	344.26 - 377.59	1.379 - 13.790	0.0279 - 0.5320	28
n-C_6	298.33 - 373.33	1.014 - 10.135	0.0300 - 0.4125	37
n-C_7	311.11 - 411.11	2.193 - 10.466	0.1000 - 0.4000	12
n-C_8	298.33 - 423.33	1.013 - 7.093	0.0280 - 0.2870	28
n-C_9	323.15 - 423.15	1.014 - 10.135	0.0329 - 0.3471	39
n-C_{10}	310.93 - 410.93	1.043 - 8.647	0.0495 - 0.3080	32
n-C_{20}	323.15 - 423.15	0.953 - 10.690	0.0512 - 0.3500	22
n-C_{28}	348.15 - 423.15	0.926 - 7.092	0.0568 - 0.2992	18
n-C_{36}	373.15 - 423.15	0.838 - 7.928	0.0511 - 0.3506	13
		Ethane [T_r= 0.9 – 1.9]		
n-C_4	303.15 - 363.40	0.441 - 4.877	0.0440 - 0.8370	34
n-C_5	310.93 - 444.26	0.345 - 6.205	0.0048 - 0.8503	28
n-C_6	310.93 - 394.26	0.393 - 5.399	0.0720 - 0.6519	48
n-C_7	338.71 - 449.82	3.923 - 7.598	0.2960 - 0.8480	8
n-C_{10}	311.11 - 411.11	0.423 - 8.236	0.1050 - 0.6380	30
n-C_{20}	323.15 - 423.15	0.504 - 6.645	0.1180 - 0.6530	17
n-C_{28}	348.15 - 423.15	0.563 - 4.394	0.1020 - 0.5200	23
n-C_{36}	373.15 - 573.05	0.368 - 4.760	0.0870 - 0.5320	24

where z_k represents the mole fraction of component "k" in a mixture, and N is the number of components in mixture. In Eqs. 8 and 9, the summations are over all chemical species, and C_{ij} is an empirical binary interaction parameter. Interaction parameter values were determined by fitting the experimental data to minimize the objective function given in Eq. 7.

Table 8 presents the summary of results for the PR EOS predictions, using the selected α functions. On average, comparable results are obtained for all the cases considered (AAD: 15% for Case 1, 3% for Case2, and 2% for Case 3). Some improvement has been achieved for Model 3 compared to Model 1 (from 17.2 % to 13.9 % overall, 29.3 % to 15.8 % for hydrogen system, 26.5 % to 23.0 % for nitrogen, and 11.6 % to 8.2 % for carbon monoxide). It is interesting to note that these improvements are mainly for the solutes that have large reduced temperatures. This indicates the improved limiting behavior for the new α function has a moderate impact of the EOS predictions, when supercritical components are involved. Twu's switching-function model (Model 2S) gives better predictions than the other models for hydrogen systems (AAD of 6 %). This is expected since Model 2S was developed based on mixture data for hydrogen and methane; however, the other solute mixtures, including carbon monoxide and nitrogen, did not do as well.

Once interaction parameters are used, variation in the qaulity of the representation among the various solutes is not significant. Further, the results indicate that, for the systems considered, using temperature-dependent interaction parameters is not highly beneficial, relative to the effort involved.

Table 8

Summary of Results for Bubble Point Calculations Using Different PR α Functions

Model	Case 1, C_{ij}=0			Case 2, C_{ij} (CN)			Case 3, C_{ij}(CN, T)		
	%ADD	RMSE bar	BIAS bar	%ADD	RMSE bar	BIAS bar	%ADD	RMSE bar	BIAS bar
				Hydrogen					
1	29.3	27.96	17.60	2.8	4.50	0.00	1.6	2.63	-0.07
1R	23.6	22.67	16.58	2.8	4.31	0.02	1.5	3.05	-0.02
2S	5.8	8.15	-4.27	2.5	3.57	0.08	1.4	3.07	0.06
3	15.8	17.03	11.35	2.7	3.81	0.02	1.4	2.32	-0.06
				Nitrogen					
1	26.5	34.96	26.33	2.3	3.73	-0.80	2.0	3.54	-0.70
1R	24.4	32.88	24.38	2.6	3.93	-0.87	1.8	3.35	-0.69
2S	30.1	36.95	28.66	2.2	3.23	-0.45	1.7	3.20	-0.38
3	23.0	31.84	23.23	2.9	4.33	-0.86	1.5	2.59	-0.40
				Methane					
1	7.8	5.22	3.38	1.8	1.12	0.15	1.3	1.02	0.16
1R	7.0	4.56	2.74	1.8	1.12	0.09	1.2	0.96	0.11
2S	7.4	4.75	2.92	1.9	1.16	0.17	1.3	1.07	0.17
3	7.1	4.56	2.60	2.0	1.25	0.17	1.3	1.05	0.18
				Ethane					
1	7.2	2.30	-0.65	3.0	1.48	0.36	2.6	1.33	0.38
1R	7.3	2.32	-0.93	3.1	1.48	0.33	2.6	1.31	0.37
2S	7.1	2.25	-0.77	3.0	1.50	0.39	2.6	1.33	0.38
3	7.3	2.29	-0.85	3.1	1.50	0.35	2.6	1.32	0.39

Table 8

Summary of Results for Bubble Point Calculations Using Different PR α Functions – *continued*

Model	Case 1, $C_{ij}=0$			Case 2, C_{ij} (CN)			Case 3, C_{ij}(CN, T)		
	%ADD	RMSE bar	BIAS bar	%ADD	RMSE bar	BIAS bar	%ADD	RMSE bar	BIAS bar
				Carbon Monoxide					
1	11.6	7.90	6.52	2.7	2.09	-0.12	1.0	1.36	-0.05
1R	9.3	6.52	3.99	2.9	2.29	0.13	1.1	1.41	-0.03
2S	19.1	12.06	7.02	2.2	1.75	0.08	1.0	1.34	0.05
3	8.2	6.07	3.52	3.1	2.41	-0.16	1.2	1.46	0.04
				Carbon Dioxide					
1	25.1	10.97	9.02	4.0	2.45	0.01	2.6	1.94	0.02
1R	24.5	10.69	8.78	4.2	2.58	0.03	2.6	1.97	-0.02
2S	25.2	11.01	9.01	3.8	2.37	0.09	2.6	1.94	0.01
3	24.8	10.87	8.92	4.0	2.51	0.02	2.6	1.95	0.01
				Overall					
1	17.2	19.46	10.16	2.7	2.81	-0.04	2.0	2.04	-0.02
1R	15.5	17.46	9.23	2.8	2.85	-0.06	2.0	2.10	-0.02
2S	17.1	17.23	7.03	2.6	2.43	0.09	1.8	2.17	0.04
3	13.9	15.98	7.07	2.9	2.86	-0.07	1.8	1.97	0.03

Perhaps, the most significant finding of this study is that the accuracy of the pure-component predictions has only a moderate impact on the quality of EOS representation of mixtures involving supercritical components. That is, in comparison potentially to mixtures containing only subcritical components, the advantages of having accurate vapor pressure predictions are outweighed by the quality of the mixing rules used. Accordingly, additional studies are required to improve the mixing rules for asymmetric mixtures.

SUMMARY

In this study, a new α function is proposed for the PR EOS, which exhibits appropriate temperature-limiting behavior. The new function was compared to the PR EOS original Soave-type α function and Twu's logarithmic-type α function. The database used to evaluate the new α function consists of a variety of molecular species including, simple, normal, and polar fluids, with emphasis on heavy hydrocarbons. The new PR EOS α function represents the vapor pressures of 1138 data points with an absolute averaged deviation of 1.1 %, including heavy hydrocarbons. In addition, the new PR EOS α function has been found more accurate for *a priori* predictions (AAD of 13.9%) of bubble point pressure and comparable to the original α function in representing 48 binary asymmetric mixtures involving diverse molecular species (AAD of 3%, using paraffin-dependent interaction parameters), without the use of switching functions.

CHAPTER 6

ALTERNATE COMBINING RULES AND INTERACTION PARAMETER GENERALIZATIONS FOR ASYMMETRIC MIXTURES

ABSTRACT

Following the work of Juris and Wenzel (1974), an alternate combining rule is proposed for cubic equations of state (CEOS). A wide variety of interactions between unlike molecules can be effectively represented by this combining rule.

The Soave-Redlich-Kwong (SRK) (Soave, 1972) and Peng-Robinson (PR) (Peng and Robinson, 1976) equations of state (EOS) have been used to assess the proposed combining rule, in comparison with the classical rules. Specifically, a study was undertaken to evaluate the predictive capability of both equations in representing the vapor-liquid equilibrium properties of asymmetric binary mixtures, involving methane, ethane, nitrogen, hydrogen, CO and CO_2 in the n-paraffins (C_4 – C_{44}).

EOS binary interaction parameters generated by the proposed combination rules are presented for the systems considered. The quality of the EOS representation is dependent on the level of complexity applied in the parameter regressions. Overall, AAD (average absolute deviation) of 1 to 3% is realized from the various regression scenarios. In addition, generalized EOS parameter correlations for system-dependent parameters have been developed. These interaction parameters represent the solubilities of the selected systems within 5%.

INTRODUCTION

Precise descriptions of the fluid-phase behavior can have significant economic impact when used in chemical engineering process calculations, such as phase separations. These descriptions must be undertaken in terms of analytical models suited for process design/development calculations. Almost all the state-of-the-art analytical models, such as EOS or activity coefficient models, have one or more empirical "interaction" parameters, for precise model tuning (Gasem, et al., 1993). Although these parameters cannot be predicted *a priori* from theory at present, they can have dramatic effect on phase behavior calculations. Typically, interaction parameters are regressed from the available experimental data, and provisions are made, through parameter generalizations, to estimate them for systems lacking experimental data; therefore, accurate parameter generalizations are necessary, since it is infeasible to conduct enough experiments to cover all binaries and all phase conditions.

Asymmetric mixtures involving light gas solutes (hydrogen, nitrogen, CO, CO_2, methane, and ethane) and hydrocarbon solvents (C_4-C_{44}) are encountered in many important industries, such as enhanced oil recovery, supercritical extraction, and Fisher-Tropsch syntheses. In this study, the CEOS have been chosen to describe the equilibrium properties of such systems. Although these simple CEOS are not as rigorous as the theoretically-based equations of state, such as the simplified-perturbed-hard-chain theory (SPHCT) EOS (Kim et al., 1986), the simplified-statistical-associating-fluid theory (SAFT) EOS (Chapmen et al., 1990) and the modified Park-Gasem-Robinson (MPGR) EOS (Row, 1998), their simplicity, relative accuracy and wide industrial use justify their further development (Gasem et al., 1993).

Proper mixing rules are required to extend EOS application to mixtures. As a result, numerous mixing rules have been evaluated and developed (see, e.g., Mansoori, 1993; Shibata and Sandler, 1989; Eubank et al., 1993; Orbey and Sandler, 1995; Twu and Coon, 1995). Nevertheless, the one-fluid theory mixing rules are found to be both simple and, in most cases, accurate. The CEOS with these mixing rules can be used to represent the systems within the experimental precision (Shibata and Sandler, 1989); and in many situations, one interaction parameter is sufficient for the purpose. The interaction parameters from these mixing rules show regular trends with solvent size variations. Although many other mixing rules such as Wong-Sandler mixing rules (Obey and Sandler, 1995) are more theoretically based and can be used to represent asymmetric mixtures precisely (Trivedi, 1996), the multiple parameters associated with these mixing rules complicate developing simple parameter generalizations. Therefore, we have elected to use the one-fluid classical quadratic mixing rules.

At the heart of all mixing rules are combining rules to account for the unlike molecular interactions. Interestingly, while the literature reflects a great interest in mixing rules, there are relatively fewer studies on combining rules, especially those pertaining to CEOS. Historically, the use of a geometric-mean combining rule for the attraction law constant ‘a’ and a linear combining rule for the co-volume ‘b’ is most common, when dealing with CEOS. In contrast, a variety of combining rules has been developed for virial-type EOS (see, e.g., Juris and Wenzel, 1974; Luongo-Ortiz and Starling, 1997). In the present work, we apply a general form of a combining rule first suggested for use in virial-type EOS by Juris and Wenzel (1974).

Once a set of mixing and combining rules were selected, binary interaction parameters were then regressed from available data to represent the mixture vapor-liquid equilibrium (VLE) properties precisely. Moreover, attempts were made to generalize these parameters for systems and phase conditions not accounted for in the existing experimental database. Literature generalization efforts have been reviewed by several investigators (see, e.g., Kordas et al., 1994-1995; Nishiumi, 1988.) Our previous parameter generalization efforts involving asymmetric mixtures have been varied in complexity (e.g., Gasem, 1986; Gasem, et al., 1993; Tong, 1994). In this study, we present new generalized correlations for EOS binary interaction parameters, which benefit from (a) an expanded binary mixture database, (b) more accurate heavy n-paraffin pure fluid properties, and (c) a more general EOS combining rule.

EQUATIONS OF STATE

The SRK EOS is:

$$p = \frac{RT}{v - b} - \frac{a}{v(v + b)} \tag{1}$$

where

$$a = a_c \alpha(T) \tag{2}$$

$$b = 0.08664 RT_c/P_c \tag{3}$$

and

$$a_c = 0.42748 R^2 T_c^2/p_c \tag{4}$$

$$\alpha(T)^{1/2} = 1 + k(1 - T_r^{1/2}) \tag{5}$$

$$k = 0.480 + 1.574\omega - 0.176\omega^2 \tag{6}$$

Similarly, the PR EOS is:

$$p = \frac{RT}{v - b} - \frac{a}{v(v + b) + b(v - b)} \tag{7}$$

where

$$a = a_c\alpha(T) \tag{8}$$

$$b = 0.0778RT_c/P_c \tag{9}$$

and

$$a_c = 0.45724R^2T_c^2/p_c \tag{10}$$

$$\alpha(T)^{1/2} = 1 + k(1 - T_r^{1/2}) \tag{11}$$

$$k = 0.37464 + 1.54226\omega - 0.26992\omega^2 \tag{12}$$

where p is the pressure, R is the gas constant, T is the temperature, a and b are EOS constants, v is the molar volume, T_c is the critical temperature, p_c is the critical pressure, T_r is the reduced temperature, $\alpha(T)$ expresses the temperature dependence in the parameter a, and ω is the acentric factor. For the PR EOS, we also use the new α function (Gao et al., 1999b),

$$\ln(\alpha(T,\omega)) = (2.000 + 0.836T_r)(1 - T_r^{(0.134+0.508\omega+0.0467\omega^2)}) \tag{13}$$

which yields more accurate vapor pressure predictions for the heavy hydrocarbons than those obtained from Eqs. 11-12.

MIXING RULES

To apply the SRK and PR EOS to mixtures, mixing rules are employed to calculate the values of a and b of the mixtures. Classic, one-fluid quadratic mixing rules are employed in this study:

$$a = \sum_i^N \sum_j^N z_i z_j a_{ij} \tag{14}$$

$$b = \sum_i^N \sum_j^N z_i z_j b_{ij} \tag{15}$$

where z_k represents the mole fraction of component "k" in a mixture, and N is the number of components in the mixture. In Eqs. 14 and 15, the summations are over all chemical species. The cross coefficients a_{ij} and b_{ij} are the parameters used in EOS calculation for the mixture of component “i” and component “j”. They are calculated using pure-substance a and b parameters according to the selected combining rules.

There are different combining rules in the literature, especially for virial-type EOS. Concerning CEOS, some attempts have been made to improve the mixture property predictions through alternate combining rules (see, e.g., Panagiotopoulos and Reid, 1986; Harismiadis et al., 1994). Nevertheless, little improvements were realized, relative to the added complexity of the proposed rules.

Of interest in this study is the general form of the combining rule described by Juris and Wenzel (1974) for the Martin-Hou EOS parameters:

$$A_{ij} = \left(\frac{A_i^N + A_j^N}{2}\right)^{1/N} \qquad (16)$$

This combining rule encompasses several rules used in the literature (N = 0, geometric or Lorentz-Berthelot rule; N = 1, linear rule; N = 1/3, Lorentz rule; N = -1, Halsey-Fender rule). In this work, we apply Eq. 16 in its most general form. That is, the combining rule exponent ‘N’ is treated as a regressed parameter; thus, the combining rule allows the experimental data for a given binary to dictate the recipe for combining the unlike molecular interactions. This treatment is similar to the approach taken by Sudibandriyo (1986) to develop new mixing rules that abide by the conformal solution theory. In this study, we call Eq. 16 the conformal combining rule. The efficiency of both the classical and conformal combining rules in representing asymmetric mixtures is evaluated in this study.

1. Classic or Lorentz-Berthelot combining rules

The classic combining rules are as follows (see, e.g., Gasem et al., 1989):

$$a_{ij} = (1 - C_{ij})(a_i a_j)^{1/2} \tag{17}$$

$$b_{ij} = 0.5(1 + D_{ij})(b_i + b_j) \tag{18}$$

C_{ij} and D_{ij} are empirical interaction parameters characterizing deviations from the defined (geometric or linear) unlike interactions between molecules "i" and "j". When i equals j, C_{ij} and D_{ij} are zero. When i does not equal j, C_{ij} and D_{ij} may not be zero. Values of C_{ij} and D_{ij} are determined by fitting the experimental data to minimize an objective function. Eqs. 17 and 18 are equivalent to Eq. 16, when the exponent in Eq. 16 is set to infinitely small value and 1, respectively.

2. Conformal combining rules

For asymmetric mixtures, the interaction between two unlike molecules can be significantly different from that represented by the geometric-mean combining rule, $a = (a_i a_j)^{1/2}$. In such cases, the binary interaction parameter used to correct for deviations from the geometric mean can require very large values (>50% correction). Clearly, in such instances, a different combining rule is more appropriate.

In this study, we adopt the following combining rules:

$$a_{ij} = \left(\frac{a_i^{N_{ij}} + a_j^{N_{ij}}}{2}\right)^{1/N_{ij}} \tag{19}$$

$$b_{ij} = \left(\frac{b_i^{M_{ij}} + b_j^{M_{ij}}}{2}\right)^{1/M_{ij}} \tag{20}$$

where the exponents N_{ij} and M_{ij} are regressed directly from the binary experimental data. In principle, these exponents should more precisely reflect the type of unlike-pair interactions than the binary interaction parameters C_{ij} and D_{ij}.

There exist direct connections between C_{ij} and N_{ij}, D_{ij} and M_{ij}, as shown below:

$$1-C_{ij}=\left(\frac{\left(\frac{a_i}{a_j}\right)^{N_{ij}/2}+\left(\frac{a_j}{a_i}\right)^{N_{ij}/2}}{2}\right)^{1/N_{ij}} \tag{21}$$

$$1-D_{ij}=\frac{2}{b_i+b_j}\left(\frac{b_i^{M_{ij}}+b_j^{M_{ij}}}{2}\right)^{1/M_{ij}} \tag{22}$$

This means the quality of the EOS presentation obtained from the classical combining rules and the conformal rules are identical at given temperature, and one set of parameters can be generated from the other. As such, use of the conformal combining rules is predicated on their ability to provide clear interpretation for the type of molecular combinations encountered, as opposed to accepting preset rules. Also, the regressed exponents may be easier to generalize. Variation of C_{ij} with N_{ij} is shown in Figure 1, which indicates that significant curvature in C_{ij} can be represented by a constant N_{ij}. This behavior is clearly illustrated by the parameters for carbon monoxide and nitrogen.

DATABASE AND DATA REDUCTION PROCEDURES

Table 1 presents the pure-fluid physical properties used in this study. As was discussed in Chapter 4, while property values for the light components originate from Reid et al. (1987), the updated ABC model is used to predict the physical properties of

Table 1

The Critical Properties and Acentric Factors Used in the Cubic Equation-of-State Evaluations

Component	p_c / MPa	T_c / K	ω	Reference
Nitrogen	3.39	126.2	0.039	Reid et al. (1987)
Hydrogen	1.30	33.2	-0.218	Reid et al. (1987)
Carbon Monoxide	3.50	132.9	0.066	Reid et al. (1987)
Carbon Dioxide	7.38	304.2	0.225	Reid et al. (1987)
Methane	4.60	190.6	0.011	Reid et al. (1987)
Ethane	3.87	305.3	0.100	Reid et al. (1987)
C_3	4.25	369.8	0.153	Reid et al. (1987)
n-C_4	3.80	425.2	0.199	Reid et al. (1987)
n-C_5	3.37	469.7	0.251	Reid et al. (1987)
n-C_6	3.01	507.5	0.299	Reid et al. (1987)
n-C_7	2.74	540.3	0.349	Reid et al. (1987)
n-C_8	2.49	568.8	0.398	Reid et al. (1987)
n-C_9	2.29	594.6	0.445	Reid et al. (1987)
n-C_{10}	2.13	618.8	0.489	Gao et al. (1999a)
n-C_{12}	1.83	658.9	0.575	Gao et al. (1999a)
n-C_{16}	1.39	720.9	0.737	Gao et al. (1999a)
n-C_{18}	1.23	745.5	0.814	Gao et al. (1999a)
n-C_{19}	1.16	756.6	0.851	Gao et al. (1999a)
n-C_{20}	1.09	766.9	0.888	Gao et al. (1999a)
n-C_{21}	1.03	776.6	0.925	Gao et al. (1999a)
n-C_{22}	0.97	785.7	0.961	Gao et al. (1999a)
n-C_{24}	0.87	802.3	1.031	Gao et al. (1999a)
n-C_{28}	0.71	830.3	1.167	Gao et al. (1999a)
n-C_{36}	0.48	871.5	1.421	Gao et al. (1999a)
n-C_{44}	0.34	899.8	1.656	Gao et al. (1999a)

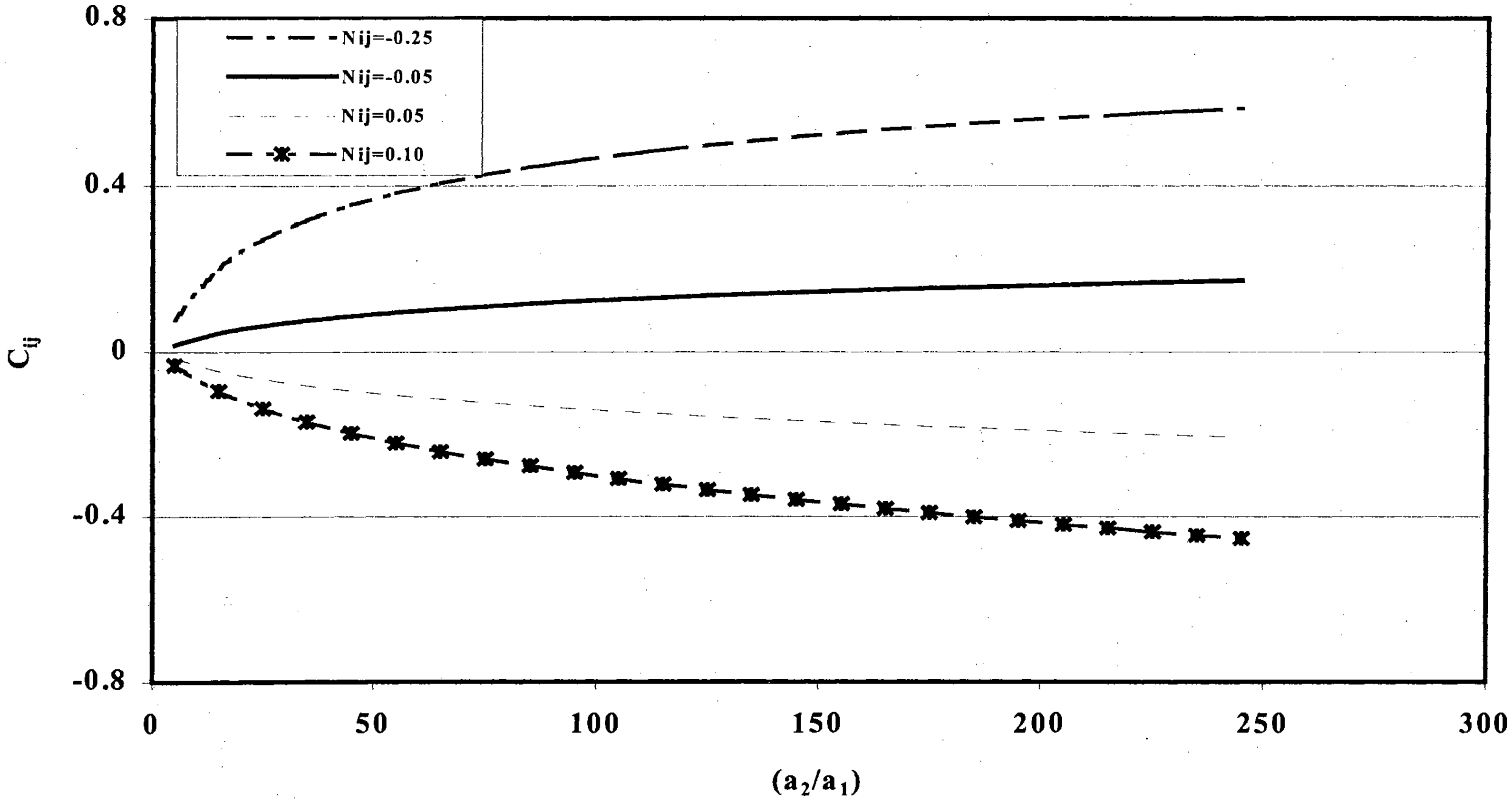

Figure 1. The Relationship between C_{ij} and (a_2/a_1) at Constant N_{ij}.

heavy n-paraffins (CN > =10), as given by Gao et al. (1999a). These properties are EOS independent. Table 2 details the sources of binary experimental data used in our evaluations, along with the temperature, pressure and composition range for each binary system. All data are utilized as isothermal p-x measurements, i.e., the bubble point pressure as a function of solute liquid mole fraction, or, alternatively, the solubility of the solute as a function of pressure. We intentionally limited the upper pressure to 90% of the critical pressure, as EOS are inherently inaccurate near the critical point of a mixture. This procedure decreases the influence on the regressed interaction parameters of data in regions where the EOS is incapable of accurate predictions.

The objective function used, SS, minimizes the sum of squared relative deviations in predicted bubble point pressures:

$$SS = \sum_{i}^{n} \left(\frac{p_{calc} - p_{exp}}{p_{exp}} \right)_i^2 \qquad (20)$$

Here, n is the number of data points, p_{calc} is the calculated pressure, and p_{exp} is the experimental pressure. Detailed procedures for data reduction are referred to Gasem (1986, 1993).

PARAMETER GENERALIZATIONS

As shown in Tables 3 and 4, five cases, involving the classical and the conformal combining rules, are evaluated. A systematic progression in the complexity of data regressions has been pursued to (a) explore the effect of variations in solute type, solvent molecular size, and temperature on EOS representation; (b) assess the correlative ability of the PR and SRK EOS; and (c) identify the optimum strategy for parameter generalization.

Table 2

The Database of Binary Systems Used in This Study

	Hydrogen				
Solvent	Temperature Range, K	Pressure Range, MPa	Solute Mole Fraction Range	NPTS	Reference
n-C_4	327.65 – 394.25	2.778 - 16.847	0.0190 - 0.1930	48	Klink et al, 1975
n-C_5	323.15	0.347 - 20.680	0.0016 - 0.1460	11	Freitag and Robinson, 1986
n-C_6	344.26 - 411.11	1.238 - 24.132	0.0105 - 0.2150	46	Nichols et al., 1957; Chapter 2 in this study
n-C_7	424.15 - 498.85	2.4203 - 8.714	0.0230 - 0.5370	22	Peter and Reinhartz, 1960
n-C_{10}	344.26 - 423.15	3.710 - 17.390	0.0367 - 0.1288	17	Park et al., 1995
n-C_{12}	344.26 - 410.93	1.422 - 123.235	0.0144 - 0.1252	24	Gao et al., 1999
n-C_{20}	323.15 - 423.15	2.230 - 12.910	0.0273 - 0.1289	22	Park et al., 1995
n-C_{28}	348.15 - 423.15	2.860 - 13.100	0.0452 - 0.1572	19	Park et al., 1995
n-C_{36}	373.15 - 423.15	3.560 - 16.750	0.0677 - 0.2271	12	Park et al., 1995
Total Number of Points				191	

Table 2

The Database of Binary Systems Used in This Study – *continued*

	Nitrogen				
Solvent	Temperature Range, K	Pressure Range, MPa	Solute Mole Fraction Range	NPTS	Reference
n-C_4	250.00 - 399.82	0.777 - 15.785	0.0040 - 0.2742	53	Brown et al., 1989; Akers et al., 1954
n-C_5	277.43 - 377.59	0.250 - 20.781	0.0022 - 0.3390	38	Kalra et al., 1977
n-C_8	322.00 - 344.30	3.227 - 35.039	0.0430 - 0.3470	10	Llave and Chung, 1988
n-C_9	322.00 - 344.30	3.723 - 34.736	0.0480 - 0.3320	12	Llave and Chung, 1988
n-C_{10}	344.26 - 410.93	3.910 - 16.040	0.0556 - 0.1967	21	Tong et al., 1999
n-C_{12}	344.26 - 410.93	1.293 - 9.549	0.0202 - 0.1251	23	Gao et al., 1999
n-C_{20}	323.20 - 423.20	3.830 - 17.230	0.0610 - 0.2121	20	Tong et al., 1999
n-C_{28}	348.20 - 423.20	4.300 - 16.470	0.0726 - 0.2578	19	Tong et al., 1999
n-C_{36}	373.20 - 423.20	5.280 - 17.990	0.1054 - 0.2970	12	Tong et al., 1999
Total Number of Points				208	

Table 2

The Database of Binary Systems Used in This Study – *continued*

	Carbon Monoxide				
Solvent	Temperature Range, K	Pressure Range, MPa	Solute Mole Fraction Range	NPTS	Reference
C_3	273.15 - 323.15	1.379 - 13.790	0.0230 - 0.3840	20	Trust and Kurata, 1971
n-C_6	323.15 - 423.15	1.179 - 8.687	0.0099 - 0.1466	18	Yi, 1992
n-C_8	463.15 - 533.15	0.669 - 6.569	0.0027 - 0.1570	42	Connolly and Kandalic, 1984
n-C_{10}	310.93 - 377.59	2.227 - 10.004	0.0385 - 0.1400	17	Yi, 1992
n-C_{12}	344.26 - 410.93	0.690 - 8.751	0.0113 - 0.1493	27	Gao et al., 1999
n-C_{20}	323.15 - 423.15	1.991 - 8.384	0.0403 - 0.1614	20	Yi, 1992
n-C_{28}	348.15 - 423.15	1.903 - 8.412	0.0463 - 0.1853	26	Yi, 1992; Srivatsan, 1991
n-C_{36}	373.15 - 423.15	1.800 - 8.956	0.0494 - 0.2099	12	Yi, 1992
Total Number of Points				182	

Table 2

The Database of Binary Systems Used in This Study – *continued*

	Carbon Dioxide				
Solvent	Temperature Range, K	Pressure Range, MPa	Solute Mole Fraction Range	NPTS	Reference
n-C_5	273.41	0.269 - 1.558	0.0451 - 0.3206	4	Cheng et al., 1989
n-C_6	303.15 - 353.15	0.862 - 7.620	0.0515 - 0.8435	19	Ohgaki and Katayama, 1976; Wagner and Wichterle, 1987
n-C_7	310.65 - 352.59	0.186 - 7.267	0.0220 - 0.9290	29	Kalra et al., 1978
n-C_{10}	310.93 - 377.59	0.689 - 8.618	0.0730 - 0.4876	14	Reamer and Sage, 1963
n-C_{16}	463.05 - 663.75	2.006 - 5.087	0.0897 - 0.2575	15	Sebastian et al., 1980
n-C_{18}	396.60 - 673.20	1.016 - 6.190	0.0519 - 0.3890	25	Kim et al., 1985
n-C_{19}	313.15 - 333.15	0.936 - 7.181	0.0899 - 0.6342	21	Fall et al., 1985
n-C_{20}	323.15 - 373.15	0.620 - 6.429	0.0730 - 0.5010	22	Gasem, 1986
n-C_{21}	318.15 - 338.15	0.931 - 7.759	0.0999 - 0.6496	15	Fall et al., 1985
n-C_{22}	323.15 - 373.15	0.962 - 7.178	0.0833 - 0.5925	34	Fall et al., 1984
n-C_{24}	373.15	1.013 - 5.066	0.0819 - 0.3531	5	Tsai and Yau, 1990

Table 2

The Database of Binary Systems Used in This Study – *continued*

	Carbon Dioxide - *continued*				
Solvent	Temperature Range, K	Pressure Range, MPa	Solute Mole Fraction Range	NPTS	Reference
n-C_{28}	348.15 - 423.15	0.807 - 9.604	0.0700 - 0.6170	22	Gasem, 1986
n-C_{36}	373.15 - 423.15	0.524 - 5.878	0.0620 - 0.4590	16	Gasem, 1986
n-C_{44}	373.15 - 423.15	0.579 - 6.112	0.0800 - 0.5020	12	Gasem, 1986
Total Number of Points				328	

Table 2

The Database of Binary Systems Used in This Study – *continued*

	Methane				
Solvent	Temperature Range, K	Pressure Range, MPa	Solute Mole Fraction Range	NPTS	Reference
n-C_4	277.59 - 377.59	1.379 - 10.342	0.0256 - 0.4513	11	Wiese et al, 1970; Roberts et al, 1962
n-C_5	344.26 - 377.59	1.379 - 13.790	0.0279 - 0.5320	28	Prodany and Williams, 1971; Talyer et a;. 1939
n-C_6	298.33 - 373.33	1.014 - 10.135	0.0300 - 0.4125	37	Shim and Kohn, 1962
n-C_7	311.11 - 411.11	2.193 - 10.466	0.1000 - 0.4000	12	Reamer, 1956
n-C_8	298.33 - 423.33	1.013 - 7.093	0.0280 - 0.2870	28	Kohn and Bradish, 1964
n-C_9	323.15 - 423.15	1.014 - 10.135	0.0329 - 0.3471	39	Shipman and Kohn, 1966
n-C_{10}	310.93 - 410.93	1.043 - 8.647	0.0495 - 0.3080	32	Darwish et al., 1993
n-C_{16}	462.45 - 623.15	2.029 - 25.260	0.0801 - 0.5958	15	Lin et al., 1980
n-C_{20}	323.15 - 423.15	0.953 - 10.690	0.0512 - 0.3500	22	Darwish et al., 1993
n-C_{28}	348.15 - 423.15	0.926 - 7.092	0.0568 - 0.2992	18	Darwish et al., 1993
n-C_{36}	373.15 - 423.15	0.838 - 7.928	0.0511 - 0.3506	13	Darwish et al., 1993

Table 2

The Database of Binary Systems Used in This Study – *continued*

Methane - *continued*					
Solvent	Temperature Range, K	Pressure Range, MPa	Solute Mole Fraction Range	NPTS	Reference
n-C_{44}	373.15 - 423.15	0.677 - 5.572	0.0501 - 0.3112	15	Darwish et al., 1993
Total Number of Points				270	

Table 2

The Database of Binary Systems Used in This Study – *continued*

	Ethane				
Solvent	Temperature Range, K	Pressure Range, MPa	Solute Mole Fraction Range	NPTS	Reference
n-C_4	303.15 - 363.40	0.441 - 4.877	0.0440 - 0.8370	34	Lhotak and Wichterle, 1981
n-C_5	310.93 - 444.26	0.345 - 6.205	0.0048 - 0.8503	28	Reamer, 1960
n-C_6	310.93 - 394.26	0.393 - 5.399	0.0720 - 0.6519	48	Robinson and Gasem, 1987
n-C_7	338.71 - 449.82	3.923 - 7.598	0.2960 - 0.8480	8	Mehra and Thodos, 1965
n-C_8	323.15 - 373.15	0.405 - 5.269	0.0470 - 0.8630	31	Rodrigues et al., 1968
n-C_{10}	311.11 - 411.11	0.423 - 8.236	0.1050 - 0.6380	30	Bufkin, 1986
n-C_{16}	285.00 - 345.00	0.575 - 6.633	0.1990 - 0.8750	30	Goede, 1989
n-C_{20}	323.15 - 423.15	0.504 - 6.645	0.1180 - 0.6530	17	Robinson and Gasem, 1987
n-C_{24}	330.00 - 360.00	0.460 - 7.820	0.1197 - 0.7833	11	Peters, 1987
n-C_{28}	348.15 - 423.15	0.563 - 4.394	0.1020 - 0.5200	23	Robinson and Gasem, 1987
n-C_{36}	373.15 - 573.05	0.368 - 4.760	0.0870 - 0.5320	24	Robinson and Gasem, 1987; Tsai et al., 1987

Table 2

The Database of Binary Systems Used in This Study – *continued*

	Ethane - *continued*				
Solvent	Temperature Range, K	Pressure Range, MPa	Solute Mole Fraction Range	NPTS	Reference
n-C_{44}	373.15 - 423.15	0.387 - 3.170	0.0986 - 0.5161	16	Robinson and Gasem, 1987
Total Number of Points				300	

Table 3

Case Studies Employed to Evaluate Cubic Equation-of-State Predictions Using C_{ij} and D_{ij}

Case	Description
1. $C_{ij}=0$, $D_{ij}=0$	The simple quadratic mixing rules are used, without any interaction parameters
2. $C_{ij}(CN)$, $D_{ij}=0$	A single value of C_{ij} is determined for each binary system, no D_{ij} is used
3. $C_{ij}(CN, T)$, $D_{ij}=0$	A separate value of C_{ij} is determined for each temperature in a system, no D_{ij} used
4. $C_{ij}(CN)$, $D_{ij}(CN)$	Both C_{ij} and D_{ij} values are determined for each system
5. $C_{ij}(CN, T)$, $D_{ij}(CN, T)$	Both C_{ij} and D_{ij} are determined for each temperature in a system

Table 4

Case Studies Employed to Evaluate Cubic Equation-of-State Predictions Using N_{ij} and M_{ij}

Case	Description
1. $N_{ij}=0$, $M_{ij}=1$	The simple quadratic mixing rules are used, without any interaction parameters
2. $N_{ij}(CN)$, $M_{ij}=1$	A single value of N_{ij} is determined for each binary system, no M_{ij} is used
3. $N_{ij}(CN, T)$, $M_{ij}=1$	A separate value of N_{ij} is determined for each temperature in a system, no M_{ij} used
4. $N_{ij}(CN)$, $M_{ij}(CN)$	Both N_{ij} and M_{ij} values are determined for each system
5. $N_{ij}(CN, T)$, $M_{ij}(CN, T)$	Both N_{ij} and M_{ij} are determined for each temperature in a system

The summary results for the PR EOS using the new α function are given in Table 5 for all the systems as specified by Cases 1-5. Case 1, where the predictions are based solely on generalized pure-fluid parameters, represents the raw potential of the EOS. The overall EOS accuracy for the systems considered is within 14%. In Case 2, we use n-paraffin-dependent C_{ij} or $C_{ij}(CN)$. This is the commonly-used approach in most industrial applications. The results for this case show significant improvement over Case 1. This is expected since binary data are used to calibrate the EOS model. A %AAD of 3.1% is obtained for this case. In Case 4, both C_{ij} (CN) and D_{ij} (CN) are used simultaneously. Here, D_{ij} is used to account for molecular size effects, as was discussed by Gasem et al. (1985, 1986). The quality of EOS representation improves some, yielding an overall AAD of 2%. Similar results are observed when in Case 3 we employ temperature-dependent parameter, C_{ij} (CN, T). Finally, we consider Case 5, which represents the ultimate precision capability of the EOS. Two temperature-dependent parameters are used C_{ij} (CN, T) and D_{ij} (CN, T) to account for variations in solvent molecular size and temperature. The overall AAD for this case is within 1% for all the solutes considered. This level of representation reflects, to a large degree, the experimental imprecision.

As expected, the regression results from both the conformal and the classical combining rules are practically identical. However, the variations in the parameter values are more significant for C_{ij} in comparison with N_{ij}, as seen in Figure 2. The optimum interaction parameters for both the classical and conformal combining rules as specified by Case 2-5 are presented in Tables A.1-A.12, Appendix A. Also given in these tables are the detailed statistics for each binary mixture.

Table 5

Summary of Results for PR Equation-of-State Representations of the Bubble Point Pressure of the Selected Systems Using the New α Function

Case	Overall Results for C_{ij}, D_{ij}		Overall Results for N_{ij}, M_{ij}	
	%AAD	RMSE, bar	%AAD	RMSE, bar
		Hydrogen		
1	16.0	18.3	15.8	17.0
2	2.7	3.84	2.7	3.82
3	1.4	2.82	1.4	2.82
4	2.5	3.78	2.6	3.76
5	1.0	1.43*	0.9	1.37*
		Nitrogen		
1	23.1	33.4	23.1	33.4
2	2.9	4.33	3.2	4.76
3	1.9	2.96	1.8	2.74
4	2.4	3.35	2.5	3.66
5	0.9	1.38	0.8	1.35

* Difference in the parameter initialization methods leads to slightly different results.

Table 5

Summary of Results for PR Equation-of-State Representations of the Bubble Point Pressure of the Selected Systems Using the New α Function - *continued*

Case	Overall Results for C_{ij}, D_{ij}		Overall Results for N_{ij}, M_{ij}	
	%AAD	RMSE, bar	%AAD	RMSE, bar
		Carbon Monoxide		
1	8.4	5.94	8.4	5.94
2	3.1	2.36	3.2	2.44
3	1.6	1.41	1.2	1.35
4	2.8	2.00	2.7	1.97
5	0.7	0.59	0.6	0.54
		Carbon Dioxide		
1	23.4	10.5	23.6	11.9
2	4.1	2.33	4.2	2.36
3	2.7	1.83	2.7	1.79
4	2.9	1.29	3.0	1.30
5	1.1	0.82	0.9	0.48

Table 5

Summary of Results for PR Equation-of-State Representations of the Bubble Point Pressure of the Selected Systems Using the New α Function - *continued*

Case	Overall Results for C_{ij}, D_{ij}		Overall Results for N_{ij}, M_{ij}	
	%AAD	RMSE, bar	%AAD	RMSE, bar
		Methane		
1	7.1	4.55	6.8	4.53
2	2.2	2.04	2.2	2.04
3	1.6	1.99	1.6	1.99
4	1.8	1.08	1.7	1.05
5	0.5	0.44	0.5	0.43
		Ethane		
1	7.2	2.29	8.8	2.53
2	3.4	1.83	3.4	1.83
3	3.1	1.59	3.1	1.60
4	1.8	0.89	1.8	0.97
5	1.0	0.46	1.0	0.64

Table 5

Summary of Results for PR Equation-of-State Representations of the Bubble Point Pressure of the Selected Systems Using the New α Function - *continued*

	Overall Results for C_{ij}, D_{ij}		Overall Results for N_{ij}, M_{ij}	
Case	%AAD	RMSE, bar	%AAD	RMSE, bar
		Overall Results		
1	13.7	16.2	13.7	16.2
2	3.1	3.11	3.1	3.26
3	2.0	4.67	2.3	4.90
4	2.4	4.49	2.4	4.31
5	0.8	1.41	0.8	1.22

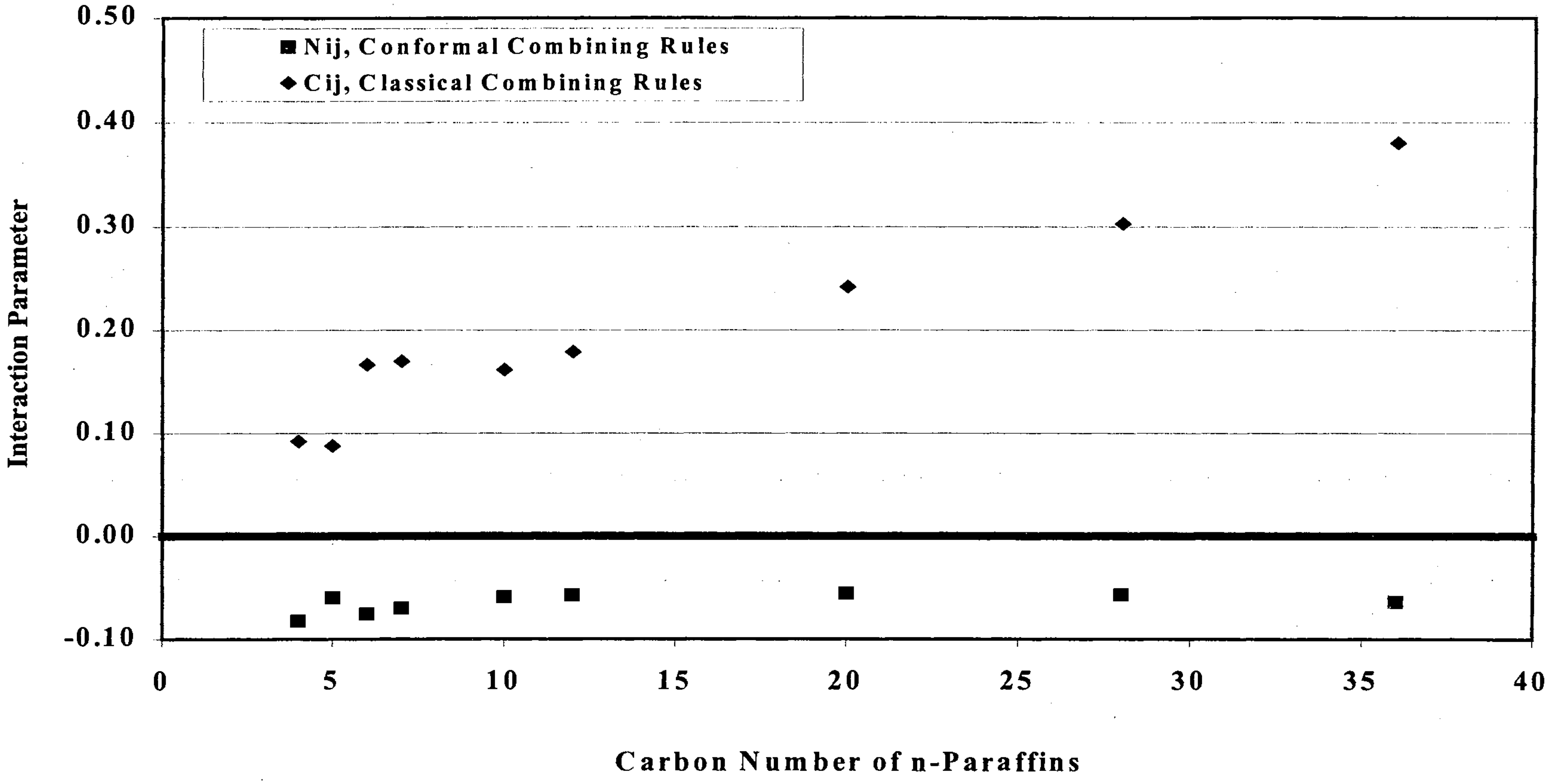

Figure 2. Comparisons of the Interaction Parameters from Classic Combining Rules and Conformal Combining Rules for Nitrogen + n-Paraffins.

Careful examination of the various cases described above leads us to believe that Case 2 provides the best opportunity for parameter generalizations. First, disallowing C_{ij}'s temperature dependence reduces the complexity of the generalized correlations with minor loss of accuracy (3% for Case 2 compared to 2% for Case 3). Second, using a single interaction parameter eliminates the parameter inter-correlation that invariably exists when using multiple parameters. Third, accuracy of 3-5% is adequate in many of the targeted industrial processes.

Tables 6 through 11 present the generalized correlations developed in this study. Specifically, generalized parameter correlations have been developed for the

1. PR EOS employing the new α function (Tables 6-7),
2. original PR EOS (Tables 8-9), and
3. SRK EOS (Tables 10-11).

In all cases, generalized correlations involving both the classical and the conformal combining rules are presented.

Careful evaluation of various correlation schemes for the interaction parameters indicated that acentric factor is a suitable correlating variable. Thus, the EOS parameters (C_{ij} / N_{ij}) for each solute are correlated in terms of the solvent acentric factor, ω. In general, linear correlations in ω or $1/\omega$ are employed. For all the models considered, the generalized predictions yield AAD from 3% for methane to 5% for CO_2 (RMSE of 1 to 6 bar, respectively). This level of accuracy represents about 50% more error than that obtained from the corresponding correlation case (Case 2). Both the classical and the conformal combining rules exhibit similar generalization capabilities, with NAAD $[(\%AAD)_{generalization} / (\%AAD)_{regression}]$ ranging from 1.1 to 1.6.

Table 6

Results of PR Equation-of-State Generalized Predictions of the Bubble Point Pressure of the Selected Systems Using the New α Function: C_{ij} and D_{ij} Approach

Systems	C_{ij}	D_{ij}	%AAD	RMSE bar	NAAD
H_2	$0.211 + 0.060\omega$	0	3.8	4.70	1.4
N_2	$0.045 + 0.231\omega$	0	3.4	5.84	1.2
CO	$0.001 + 0.107\omega$	0	3.7	3.29	1.2
CO_2	$0.139 - 0.062\omega$	0	5.5	2.58	1.3
CH_4	$0.053 - 0.063\omega$	0	2.9	1.97	1.3
C_2H_6	$0.035 - 0.072\omega$	0	5.0	2.00	1.5

Table 7

Results of PR Equation-of-State Generalized Predictions of the Bubble Point Pressure of the Selected Systems Using the New α Function: N_{ij} and M_{ij} Approach

Systems	N_{ij}	M_{ij}	%AAD	RMSE bar	NAAD
H_2	$-0.023 - 0.015/\omega$	1	3.6	4.76	1.3
N_2	-0.062	1	4.1	5.74	1.3
CO	-0.021	1	3.6	3.27	1.1
CO_2	$0.042 - 0.067/\omega$	1	5.3	2.50	1.2
CH_4	$0.017 - 0.014/\omega$	1	3.0	1.95	1.4
C_2H_6	$0.033 - 0.020/\omega$	1	4.6	2.0	1.4

Table 8

Results of PR Equation-of-State Generalized Predictions of the Bubble Point Pressure of the Selected Systems Using the Original α Function: C_{ij} and D_{ij} Approach

Systems	C_{ij}	D_{ij}	%AAD	RMSE bar	NAAD
H_2	$0.323 + 0.149\omega$	0	4.3	5.74	1.6
N_2	$0.044 + 0.284\omega$	0	2.9	4.87	1.1
CO	0.165ω	0	3.4	3.12	1.1
CO_2	$0.141 - 0.059\omega$	0	5.2	2.51	1.3
CH_4	$0.048 - 0.033\omega$	0	3.0	2.10	1.3
C_2H_6	$0.017 - 0.047\omega$	0	5.0	2.11	1.6

Table 9

Results of PR Equation-of-State Generalized Predictions of the Bubble Point Pressure of the Selected Systems Using the Original α Function: N_{ij} and M_{ij} Approach

Systems	N_{ij}	M_{ij}	%AAD	RMSE bar	NAAD
H_2	$-0.060 - 0.029/\omega$	1	4.4	6.45	1.6
N_2	-0.076	1	3.7	4.71	1.5
CO	-0.032	1	3.4	3.14	1.1
CO_2	$0.038 - 0.066/\omega$	1	5.2	2.77	1.3
CH_4	$0.010 - 0.014/\omega$	1	3.0	2.10	1.3
C_2H_6	$0.034 - 0.022/\omega$	1	4.8	2.03	1.5

Table 10

Results of SRK Equation-of-State Generalized Predictions of the Bubble Point Pressure of the Selected Systems: C_{ij} and D_{ij} Approach

Systems	C_{ij}	D_{ij}	%AAD	RMSE bar	NAAD
H_2	$0.359 + 0.173\omega$	0	4.7	6.21	1.7
N_2	$0.032 + 0.314\omega$	0	2.8	4.51	1.2
CO	$-0.019 + 0.176\omega$	0	3.4	2.76	1.1
CO_2	$0.146 - 0.045\omega$	0	4.8	2.41	1.1
CH_4	$0.009 + 0.009\omega$	0	3.0	2.23	1.3
C_2H_6	$0.013 - 0.040\omega$	0	4.8	2.11	1.4

Table 11

Results of SRK Equation-of-State Generalized Predictions of the Bubble Point Pressure of the Selected Systems: N_{ij} and M_{ij} Approach

Systems	N_{ij}	M_{ij}	%AAD	RMSE, bar	NAAD
H_2	$-0.064 - 0.023/\omega$	1	4.8	6.41	1.6
N_2	-0.071	1	3.1	4.98	1.2
CO	-0.028	1	3.5	3.42	1.1
CO_2	$0.033 - 0.066/\omega$	1	4.8	2.60	1.1
CH_4	$0.007 - 0.011/\omega$	1	3.1	2.14	1.3
C_2H_6	$0.027 - 0.019/\omega$	1	4.8	1.98	1.4

Figure 3 depicts the generalized correlations for the various solutes in comparison with the regressed parameters of Case 2. This figure presents only the results for the conformal combining rule using the new PR EOS α function. As illustrated, the current generalizations reproduce the regressed parameters reasonably well.

DISCUSSION

The conformal combining rule offers a clear interpretation for the numerical values of binary interaction parameter. As illustrated in Figure 4, variation in the value of N_{ij} indicates differences in the operative combining rule. For the asymmetric mixtures considered, the regressed values of N_{ij} indicate that using the geometric-mean combining rule for 'a' is suitable, with the possible exception of CO_2. Moreover, the majority of the mixtures have small negative N_{ij} values (corresponding to positive C_{ij} values), which signifies a leaning toward the Halsey-Fender combining rule. So, beyond the benefit of having a flexible combining rule, we gain some insight of how the unlike molecules are interacting. For example, previous concerns about using large values of C_{ij} ($C_{ij} > 0.2$) can be alleviated, knowing that large C_{ij} values indicate unlike molecule combinations representative of both the geometric-mean and the Halsey-Fender rules.

The present efforts to improve CEOS predictions for asymmetric mixtures have been effective in many regards, including developing

1. accurate correlations for predicting the heavy n-paraffin critical properties and acentric factors,
2. improved temperature-dependence α function for the PR EOS to predict accurately vapor pressures of heavy hydrocarbons,

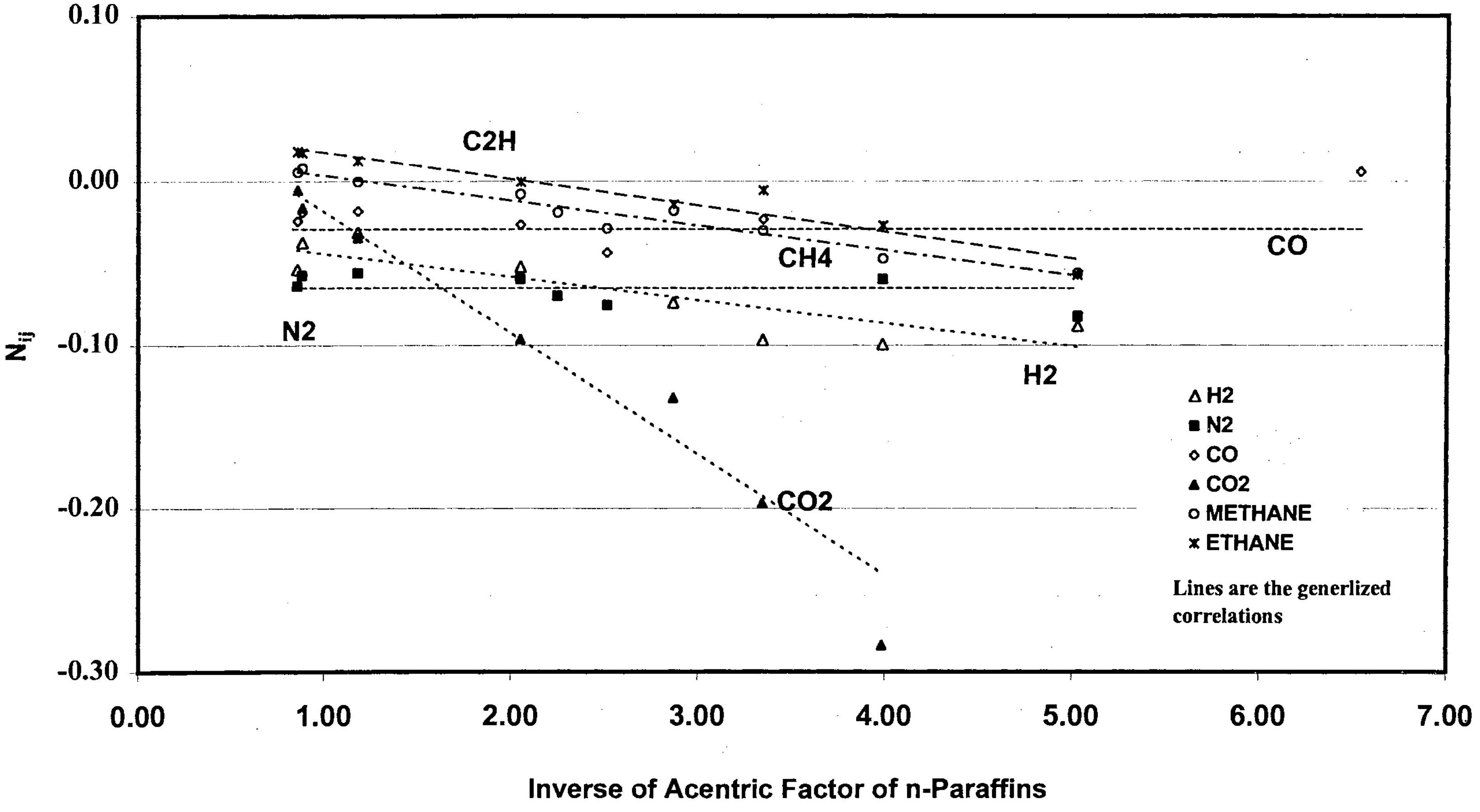

Figure 3. Generalized Parameters for the Asymmetric Mixtures Considered.

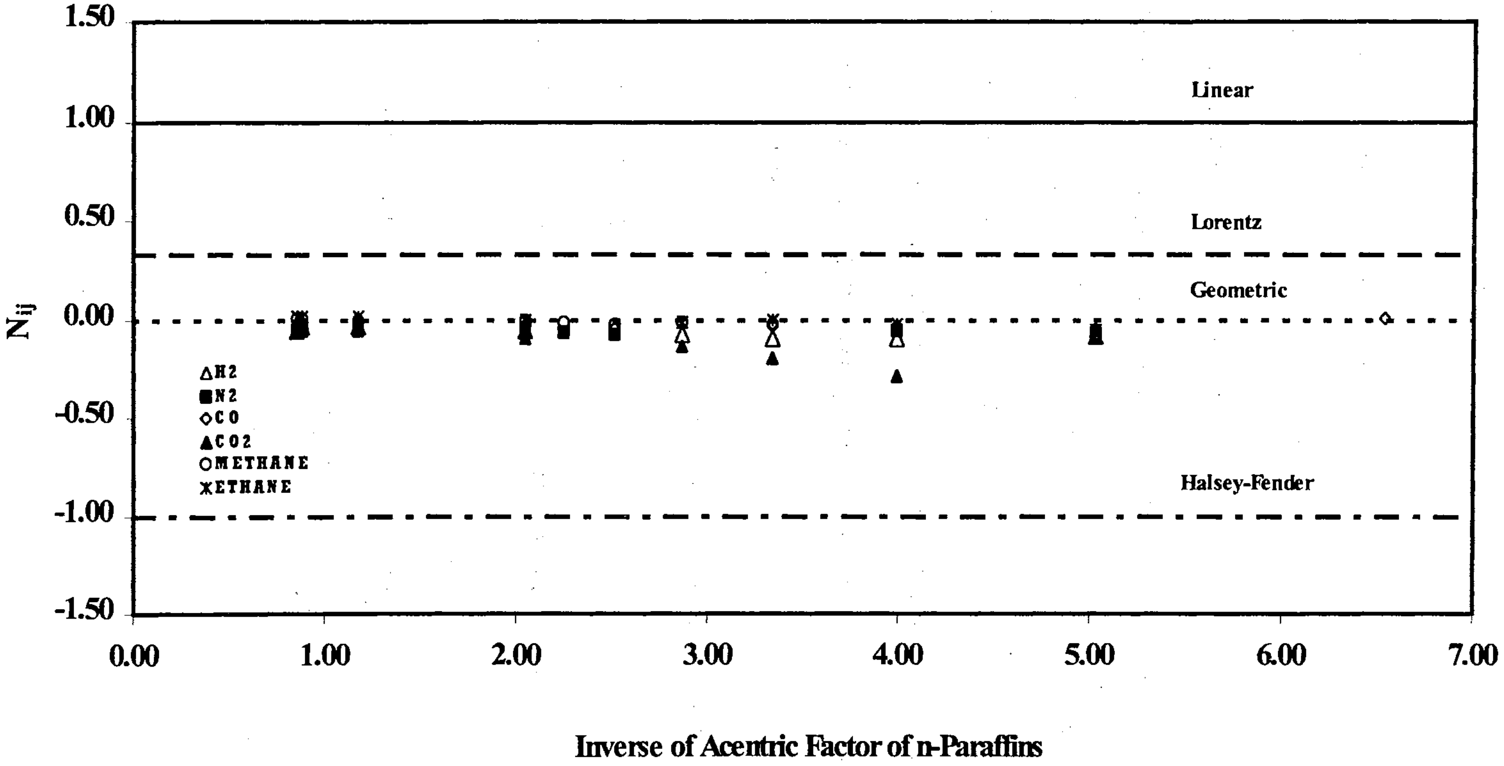

Figure 4. Comparison of Equation-of-State Combining Rules.

3. an alternate EOS combining rule, and
4. useful generalized-parameter correlations for two widely-used EOS.

More importantly, this study delineated several issues relating to the merits of using CEOS for asymmetric mixtures and their capability to represent such systems. First, our results clearly indicate that the accuracy of the pure-component predictions has only a moderate impact on the quality of EOS representation of mixtures involving supercritical components; that is, the advantages of having accurate vapor pressure predictions and appropriate liming behavior for the supercritical components are outweighed by the deficiencies of the mixing rules used. The nitrogen binaries provide a good example for this situation. Although, our current PR EOS predicts the vapor pressures of all components accurately and the compressibility factors of nitrogen equally well (AAD of 1-2%), the *a priori* predictions for the binary data yield over 20% average error. These results strongly suggest that additional studies are required to improve the mixing rules for asymmetric mixtures. Second, the attraction for using the simple CEOS should not mask our need to develop theoretically-based EOS models. The desire to associate physically-meaningful interpretation to EOS model parameters is dependent on our ability to develop EOS models based on sound theory, which accounts in fundamental terms for the molecular interactions.

SUMMARY

Following the work of Juris and Wenzel (1974), an alternate combining rule is proposed for the CEOS. The SRK and PR EOS have been used to assess the proposed combining rule, in comparison with the classical rules. Specifically, a study was undertaken to evaluate the predictive capability of both equations in representing the vapor-liquid equilibrium properties of asymmetric binary mixtures, involving methane, ethane, nitrogen, hydrogen, CO and CO_2 in the n-paraffins (C_4 – C_{44}).

EOS binary interaction parameters generated by the proposed combination rule are presented for the systems considered. The quality of the EOS representation is dependent on the level of complexity applied in the parameter regressions. Overall, AAD of 1 to 3% are realized from the various regression scenarios.

In addition, generalized EOS parameter correlations for system-dependent parameters have been developed. These interaction parameters represent the solubilities of the selected systems within 5 %.

CHAPTER 7

CONCLUSIONS AND RECOMMENDATIONS

The conclusions drawn in study are presented for each topic separately in the Summary sections of Chapters 2, 4-6.

Based on the studies conducted, the following recommendations are made:

1. Develop a new experimental facility which is (a) free of mercury, (b) fully automated, and (c) capable of providing phase density measurements.
2. Conduct experiments on selected ternary systems.
3. Develop techniques for measuring the critical properties of heavy hydrocarbons.
4. Conduct molecular simulations to improve our understanding of the limiting behavior of critical properties.
5. Test the viability of the new PR α functions in representing mixtures containing only subcritical components.
6. Evaluate the quality of derivative-property predictions using the new PR α function.
7. Develop improved mixing rules for the cubic equations of state.
8. Direct more modeling efforts to theoretically-based equations of state.

REFERENCES

1. Akers, W. W.; Attwell, L. L.; Robinson, J. A. Volumetric and Phase Behavior of Nitrogen-Hydrocarbon System: Nitrogen-Butane System. *Ind. Eng. Chem.*, **1954**, *46*, 2539-2540.

2. Ambrose, D. The Correlation and Estimation of Vapor Pressures V. Observations on Wagner's Method of Fitting Equations to Vapor Pressures. *J. Chem. Thermodyn.*, **1986**, *18*, 45-51.

3. Ambrose, D.; Tsonopoulos C. Vapor-Liquid Critical Properties of Elements and Compounds. 2. Normal Alkanes. *J. Chem. Eng. Data,* **1995**, *40*, 531-546.

4. Androulakis, I. P.; Kalospiros, N. S.; Tassios, D. P. Thermophysical Properties of Pure Polar and Nonpolar Compounds with a Modified VdW-711 Equation of State. *Fluid Phase Equilib.*, **1989**, *45*, 135-163.

5. Boston, J. F.; Mathias, P., M. The Preceedings of the 2nd International Conference on Phase Equilibria and Fluid Properties in the Chemical Process Industries, West Berlin, March 1980, 823-849.

6. Boukouvalas, C.; Spiliotis, N.; Coutsikos, P.; Tzouvaraz, N.; Tassios, D. Predictions of Vapor-Liquid Equilibrium with the LCVM model: A Linear Combination of the Vidal and Michelsen Mixing Rules Coupled with the Original UNIFC and the t-mPR Equation of State. *Fluid Phase Equilib.*, **1994**, *92*, 75-82.

7. Brown, T. S.; Niesen, V. G.; Sloan, E. D.; Kidnay, A. J. Vapor-Liquid Equilibria for the Binary Systems of Nitrogen, Carbon Dioxide and n-Butane at Temperatures from 220 to 344 K. *Fluid Phase Equilib.*, **1989**, *53*, 7-14.

8. Bufkin, B. *High Pressure Solubilities of Carbon Dioxide and Ethane in Selected Paraffinic, Naphthenic and Aromatic Solvents.* M.S. Thesis. Oklahoma State University, Stillwater, OK., 1986.

9. Carrier, B.; Rogalski, M.; Peneloux, A. Correlation and Prediction of Physical Properties of Hydrocarbons with the Modified Peng-Robinson Equation of State. 1. Low and Medium Vapor Pressures, *Ind. Eng. Chem. Res.*, **1988**, *27*, 1714-1718.

10. Chapman, W. G.; Gubbins, K. E.; Jackson, G.; Radosz, M. New Reference Equation of State for Associating Liquids. *Ind. Eng. Chem. Res.*, **1990**, *29*, 1709-1721.

11. Cheng, H.; de Fernandez, P. M. E.; Zollweg, J. A.; Streett., W. B. Vapor-Liquid Equilibria in the System Carbon Dioxide + n-Pentane from 252 to 458 K at Pressures to 10 MPa. *J. Chem. Eng. Data,* **1989**, *34*, 319-323.

12. Connolly, J. F.; Kandalic, G. A. Thermodynamic Properties of Dilute Solutions of Carbon Monoxide in a Hydrocarbon. *J. Chem. Thermodyn.*, **1984**, *16*, 1129-1139.

13. Constantinou, L.; Gani, R.; O'Connel, J. P. Estimation of the Acentric Factor and the Liquid Molar Volume at 298 K Using a New Group Contribution Method. *Fluid Phase Equilib.*, **1995**, *103*, 11-22.

14. Danesh, A.; Xu, D. H.; Tehrani, D, H.; Todd, A. C. Improving Predictions of Equation of State by Modifying Its Parameters for Supercritical Components of Hydrogen Reservoir Fluids. *Fluid Phase Equilib.*, **1995**, *112*, 45-61.

15. Darwish, N. A.; Fathikalajahi, J.; Gasem, K. A. M.; Robinson, R. L., Jr. Solubility of Methane in Heavy Normal Paraffins at Temperatures from 323 to 423 K and Pressures to 10.7 MPa. *J. Chem. Eng. Data,* **1993**, *38*, 44-48.

16. Ely, H. F.; Hanley, H. J. M., NBS Technical Note, 1981, 1039-1050.

17. Eubank, P. T.; Shyu, G. S.; Hanif, N. S. M. New Procedures for Application of the Wong-Sandler Mixing Rules to the Prediction of Vapor-Liquid Equilibria. *Ind. Eng. Chem.* Res., **1995**, *34*, 314-323.

18. Fall, D. J.; Fall, J. L.; Luks, K. D. Liquid-Liquid-Vapor Immiscibility Limits in Carbon Dioxide + n-Paraffin Mixtures. *J. Chem. Eng. Data,* **1985**, *30*, 82-88.

19. Fall, D. J.; Fall, J. L.; Luks, K. D. Phase Equilibria Behavior of the Systems Carbon Dioxide + n-Dotriacontane and Carbon Dioxide + n-Docosane. *J. Chem. Eng. Data,* **1984**, *29*, 413-417.

20. Flory, P. J.; Orwoll, R. A.; Vrij, A. Statistical Thermodynamics of Chain Molecule Liquids. I. An Equation of State for Normal Paraffin Hydrocarbon. *J. Am. Chem. Soc.*, **1964**, *86*, 3507-3514.

21. Floter, E.; Loos, T. W. D.; Arons, J. D. S. Improved Modeling of the Phase Behavior of Asymmetric Hydrocarbon Mixtures with the Peng-Robinson Equation of State Using a Different Temperature Dependency of the Parameter 'a'. *Ind. Eng. Chem. Res.*, **1998**, *37*, 1651-1662.

22. Freitag, N. P.; Robinson, D. B. Equilibrium Phase Properties of the Hydrogen-Methane-Carbon dioxide, Hydrogen-Carbon Dioxide-n-Pentane and Hydrogen-n-Pentane Systems. *Fluid Phase Equilib.*, **1986,** *31,* 183-201.

23. Gao, W.; Gasem, K. A. M.; Robinson, R. L., Jr. Solubilities of Nitrogen in Selected Naphthenic and Aromatic Hydrocarbons at Temperatures from 344 to 433 K and Pressures to 22.8 MPa. *J. Chem. Eng. Data,* **1999**, *44*, 185-189.

24. Gao, W.; Gasem, K. A. M.; Robinson, R. L., Jr. Updated ABC Model for the Prediction of Heavy N-Paraffins Physical Properties, Submitted to Fluid Phase Equilib., **1999**a.

25. Gao, W.; Gasem, K. A. M.; Robinson, R. L., Jr. Modifying the Temperature Dependence of the Peng-Robinson Equation of State, Submitted to Fluid Phase Equilib., **1999**b.

26. Gao, W.; Gasem K. A. M.; Robinson R. L., Jr. Alternate Combining Rules and Parameter Generalizations for Asymmetric Mixtures, Submitted to Fluid Phase Equilib., **1999**c.

27. Gasem, K. A. M. *Binary Vapor-Liquid Phase Equilibrium for Carbon Dioxide + Heavy Normal Paraffins*. Ph.D. Dissertation, Oklahoma State University, Stillwater, OK, **1986**.

28. Gasem, K. A. M., Robinson, R. L., Jr. *Phase Behavior of Light Gases in Hydrocarbon and Aqueous Solvents*. DOE Proposal, **1995**.

29. Gasem, K. A. M.; Ross, C. H.; Robinson, R. L. Jr. Prediction of Ethane and CO2 Solubilities in Heavy Normal Paraffins Using Generalized-Parameters Soave and Peng-Robinson Equations of State. *Can. J. Chem. Eng*., **1993**, *71*, 805-816.

30. Goede, R.; Peters, C. J.; Kooi, H. J. V. D.; Lichtenthaler R.N. Phase Equilibria in Binary Mixtures of Ethane and Hexadecane. *Fluid Phase Equilib*., **1989**, *50*, 305-314.

31. Harismiadis, V. I.; Panagiotopoulos, A. Z.; Tassios, D. P. Phase Equilibria of Binary Lennard-Jones Mixtures with Cubic Equations of State. *Fluid Phase Equilib*., **1994**, *94*, 1-18.

32. Harmens, A.; Knapp, H.; Three Parameter Cubic Equation of State for Normal Fluids. *Ind. Eng. Chem. Fund*., **1980**, *19*, 291-294.

33. Heyen, G.; In Proceedings of the 2nd International Conference on Phase Equilibria and Fluid Properties in the Chemical Industry, DECHEMA, Frankfurt/Main, **1980**, 9-13.

34. Hoshino, D.; Nagahama, K.; Hirata, M. Prediction of Acentric Factor of Alkanes by the Group Contribution Method. *J. Chem. Eng. Japan,* **1982**, *15*, 13-15.

35. Juris, K.; Wenzel, L. A. Joule-Thomson Effects in CF_4-CHF_3 Mixtures, *AIChE Symposium Series*, **1974**, *70*, 70-79.

36. Kalra, H.; Kubota, H.; Robinson, D. B.; Ng, H. Equilibrium Phase Properties of the Carbon Dioxide-n-Heptane System. *J. Chem. Eng. Data,* **1978**, *23*, 317-321.

37. Kalra, H.; Robinson, D. B.; Besserer, G. J. The Equilibrium Phase Properties of the Nitrogen-n-Pentane System. *J. Chem. Eng. Data,* **1977,** *22,* 215-218.

38. Kim, C. H.; Vimalchand, P.; Donohue, M.D.; Sandler, S.I. Local Composition Model for Chainlike Molecules: A New Simplified Version of the Perturbed Hard Chain Theory. *AIChE J.*, **1986**, *32*, 1726.

39. Kim, H.; Lin, H.; Chao, K. C. Vapor-Liquid Equilibrium in Binary Mixtures of Carbon Dioxide + n-PropylCyclohexane and Carbon Dioxide + n-Octadecane. *AIChE Symp. Ser.*, **1985**, *81*, 96-101.

40. Klink, A. E.; Cheh, H. Y.; Amick, E. H., Jr. The Vapor-Liquid Equilibrium of the Hydrogen - n-Butane System at Elevated Pressures. *AIChE J.*, **1975**, *21*, 1142-1148.

41. Kohn, J. P.; Bradish, W. F. Multiphase and Volumetric Equilibria of the Methane-n-Octane System at Temperatures between -1100 and 1500 C. *J. Chem. Eng. Data,* **1964,** *9,* 5-8.

42. Kordas, A.; Magoulas, K.; Stamataki, S.; Tassios, D. Methane-Hydrocarbon Interaction Parameters Correlation for the Peng-Robinson and the t-mPR Equation of State. *Fluid Phase Equilib.*, **1995**, *112*, 33-44.

43. Kordas, A.; Tsoutsouras, K.; Stamataki, S.; Tassios, D. Generalized Correlation for the Interaction Coefficients of CO2-Hydrocarbon Binary Mixtures. *Fluid Phase Equilib.*, **1994**, *93*, 141-166.

44. Kreglewski, A.; Zwolinski, B. J. Vapor Pressures and Boiling Points of Normal Alkanes, C_{21} to C_{100}. *J. Chem. Eng. Data*, **1966**, *11*, 253-255.

45. Kudcgadker, A. P.; Alani, G. H.; Zwolinski, B. J. Critical Constants of Organic Substances. *Chem. Rev.*, **1986**, *68*, 723-725.

46. Kurata, M.; Isida, S. Theory of Normal Paraffins Liquids. *J. Chem. Phys.*, **1955**, *23*, 1126-1131.

47. Lhotak, V.; Wichterle, I. Vapor-Liquid Equilibrium in the Ethane-n-Butane System at High Pressures. *Fluid Phase Equilib.*, **1981**, *6*, 229-235.

48. Lin, H. M.; Sebastian, H. M.; Chao, K. C. Gas-Liquid Equilibrium in Hydrogen + n-Hexadecane and Methane + n-Hexadecane at Elevated Temperatures and Pressures. *J. Chem. Eng. Data,* **1980,** *25*, 252-254.

49. Llave, F. M.; Chung, T. H. Vapor-Liquid Equilibrium of Nitrogen-Hydrocarbon Systems at Elevated Pressures. *J. Chem. Eng. Data,* **1988,** *33*, 123-128.

50. Magoulas, C.; Tassios, D. Thermophysical Properties of n-Alkanes from C_1 to C_{20} and Their Prediction for Higher Ones. *Fluid Phase Equilib.*, **1990**, *56*, 119-140.

51. Mansoori, A. G. Mxing Rules for Cubic Equation of State. In: Chao, K.C.; Robinson, Jr., R.L., ed. Equation of State: theories and applications. Washington, D.C.: American Chemical Society. **1986**, 314-330.

52. Mansoori, A. G. Radial Distribution Functions and Their Role in Modeling of Mixtures Behavior. *Fluid Phase Equilib.*, **1993**, *87*, 1-22.

53. Marano, J.J.; Holder, G.D. A General Equatuion for Correlating the Thermophysical Properties of n-paraffins, n-olefins, and other homologous series: I. Formalism for Developing Asymptotic Behavior Correlations. *Ind. Eng. Chem. Res.*, **1997**, *36*, 1887-1894.

54. Mathias, P. M. A Versatile Phase Equilibrium Equation of State. *Ind. Eng. Chem. Pro. Design Dev.*, **1983**, *22*, 385-391.

55. Mathias, P.M.; Copeman, T.W. Extension of the Peng-Robinson Equation of State to Complex Mixtures: Evaluation of the Various Forms of the Local Composition Concept. *Fluid Phase Equilib.*, **1983**, *13*, 91-108.

56. Mehra, V. S.; Thodos, G. Vapor-Liquid Equilibrium in the Ethane-n-Heptane System. *J. Chem. Eng. Data,* **1965**, *10*, 211-214.

57. Melham, G.H.; Siani, R.; Goodwin, G.M. A Modified Peng-Robinsion Equation of State. *Fluid Phase Equilib.*, **1989**, *47*, 189.

58. Morgan, D.L.; Kobayashi, R. Direct Vapor Pressure Measurements of Ten n-Alkanes in the C10-C28 range. *Fluid Phase Equilib.,* **1994**, *97*, 211-242.

59. Nichols, W. B.; Reamer, H. H.; Sage, B. H. Volumetric and Phase Behavior in the Hydrogen-n-Hexane System, *AIChE J.*, **1957**, *3,* 262-267.

60. Nikitin, E. D.; Pavlov, P. A.; Bessonova, N.V. *J. Chem. Thermodyn.*, **1994**, *26*, 177-182.

61. Nikitin, E. D.; Pavlov, P. A.; Popov, A. P. Vapor-Liquid Critical Temperatures and Pressures of Normal Alkanes with from 19 to 36 Carbon Atoms, Naphthalene and m-Terphenyl Determined by the Pulse-Heating Technique. *Fluid Phase Equilib.*, **1997**, *141*, 155-164.

62. Nishiumi, H.; Arai, T. Generalization of the Binary Interacion Parameter of the Peng-Robinson Equation of State by Component Family. *Fluid Phase Equilib.*, **1988**, *42*, 43-62.

63. Ohgaki, K.; Katayama, T. Isothermal Vapor-Liquid Equilibrium Data for Binary Systems Containing Carbon Dioxide at High Pressures: Methanol-Carbon Dioxide, n-Hexane-Carbon Dioxide, and Benzene-Carbon Dioxide Systems. *J. Chem. Eng. Data,* **1976**, *21*, 53-55.

64. Orbey, H.; Sandler, S. I. Reformulation of Wong-Sandler Mixing Rule for Cubic Equations of State. *AIChE J.*, **1995**, *41*, 683-690.

65. Panagiotopoulos, A. Z.; Reid, R. C. New Mixing Rules for Cubic Equations of State for Highly Polar Asymmetric Mixtures. *Fluid Phase Equilib.*, **1986**, *29*, 525-534.

66. Park, J.; Robinson, R. L., Jr., Gasem, K. A. M. Solubilities of Hydrogen in Heavy Normal Paraffins at Temperatures from 323.2 to 423.2 K and Pressures to 17.4 MPa. *J. Chem. Eng. Data,* **1995**, *40*, 241-244.

67. Park, J.; Robinson, R. L., Jr., Gasem, K. A. M. Solubilities of Hydrogen in Aromatic Hydrocarbons from 323 to 433 K and Pressures to 21.7 MPa. *J. Chem. Eng. Data,* **1995**, *40,* 70-73.

68. Peng, D. Y.; Robinson, D. B. A New Two-Constant Equation of State. *Ind. Eng. Chem. Fundam.* **1976**, *15*, 59-64.

69. Peter, S.; Reinhartz, K. The Phase Equilibria of the System Hydrogen-n-Heptane, Hydrogen-Methylcyclohexane and Hydrogen-2,2,4-Trimethylpentane at Higher Pressure and Temperature. *Zeit. fur. Phys. Chem.* **1960**, *24*, 103-119.

70. Peters, C. J.; Kooi, V. D. H. J.; Arons, D. S. J. Measurements and Calculations of Phase Equilibria for Ethane +Tetracosane and p, V, T of Liquid Tetracosane. *J. Chem. Thermodyn.*, **1987**, *19*, 395-405.

71. Prodany, N. W.; Williams, B. Vapor-Liquid Equilibria in Methane-Hydrocarbon Systems. *J. Chem. Eng. Data*, **1971**, *16*, 1-6.

72. Reamer, H. H.; Sage, B. H. Phase Equilibria in Hydrocarbon Systems. Volumetric and Phase Behavior of the n-Decane-CO2 System. *J. Chem. Eng. Data,* **1963**, *8*, 508-513.

73. Reamer, H. H.; Sage, B. H.; Lacey, W. N. Volumetric and Phase Behavior of the Methane-n-Heptane System. *Chem. Eng. Data Ser.*, **1956**, *1*, 29-42.

74. Reamer, H. H.; Sage, B. H.; Lacey, W.N. Phase Equilibria in Hydrocarbon Systems. Volumetric and Phase Behavior of Ethane-n-Pentane System *J. Chem. Eng. Data,* **1960**, *5*, 44-50.

75. Redlich, O.; Kwong, J. N. S. On Thermodynamics os Solutions V: An Equation of State. Fugacities of Gaseous Solutions. *Chem. Rev.*, **1949**, *44*, 233-244.

76. Reid, R. C.; Prausnitz, J. M.; Poling, B. E. The Properties of Gases and Liquids, 4th ed. McGraw-Hill, New York, **1987**.

77. Riazi, M.R.; Al-Sahhaf, T.A.; Al-Shammari, M.A. A Generalized Method for Estimation of Critical Constants. *Fluid Phase Equilib.*, **1998**, *147*, 1-6.

78. Rijkers, M. P. W. M. Ph.D. Dissertation, TU Deft, Delft, **1991**.

79. Roberts, L. R.; Wang, R. H.; Azarnoosh, A.; McKetta, J. J. Methane-n-Butane System in the Two-Phase Region. *J. Chem. Eng. Data,* **1962**, *7*, 484-485.

80. Robinson, R. L., Jr.; Gasem, K. A. M. Phase Behavior of Coal Fluids: Data for Correlation Development. DE-FG22-83PC60039-12, Final Report, Department of Energy. **1987**.

81. Rodrigues, A. B. J.; McCaffrey, D. S., Jr.; Kohn, J. P. Heterogeneous Phase and Volumetric Equilibrium in the Ethane-n-Octane System. *J. Chem. Eng. Data,* **1968**, *13*, 164-168.

82. Row, K. H. *Evaluation of the Modified Park-Gasem-Robinson Equation of State and Calculation of Calorimetric Properties Using Equations Of State*. Ph.D. Dissertation. Oklahoma State University, Stillwater, OK, **1998**.

83. Sandler, S. I. The Generalized van der Waals Partition. I. Basic Theory. *Fluid Phase Equilib.*, **1985**, *19*, 233-239.

84. Schwartzentruber, J.; Renon, H.; Watanasiri, S. User-Friendly Equation of State *Chem. Eng.*, **1990**, *3*, 118-124.

85. Sebastian, H. M.; Simnick, J. J.; Lin, H.; Chao, K. C. Vapor-Liquid Equilibrium in Binary Mixtures of Carbon Dioxide + n-Decane and Carbon Dioxide + n-Hexadecane. *J. Chem. Eng. Data,* **1980**, *25*, 138-140.

86. Shaver, R. D.; Robinson, R. L. Jr.; Gasem, K. A. M. Modified SPHCT EOS for Improved Predictions of Equilibrium and Volumetric Properties of Pure Fluids. *Fluid Phase Equilib.*, **1995**, *112*, 223-235.

87. Shaver, R. D.; Robinson, R. L., Jr.; Gasem, K. A. M. Framework for the prediction of saturation properties. Vapor pressures. *Fluid Phase Equilib.*, **1991**, *64*, 141-163.

88. Shibate, S. K.; Sandler, S. L. High-Pressure Vapor-Liquid Equilibria of Mixtures of Nitrogen, Carbon Dioxide and Cyclohexane. *J. Chem. Eng. Data,* **1989**, *34*, 419-424.

89. Shim, J.; Kohn, J. P. Multiphase and Volumetric Equilibria of Methane-n-Hexane Binary System at Temperatures between 1100 and 1500 C. *J. Chem. Eng. Data,* **1962**, *7*, 3-8.

90. Shipman, L. M.; Kohn, J. P. Heterogeneous Phase and Volumetric Equilibrium in the Methane-n-Nonane System. *J. Chem. Eng. Data,* **1966**, *11*, 176-180.

91. Simmrock, K. H.; Janowsky, R.; Ohnsorge, A. Critical Data of Pure Substances. DECHEMA Chemistry series, Vol. II., **1986**.

92. Soave, G. Application of the Redlich-Kwong-Soave Equation of State to Solid-Liquid Equilibria Calculations. *Chem. Eng. Sci.*, **1979**, *34*, 225-229.

93. Soave, G. Equilibrium Constants from a Modified Redlich-Kwong Equation of State. *Chem. Eng. Sci.,* **1972**, *27*, 1197-1203.

94. Soave, G. Improvements of the van der Waals Equations of State. *Chem. Eng. Sci.*, **1984**, *39*, 357-369.

95. Soave, G. Improving the Treatment of Heavy Hydrocarbons by the SRK EOS *Fluid Phase Equilib.*, **1993**, *84*, 339-342.

96. Srivatsan, S.; Yi, X.; Robinson, Jr., R. L.; Gasem, K. A. M. Solubilities of Carbon Monoxide in Heavy Normal Paraffins at Temperatures from 311 to 423 K and Pressures to 10.2 MPa. *J. Chem. Eng. Data,* **1995**, *40*, 237-240.

97. Stryjek, R.; Vera, J. H. PRSV - An Improved Peng-Robinson Equation of State with New Mixing Rules for Strongly Nonideal Mixtures. *Can. J. Chem. Eng.*, **1986**, *64*, 334-340.

98. Stryjek, R.; Vera, J.H. PRSV: An Improved Peng-Robinson Equation of State for Pure Compounds and Mixtures. *Can. J. Chem. Eng.* **1986**, *64*, 323-333.

99. Sudibandriyo, M. *Improved Methods for Phase Density Predictions: CO_2 + Hydrocarbons*. M.S. Thesis. Oklahoma State University. Stillwater, OK., **1991**.

100. Teja, A.S.; Lee, R. J.; Rosenthal, D.; Anselme, M. Correlation of the Critical Properties Alkanes and Alkanols. *Fluid Phase Equilib.*, **1990**, *56*, 153-169.

101. Tong, J. *Solubility Data for Nitrogen in n-Paraffins and Equation-of-State Methods to Describe Light Gas Solubilities in Hydrocarbons*. M.S. Thesis. Oklahoma State University, Stillwater, OK, **1994**.

102. Tong, J.; Gao, W.; Gasem, K. A. M.; Robinson, R. L., Jr. Solubilities of Nitrogen in Heavy Normal Paraffins from 323 to 423 K at Pressures to 18.0 MPa. *J. Chem. Eng. Data,* **1999**, *44*, 784-787.

103. Trebbe, M. A.; Bishnoi, P. R. Accuracy and Consistency Comparisons of Ten Cubic Equations of State ofr Polar and Non-Polar Compounds. *Fluid Phase Equilib.*, **1986**, *29*, 465-474.

104. Trivedi, N. *A New Framework for Vapor-Liquid Equilibrium Calculations*. M.S. Thesis. Oklahoma State University. Stillwater, OK., **1996**.

105. Trust, D. B.; Kurata, F. Vapor-Liquid and Liquid-Liquid Vapor Phase Behavior of the Carbon Monoxide-Propane and the Carbon Monoxide-Ethane Systems *AIChE J.*, **1971**, *17*, 415-419.

106. Tsai, F.; Huang, S. H.; Lin, H.; Chao, K. C. Solubility of Methane, Ethane, Carbon Dioxide in n-Hexatriacontane. *J. Chem. Eng. Data*, **1987**, *32*, 467-469.

107. Tsai, F.; Yau, J. Solubility of Carbon Dioxide in n-Tetracosane and in n-Dotriacontane. *J. Chem. Eng. Data,* **1990,** *35,* 43-45.

108. Tsonopoulos, C. Critical Constants of Normal Alkanes from Methane to Polyethylene. *AIChE J.*, **1987**, *33*, 2080-2083.

109. Twu, C. H.; Bluck, D.; Cunningham, J. R.; Coon, J. E. A Cubic Equation of State with a New Alpha Function and a New Mixing Rule. *Fluid Phase Equilib.*, **1991**, *69*, 33-50.

110. Twu, C.H.; Coon, J.E.; Cunnungham, J.R. A New Generalized Alpha Function for a Cubic Equation of State. Part I. Peng-Robinson Equation. *Fluid Phase Equilib.*, **1995**, *105*, 49-61.

111. Twu, C.H.; Coon, J.E.; Cunnungham, J.R. A New Generalized Alpha Function for a Cubic Equation of State. Part II. Soave-Redlich-Kuong Equation. *Fluid Phase Equilib.*, **1995**, *105*, 61-69.

112. Vidal, J. Equations of State – Reworking the Old Form. *Fluid Phase Equilib.*, **1983**, *13*, 15-20.

113. Wagner, Z.; Wichterle, I. High-Pressure Vapour-Liquid Equilibrium in Systems Containing Carbon Dioxide, 1-Hexene, And N-Hexane. *Fluid Phase Equilib.*, **1987**, *33*, 109-123.

114. Wiese, H. C.; Jacobs, J.; Sage, B. H. Phase Equilibria in Hydrocarbon Systems. Phase Behavior in the Methane-Propane-n-Butane System. *J. Chem. Eng. Data,* **1970**, *15*, 82-91.

115. Wilson, G. M.; J. Vapor-Liquid Equilibrium Correlated by means of a Modified Redlich-Kwong Equation of State. *Amer. Chem. Soci.*, **1964**, *86*, 127-135.

116. Wong, D. S. H.; Sandler, S. I. A Theortically Correct Mixing Rule for Cubic Equations of State. *AIChE J.*, **1992**, *38*, 671-680.

117. Yi, X. *Binary Vapor-Liquid Phase Equilibrium for Carbon Monoxide + Hydrocarbons*. M.S. Thesis. Oklahoma State University, Stillwater, OK., **1992**.

118. Young, H. D., Statistical Treatment of Experimental Data, McGRAW-HILL BOOK COMPANY, INC. **1962**.

119. Yu, J. M.; Lu, B.C.-Y. Simultaneous calculation of VLE and Saturated Liquid and Vapor Volumes by means of a 3P1T Cubic EOS. *Fluid Phase Equilib.*, **1987**, *34*, 1-19.

APPENDIXE A

PR EOS Interaction Parameters for Hydrogen, Nitrogen, Carbon Monoxide, Carbon Dioxide, Methane, and Ethane in n-Paraffins

Table A.1

PR EOS Interaction Parameters for Methane + n-Paraffins Systems Using the New α Function: C_{ij} And D_{ij} Approach

		Case Number									
		2		3		4			5		
CN	T, K	C_{ij}	%ADD	$C_{ij}(T)$	%ADD	C_{ij}	D_{ij}	%ADD	$C_{ij}(T)$	$D_{ij}(T)$	%ADD
4	277.59	0.034	1.0	0.033	0.6	0.043	-0.011	0.7	0.038	-0.006	0.4
	344.26			0.033	0.8				0.044	-0.013	0.2
	377.59			0.050	0.2				0.050	0.000	0.2
5	377.59	0.040	1.2	0.042	1.1	0.043	-0.004	1.1	0.037	0.007	1.0
	344.26			0.037	1.1				0.049	-0.011	0.6
6	298.33	0.032	0.6	0.032	0.5	0.030	0.002	0.6	0.032	0.000	0.5
	323.33			0.031	0.4				0.028	0.002	0.4
	348.33			0.034	0.3				0.033	0.001	0.3
	373.33			0.036	0.3				0.036	0.000	0.3
7	311.11	0.023	0.7	0.024	0.1	0.028	-0.003	0.6	0.024	0.000	0.1
	344.44			0.020	0.7				0.037	-0.010	0.0
	377.78			0.022	0.5				0.035	-0.008	0.0
	411.11			0.031	0.6				0.061	-0.017	0.0
8	298.33	0.043	1.8	0.040	1.0	0.010	0.015	1.4	0.028	0.006	0.8
	348.33			0.040	1.5				0.000	0.018	0.3
	373.33			0.047	2.6				-0.043	0.041	0.6
	423.33			0.051	1.2				-0.008	0.028	0.3
9	323.15	0.032	2.0	0.035	1.3	0.051	-0.008	1.7	0.056	-0.009	0.3
	348.15			0.029	2.1				0.077	-0.022	0.3
	373.15			0.039	0.6				0.026	0.006	0.2
	423.15			0.018	1.5				0.049	-0.015	1.1

Table A.1

PR EOS Interaction Parameters for Methane + n-Paraffins Systems Using the New α Function: C_{ij} And D_{ij} Approach - *continued*

		Case Number									
		2		3		4			5		
CN	T, K	C_{ij}	%ADD	$C_{ij}(T)$	%ADD	C_{ij}	D_{ij}	%ADD	$C_{ij}(T)$	$D_{ij}(T)$	%ADD
10	310.93	0.015	1.7	0.022	1.1	0.024	-0.004	1.6	0.038	-0.006	0.2
	344.26			0.014	0.5				0.029	-0.006	0.3
	377.59			0.008	0.9				0.036	-0.011	0.2
	410.93			0.005	0.9				0.039	-0.014	0.3
16	462.45	-0.006	5.0	-0.007	5.4	0.063	-0.025	2.1	0.062	-0.026	0.3
	542.65			-0.019	3.8				0.089	-0.035	0.6
	623.15			0.090	1.5				0.236	-0.041	1.2
20	323.15	-0.004	4.4	0.013	1.4	-0.011	0.001	4.4	0.052	-0.007	0.5
	373.15			-0.017	2.4				0.065	-0.016	0.2
	423.15			-0.029	2.5				0.065	-0.021	0.3
28	348.15	-0.039	3.9	-0.026	3.1	0.051	-0.012	3.5	0.069	-0.012	0.8
	373.15			-0.039	3.5				0.113	-0.019	0.8
	423.15			-0.065	2.5				0.042	-0.015	0.4
36	373.15	-0.032	4.1	-0.019	3.0	0.088	-0.012	2.4	0.077	-0.010	0.7
	423.15			-0.054	3.5				0.078	-0.013	1.0
44	373.15	-0.022	2.7	-0.012	2.5	0.076	-0.007	2.4	0.097	-0.008	0.9
	423.15			-0.037	2.8				0.099	-0.011	0.6
RMSE			2.040		1.992			1.075			0.437
BIAS			0.237		0.344			-0.026			0.005
%AAD			2.2		1.6			1.8			0.5
NPTS			270		270			270			270

RMSE, Bar; BIAS, Bar.

Table A.2

PR EOS Interaction Parameters for Methane + n-Paraffins Systems Using the New α Function: N_{ij} And M_{ij} Approach

		Case Number									
		2		3		4			5		
CN	T, K	N_{ij}	%ADD	$M_{ij}(T)$	%ADD	N_{ij}	M_{ij}	%ADD	$N_{ij}(T)$	$M_{ij}(T)$	%ADD
4	277.59	-0.056	1.0	-0.054	0.6	-0.071	0.904	0.6	-0.063	0.946	0.4
	344.26			-0.054	0.8				-0.073	0.879	0.2
	377.59			-0.082	0.2				-0.080	1.013	0.2
5	377.59	-0.047	1.2	-0.050	1.1	-0.051	0.976	1.1	-0.043	1.043	1.0
	344.26			-0.044	1.1				-0.058	0.932	0.6
6	298.33	-0.030	0.6	-0.030	0.5	-0.028	1.008	0.6	-0.030	0.998	0.5
	323.33			-0.029	0.4				-0.023	1.021	0.3
	348.33			-0.032	0.3				-0.031	1.003	0.3
	373.33			-0.033	0.3				-0.030	1.011	0.3
7	311.11	-0.018	0.7	-0.019	0.1	-0.022	0.985	0.6	-0.019	0.998	0.1
	344.44			-0.015	0.7				-0.029	0.958	0.0
	377.78			-0.017	0.5				-0.027	0.968	0.0
	411.11			-0.024	0.6				-0.048	0.929	0.0
8	298.33	-0.029	1.8	-0.027	1.0	-0.007	1.057	1.4	-0.018	1.023	0.8
	348.33			-0.027	1.5				0.000	1.069	0.3
	373.33			-0.032	2.6				0.027	1.160	0.6
	423.33			-0.034	1.2				0.005	1.109	0.3
9	323.15	-0.019	2.0	-0.021	1.3	-0.030	0.971	1.8	-0.033	0.968	0.3
	348.15			-0.017	2.1				-0.047	0.925	0.3
	373.15			-0.023	0.6				-0.015	1.021	0.2
	423.15			-0.010	1.5				-0.029	0.951	1.1

Table A.2

PR EOS Interaction Parameters for Methane + n-Paraffins Systems Using the New α Function: N_{ij} And M_{ij} Approach - *continued*

		Case Number									
		2		3		4			5		
CN	T, K	N_{ij}	%ADD	$M_{ij}(T)$	%ADD	N_{ij}	M_{ij}	%ADD	$N_{ij}(T)$	$M_{ij}(T)$	%ADD
10	310.93	-0.008	1.7	-0.012	1.1	-0.016	0.981	1.7	-0.020	0.980	0.2
	344.26			-0.007	0.5				-0.014	0.984	0.3
	377.59			-0.004	0.9				-0.019	0.967	0.2
	410.93			-0.003	0.9				-0.021	0.955	0.3
16	462.45	0.002	5.0	0.002	5.4	-0.022	0.943	2.1	-0.021	0.941	0.3
	542.65			0.006	3.8				-0.031	0.920	0.6
	623.15			-0.031	1.5				-0.091	0.905	1.1
20	323.15	0.001	4.4	-0.004	1.4	0.000	0.999	4.4	-0.015	0.985	0.5
	373.15			0.005	2.4				-0.019	0.968	0.2
	423.15			0.008	2.5				-0.019	0.957	0.3
28	348.15	0.008	3.9	0.005	3.1	-0.010	0.980	3.5	-0.015	0.978	0.8
	373.15			0.008	3.5				-0.025	0.965	0.8
	423.15			0.013	2.5				-0.009	0.974	0.4
36	373.15	0.005	4.1	0.003	3.0	-0.015	0.980	2.4	-0.014	0.983	0.7
	423.15			0.009	3.5				-0.015	0.977	1.0
44	373.15	0.003	2.6	0.002	2.5	-0.012	0.988	2.4	-0.015	0.987	0.9
	423.15			0.005	2.8				-0.016	0.983	0.6
RMSE			2.040		1.989			1.074			0.437
BIAS			0.234		0.343			-0.040			0.009
%AAD			2.2		1.6			1.8			0.5
NPTS			270		270			270			270

Table A.3

PR EOS Interaction Parameters for Ethane + n-Paraffins Systems Using the New α Function: C_{ij} And D_{ij} Approach

		Case Number									
		2		3		4			5		
CN	T, K	C_{ij}	%ADD	$C_{ij}(T)$	%ADD	C_{ij}	D_{ij}	%ADD	$C_{ij}(T)$	$D_{ij}(T)$	%ADD
4	303.15	0.009	1.5	0.008	1.7	0.015	-0.008	1.5	-0.009	0.023	1.7
	323.15			0.010	1.4				0.043	-0.041	1.0
	343.17			0.004	1.4				0.027	-0.031	1.4
	363.40			0.013	1.1				0.042	-0.036	1.0
5	310.93	0.008	0.9	0.006	0.6	0.009	-0.002	0.9	0.002	0.004	0.4
	377.59			0.011	0.8				0.026	-0.020	0.6
	444.26			0.051	1.9				0.281	-0.248	0.9
6	310.93	0.002	0.7	0.004	0.2	0.007	-0.005	0.7	0.005	-0.001	0.2
	338.71			0.000	0.7				0.007	-0.008	0.3
	366.48			0.000	0.4				0.006	-0.007	0.2
	394.26			0.005	0.8				0.020	-0.017	0.2
7	338.71	0.006	3.7	-0.009	0.7	0.010	-0.012	3.7	-0.006	-0.016	0.4
	449.82			0.026	4.2				0.077	-0.101	1.7
8	323.15	0.021	1.9	0.015	1.2	0.016	0.005	1.9	0.024	-0.013	0.3
	348.15			0.022	1.7				0.017	0.005	1.7
	373.15			0.024	2.6				0.022	0.001	2.6
10	311.11	0.000	2.0	0.004	0.9	0.004	-0.004	1.9	0.007	-0.002	0.7
	344.44			-0.001	1.2				0.006	-0.006	0.6
	377.78			-0.006	1.4				0.000	-0.006	0.6
	411.11			-0.009	2.3				0.010	-0.018	0.4

Table A.3

PR EOS Interaction Parameters for Ethane + n-Paraffins Systems Using the New α Function: C_{ij} And D_{ij} Approach - *continued*

		Case Number									
		2		3		4			5		
CN	T, K	C_{ij}	%ADD	$C_{ij}(T)$	%ADD	C_{ij}	D_{ij}	%ADD	$C_{ij}(T)$	$D_{ij}(T)$	%ADD
16	285.00	0.006	4.3	0.015	2.5	0.019	-0.011	2.3	0.024	-0.011	1.4
	295.00			0.008	3.8				0.023	-0.011	1.2
	305.00			0.007	3.7				0.021	-0.011	0.8
	315.00			0.004	3.4				0.012	-0.007	2.4
	325.00			0.001	3.8				0.011	-0.008	2.6
	335.00			0.003	6.6				0.025	-0.017	2.1
	345.00			-0.007	4.8				0.015	-0.013	0.0
20	323.15	-0.029	7.0	-0.026	7.4	0.015	-0.022	2.6	0.018	-0.021	0.7
	373.15			-0.021	6.3				0.013	-0.021	0.8
	423.15			-0.050	4.8				0.013	-0.028	0.2
24	330.00	-0.033	5.5	-0.039	1.5	0.008	-0.015	4.6	-0.037	0.000	1.6
	340.00			-0.039	1.6				-0.043	0.001	1.7
	350.00			-0.017	9.9				0.024	-0.023	3.3
	360.00			-0.042	3.2				0.001	-0.016	0.2
28	348.15	-0.056	6.9	-0.049	6.1	0.005	-0.019	2.4	0.007	-0.019	0.9
	373.15			-0.055	6.8				-0.001	-0.016	1.1
	423.15			-0.080	4.8				-0.004	-0.022	0.6
36	373.15	-0.075	7.0	-0.079	7.6	0.012	-0.021	1.8	0.001	-0.017	0.7
	423.15			-0.079	7.9				0.015	-0.023	1.2
	373.15			-0.054	9.2				0.032	-0.024	2.7
	473.05			-0.090	3.9				-0.005	-0.018	1.2
	573.05			-0.089	2.0				0.002	-0.018	0.6

Table A.3

PR EOS Interaction Parameters for Ethane + n-Paraffins Systems Using the New α Function: C_{ij} And D_{ij} Approach - *continued*

		Case Number									
		2		3		4			5		
CN	T, K	C_{ij}	%ADD	$C_{ij}(T)$	%ADD	C_{ij}	D_{ij}	%ADD	$C_{ij}(T)$	$D_{ij}(T)$	%ADD
44	373.15	-0.113	8.6	-0.111	10.7	0.002	-0.020	1.6	0.011	-0.022	1.0
	423.15			-0.115	5.8				-0.018	-0.016	0.9
RMSE			1.830		1.595			0.894			0.461
BIAS			0.422		0.440			0.030			0.019
%AAD			3.4		3.1			1.8			1.0
NPTS			300		300			300			300

Table A.4

PR EOS Interaction Parameters for Ethane + n-Paraffins Systems Using the New α Function: N_{ij} And M_{ij} Approach

		Case Number									
		2		3		4			5		
CN	T, K	N_{ij}	%ADD	$M_{ij}(T)$	%ADD	N_{ij}	M_{ij}	%ADD	$N_{ij}(T)$	$M_{ij}(T)$	%ADD
4	303.15	-0.057	1.5	-0.054	1.7	-0.112	0.740	1.5	0.062	1.584	1.7
	323.15			-0.064	1.4				-0.289	0.006	1.0
	343.17			-0.027	1.4				-0.220	0.006	1.5
	363.40			-0.088	1.1				-0.293	0.053	1.0
5	310.93	-0.027	0.9	-0.021	0.6	-0.036	0.956	0.9	-0.008	1.060	0.4
	377.59			-0.038	0.8				-0.093	0.735	0.6
	444.26			-0.186	1.9				-0.400	0.051	1.2
6	310.93	-0.005	0.7	-0.009	0.2	-0.017	0.951	0.7	-0.011	0.993	0.2
	338.71			0.000	0.7				-0.018	0.926	0.3
	366.48			0.001	0.4				-0.015	0.941	0.2
	394.26			-0.013	0.8				-0.048	0.843	0.2
7	338.71	-0.011	3.7	0.015	0.7	-0.019	0.909	3.8	0.010	0.890	0.4
	449.82			-0.048	4.2				0.002	1.117	5.8
8	323.15	-0.030	1.9	-0.022	1.2	-0.023	1.030	1.9	-0.035	0.926	0.3
	348.15			-0.032	1.7				-0.025	1.029	1.7
	373.15			-0.035	2.6				-0.027	1.025	2.5
10	311.11	0.000	2.0	-0.004	0.9	-0.005	0.980	1.8	-0.007	0.991	0.8
	344.44			0.001	1.2				-0.006	0.972	0.6
	377.78			0.006	1.4				0.000	0.973	0.6
	411.11			0.009	2.3				-0.010	0.920	0.4

Table A.4

PR EOS Interaction Parameters for Ethane + n-Paraffins Systems Using the New α Function: N_{ij} And M_{ij} Approach - *continued*

		Case Number									
		2		3		4			5		
CN	T, K	N_{ij}	%ADD	$N_{ij}(T)$	%ADD	N_{ij}	M_{ij}	%ADD	$N_{ij}(T)$	$M_{ij}(T)$	%ADD
16	285.00	-0.003	4.3	-0.009	2.5	-0.011	0.968	2.3	-0.014	0.968	1.4
	295.00			-0.005	3.8				-0.013	0.968	1.2
	305.00			-0.004	3.6				-0.012	0.968	0.8
	315.00			-0.002	3.4				-0.007	0.979	2.3
	325.00			-0.001	3.8				-0.006	0.977	2.6
	335.00			-0.001	6.6				-0.014	0.952	2.1
	345.00			0.004	4.8				-0.008	0.963	0.0
20	323.15	0.013	7.1	0.011	7.4	-0.007	0.946	2.6	-0.008	0.950	0.7
	373.15			0.009	6.3				-0.006	0.949	0.8
	423.15			0.022	4.8				-0.006	0.933	0.2
24	330.00	0.012	5.5	0.014	1.5	0.000	0.973	4.3	0.024	1.016	0.0
	340.00			0.014	1.6				0.016	1.003	1.6
	350.00			0.007	9.8				-0.009	0.950	3.3
	360.00			0.015	3.2				0.000	0.966	0.1
28	348.15	0.017	6.9	0.015	6.1	-0.002	0.961	2.4	-0.002	0.963	0.9
	373.15			0.017	6.8				0.000	0.967	1.1
	423.15			0.025	4.8				0.000	0.955	0.7
36	373.15	0.018	7.0	0.019	7.6	0.000	0.968	1.9	0.000	0.969	0.7
	423.15			0.019	7.9				-0.003	0.959	1.2
	373.15			0.013	9.2				-0.008	0.957	2.7
	473.05			0.022	3.9				0.002	0.968	1.2
	573.05			0.022	2.0				0.000	0.969	0.6

Table A.4

PR EOS Interaction Parameters for Ethane + n-Paraffins Systems Using the New α Function: N_{ij} And M_{ij} Approach - *continued*

		Case Number									
		2		3		4			5		
CN	T, K	C_{ij}	%ADD	$C_{ij}(T)$	%ADD	C_{ij}	D_{ij}	%ADD	$C_{ij}(T)$	$D_{ij}(T)$	%ADD
44	373.15	0.022	8.6	0.022	10.7	0.000	0.967	1.6	-0.003	0.962	1.0
	423.15			0.023	5.8				0.004	0.974	0.9
RMSE			1.830		1.602			0.967			0.637
BIAS			0.426		0.444			0.052			0.064
%AAD			3.4		3.1			1.8			1.0
NPTS			300		300			300			300

Table A.5

PR EOS Interaction Parameters for Hydrogen + n-Paraffins Systems Using the New α Function: C_{ij} And D_{ij} Approach

		Case Number									
		2		3		4			5		
CN	T, K	C_{ij}	%ADD	$C_{ij}(T)$	%ADD	C_{ij}	D_{ij}	%ADD	$C_{ij}(T)$	$D_{ij}(T)$	%ADD
4	327.65	0.215	4.7	0.178	4.1	0.093	0.030	4.5	-0.481	0.155	1.3
	344.25			0.191	3.1				-0.384	0.143	1.4
	360.95			0.245	2.5				-0.158	0.106	1.4
	377.55			0.355	2.5				-0.009	0.098	1.8
	394.25			0.482	1.7				0.039	0.098	2.2
5	323.15	0.272	2.3	0.272	2.3	-0.039	0.055	1.6	-0.039	0.055	1.6
6	344.26	0.275	1.5	0.261	1.1	0.383	-0.017	1.3	-0.016	0.040	1.1
	377.59			0.290	0.5				0.219	0.012	0.4
	410.93			0.449	0.0				0.371	0.012	0.0
7	424.15	0.251	2.5	0.228	1.3	0.274	-0.005	2.5	0.289	-0.012	1.1
	471.65			0.284	2.5				0.173	0.031	1.9
10	344.26	0.231	0.7	0.227	0.7	0.209	0.002	0.7	0.233	0.000	0.7
	373.15			0.227	0.2				0.228	0.000	0.2
	423.15			0.252	0.3				0.252	0.000	0.3
12	344.26	0.208	1.3	0.198	1.1	0.192	0.001	1.3	0.206	-0.001	1.1
	377.59			0.233	0.8				0.242	-0.001	0.9
	410.93			0.194	0.7				0.195	0.000	0.7
20	323.15	0.212	2.4	0.246	0.8	-0.226	0.020	2.0	0.020	0.010	0.2
	373.15			0.198	0.6				-0.007	0.009	0.6
	423.15			0.145	0.3				-0.012	0.007	0.2

Table A.5

PR EOS Interaction Parameters for Hydrogen + n-Paraffins Systems Using the New α Function: C_{ij} And D_{ij} Approach - *continued*

		Case Number									
		2		3		4			5		
CN	T, K	C_{ij}	%ADD	$C_{ij}(T)$	%ADD	C_{ij}	D_{ij}	%ADD	$C_{ij}(T)$	$D_{ij}(T)$	%ADD
28	348.15	0.293	3.8	0.355	0.5	-0.161	0.014	3.6	0.162	0.006	0.2
	373.15			0.307	0.4				0.174	0.004	0.1
	423.15			0.192	0.4				0.111	0.003	0.4
36	373.15	0.433	2.7	0.473	0.8	0.178	0.006	2.5	0.470	0.000	0.8
	423.15			0.372	0.5				0.368	0.000	0.5
RMSE			3.842		2.820			3.784			1.432
BIAS			0.003		-0.279			0.168			-0.016
%AAD			2.7		1.4			2.5			1.0
NPTS			191		191			191			191

Table A.6

PR EOS Interaction Parameters for Hydrogen + n-Paraffins Systems Using the New α Function: N_{ij} And M_{ij} Approach

		Case Number									
		2		3		4			5		
CN	T, K	N_{ij}	%ADD	$M_{ij}(T)$	%ADD	N_{ij}	M_{ij}	%ADD	$N_{ij}(T)$	$M_{ij}(T)$	%ADD
4	327.65	-0.088	4.7	-0.072	4.1	-0.030	1.159	4.5	0.146	1.831	1.3
	344.25			-0.077	3.1				0.118	1.742	1.4
	360.95			-0.103	2.5				0.054	1.543	1.4
	377.55			-0.162	2.5				0.013	1.539	1.8
	394.25			-0.250	1.7				-0.032	1.511	1.4
5	323.15	-0.099	2.3	-0.099	2.3	0.007	1.206	1.6	0.007	1.206	1.6
6	344.26	-0.088	1.4	-0.083	1.1	-0.132	0.948	1.3	0.004	1.136	1.1
	377.59			-0.094	0.5				-0.064	1.044	0.4
	410.93			-0.167	0.0				-0.124	1.044	0.0
7	424.15	-0.071	2.5	-0.063	1.3	-0.079	0.985	2.5	-0.084	0.965	1.1
	471.65			-0.082	2.5				-0.046	1.096	1.9
10	344.26	-0.052	0.7	-0.051	0.7	-0.043	1.009	0.7	-0.007	1.045	0.2
	373.15			-0.051	0.2				-0.035	1.016	0.2
	423.15			-0.057	0.3				-0.026	1.032	0.2
12	344.26	-0.041	1.4	-0.039	1.1	-0.005	1.032	1.3	0.000	1.034	0.8
	377.59			-0.047	0.8				-0.001	1.041	0.4
	410.93			-0.038	0.7				0.003	1.038	0.6
20	323.15	-0.031	2.4	-0.037	0.8	-0.005	1.014	2.1	-0.005	1.017	0.3
	373.15			-0.029	0.6				-0.001	1.016	0.6
	423.15			-0.020	0.3				0.002	1.014	0.3

Table A.6

PR EOS Interaction Parameters for Hydrogen + n-Paraffins Systems Using the New α Function: N_{ij} And M_{ij} Approach - *continued*

		Case Number									
		2		3		4			5		
CN	T, K	N_{ij}	%ADD	$M_{ij}(T)$	%ADD	N_{ij}	M_{ij}	%ADD	$N_{ij}(T)$	$M_{ij}(T)$	%ADD
28	348.15	-0.037	3.8	-0.048	0.5	0.002	1.017	3.6	-0.033	1.005	0.3
	373.15			-0.040	0.4				-0.027	1.005	0.1
	423.15			-0.023	0.4				-0.011	1.005	0.4
36	373.15	-0.054	2.7	-0.061	0.8	-0.026	1.008	2.6	-0.054	1.002	0.7
	423.15			-0.044	0.5				-0.030	1.004	0.3
RMSE			3.828		2.820			3.764			1.373
BIAS			0.000		-0.277			0.172			0.005
%AAD			2.7		1.4			2.6			0.9
NPTS			191		191			191			191

Table A.7

PR EOS Interaction Parameters for Nitrogen + n-Paraffins Systems Using the New α Function: C_{ij} And D_{ij} Approach

		Case Number									
		2		3		4			5		
CN	T, K	C_{ij}	%ADD	$C_{ij}(T)$	%ADD	C_{ij}	D_{ij}	%ADD	$C_{ij}(T)$	$D_{ij}(T)$	%ADD
4	250.00	0.092	3.1	0.101	2.2	0.008	0.043	2.0	0.040	0.030	0.5
	277.00			0.099	2.5				0.028	0.036	0.9
	311.09			0.078	2.2				0.013	0.036	0.9
	344.43			0.093	7.6				0.001	0.041	0.5
	366.48			0.060	2.3				-0.065	0.073	0.7
	399.82			0.048	2.4				-0.092	0.063	4.5
5	277.43	0.088	3.7	0.093	2.9	0.036	0.023	2.9	0.094	0.000	2.8
	310.71			0.092	3.3				0.042	0.022	2.0
	344.26			0.086	2.4				0.013	0.033	1.4
	377.59			0.026	2.1				0.085	-0.033	1.7
8	322.00	0.167	2.8	0.173	2.7	0.098	0.022	1.5	0.082	0.028	0.3
	344.30			0.161	2.7				0.100	0.019	0.8
9	322.00	0.170	2.4	0.177	2.0	0.131	0.011	2.3	0.131	0.013	1.0
	344.30			0.160	1.7				0.139	0.006	1.4
10	344.26	0.162	1.8	0.172	0.3	0.099	0.014	1.6	0.145	0.006	0.1
	377.59			0.156	0.3				0.131	0.006	0.2
	410.93			0.142	0.4				0.095	0.010	0.2
12	344.26	0.179	1.0	0.184	0.2	0.143	0.006	1.0	0.185	0.000	0.2
	377.59			0.178	0.8				0.174	0.001	0.8
	410.93			0.168	1.0				0.164	0.001	0.9

Table A.7

PR EOS Interaction Parameters for Nitrogen + n-Paraffins Systems Using the New α Function: C_{ij} And D_{ij} Approach - *continued*

		Case Number									
		2		3		4			5		
CN	T, K	C_{ij}	%ADD	$C_{ij}(T)$	%ADD	C_{ij}	D_{ij}	%ADD	$C_{ij}(T)$	$D_{ij}(T)$	%ADD
20	323.20	0.242	5.0	0.267	0.4	0.282	-0.004	5.0	0.266	0.000	0.4
	373.20			0.225	0.7				0.225	0.000	0.7
	423.20			0.182	0.6				0.181	0.000	0.6
28	348.20	0.303	3.0	0.321	0.6	0.342	-0.003	2.9	0.322	0.000	0.6
	373.20			0.302	0.9				0.302	0.000	0.9
	423.20			0.260	0.5				0.260	0.000	0.5
36	373.20	0.380	2.0	0.392	0.2	0.394	-0.001	2.0	0.394	0.000	0.2
	423.20			0.360	0.4				0.361	0.000	0.4
RMSE			4.330		6.263			3.348			1.382
BIAS			-0.857		-0.880			-0.196			0.103
%AAD			2.9		1.9			2.4			0.9
NPTS			208		208			208			208

Table A.8

PR EOS Interaction Parameters for Nitrogen + n-Paraffins Systems Using the New α Function: N_{ij} And M_{ij} Approach

		Case Number									
		2		3		4			5		
CN	T, K	N_{ij}	%ADD	$M_{ij}(T)$	%ADD	N_{ij}	M_{ij}	%ADD	$N_{ij}(T)$	$M_{ij}(T)$	%ADD
4	327.65	-0.083	3.6	-0.094	2.2	0.000	1.371	2.0	-0.035	1.231	0.5
	344.25			-0.090	2.5				-0.024	1.282	0.9
	360.95			-0.068	2.2				-0.010	1.281	0.9
	377.55			-0.068	6.9				0.000	1.320	0.5
	394.25			-0.048	2.3				0.050	1.588	0.7
5	323.15			-0.037	2.4				0.067	1.502	4.6
6	344.26	-0.060	3.9	-0.066	2.9	-0.019	1.149	2.9	-0.067	0.997	2.8
	377.59			-0.064	3.3				-0.028	1.124	2.0
	410.93			-0.057	2.4				-0.008	1.191	1.4
7	424.15			-0.016	2.1				-0.055	0.817	1.7
	471.65	-0.076	2.9	-0.080	2.7	-0.042	1.078	1.6	-0.036	1.100	0.3
10	344.26			-0.072	2.7				-0.043	1.068	0.8
	373.15	-0.070	2.6	-0.074	2.0	-0.052	1.036	2.4	-0.053	1.040	1.0
	423.15			-0.065	1.7				-0.055	1.020	1.4
12	344.26	-0.060	2.2	-0.065	0.3	-0.024	1.059	1.7	-0.054	1.017	0.1
	377.59			-0.057	0.3				-0.047	1.017	0.2
	410.93			-0.051	0.4				-0.033	1.031	0.2
20	323.15	-0.057	1.3	-0.060	0.2	-0.033	1.031	1.2	-0.066	0.994	0.2
	373.15			-0.057	0.8				-0.035	1.028	0.7
	423.15			-0.053	1.0				-0.017	1.048	0.7

Table A.8

PR EOS Interaction Parameters for Nitrogen + n-Paraffins Systems Using the New α Function: N_{ij} And M_{ij} Approach - *continued*

		Case Number									
		2		3		4			5		
CN	T, K	N_{ij}	%ADD	$M_{ij}(T)$	%ADD	N_{ij}	M_{ij}	%ADD	$N_{ij}(T)$	$M_{ij}(T)$	%ADD
28	348.15	-0.056	5.5	-0.063	0.4	-0.050	1.004	5.5	-0.071	0.994	0.2
	373.15			-0.051	0.7				-0.067	0.987	0.3
	423.15			-0.039	0.6				-0.054	0.987	0.3
28	348.15	-0.057	3.3	-0.062	0.6	-0.061	0.998	3.3	-0.075	0.993	0.3
	373.15			-0.057	0.9				-0.077	0.989	0.5
	423.15			-0.047	0.5				-0.057	0.994	0.2
36	373.15	-0.064	2.3	-0.067	0.2	-0.069	0.998	2.3	-0.069	0.999	0.3
	423.15			-0.059	0.4				-0.067	0.996	0.2
RMSE			4.762		6.433			3.657			1.350
BIAS			-0.879		-0.832			-0.049			0.070
%AAD			3.2		1.8			2.5			0.8
NPTS			208		208			208			208

Table A.9

PR EOS Interaction Parameters for Carbon Monoxide + n-Paraffins Systems Using the New α Function: C_{ij} And D_{ij} Approach

		Case Number									
		2		3		4			5		
CN	T, K	C_{ij}	%ADD	$C_{ij}(T)$	%ADD	C_{ij}	D_{ij}	%ADD	$C_{ij}(T)$	$D_{ij}(T)$	%ADD
3	273.15	-0.006	5.1	-0.001	5.0	-0.006	0.000	5.1	-0.071	0.055	1.7
	298.15			-0.016	1.8				-0.049	0.030	0.4
	323.15			0.041	7.8				-0.020	0.030	5.1
6	323.15	0.042	1.1	0.046	0.4	0.038	0.001	1.1	0.061	-0.005	0.3
	373.15			0.030	0.9				0.031	0.000	0.9
	423.15			0.042	0.4				0.042	0.000	0.4
8	463.15	0.108	1.6	0.061	0.1	0.376	-0.066	1.4	0.107	-0.011	0.1
	473.15			0.074	0.1				0.118	-0.010	0.1
	483.15			0.092	0.2				0.095	-0.001	0.2
	493.15			0.112	0.4				0.114	-0.001	0.4
	503.15			0.149	0.3				0.150	0.000	0.3
	513.15			0.192	0.4				0.192	0.000	0.4
	523.15			0.207	1.0				0.207	0.000	1.0
	533.15			0.332	0.3				0.327	0.001	0.3
10	310.93	0.072	3.3	0.089	0.5	0.166	-0.020	3.1	0.119	-0.007	0.2
	344.26			0.065	0.3				0.081	-0.003	0.3
	377.59			0.041	0.5				0.070	-0.006	0.2
12	344.26	0.071	3.5	0.092	2.2	-0.097	0.029	2.9	-0.152	0.042	0.9
	377.59			0.074	2.6				-0.128	0.034	1.3
	410.93			0.035	0.7				-0.039	0.013	0.6
	344.26			0.088	1.8				0.214	-0.022	1.4

Table A.9

PR EOS Interaction Parameters for Carbon Monoxide + n-Paraffins Systems Using the New α Function: C_{ij} And D_{ij} Approach - *continued*

		Case Number									
		2		3		4			5		
CN	T, K	C_{ij}	%ADD	$C_{ij}(T)$	%ADD	C_{ij}	D_{ij}	%ADD	$C_{ij}(T)$	$D_{ij}(T)$	%ADD
20	323.15	0.086	6.5	0.133	0.8	0.116	-0.003	6.4	0.245	-0.012	0.3
	373.15			0.070	0.9				0.189	-0.012	0.2
	423.15			-0.001	2.3				0.202	-0.019	0.2
28	373.15	0.111	3.2	0.102	0.7	0.232	-0.009	3.1	0.100	0.000	0.7
	423.15			0.061	0.9				0.059	0.000	0.9
	348.15			0.134	2.5				0.130	0.000	2.5
	373.15			0.130	0.4				0.128	0.000	0.4
	423.15			0.083	1.8				0.094	-0.001	1.8
36	373.15	0.210	3.3	0.238	2.1	-0.005	0.010	3.3	-0.026	0.013	0.7
	473.05			0.154	2.1				-0.301	0.022	1.0
	572.95			0.161	1.3				-0.286	0.021	0.7
RMSE			2.297		2.798			3.729			1.728
BIAS			-0.292		-0.278			-0.439			-0.109
%AAD			3.1		1.5			3.1			0.8
NPTS			182		182			182			182

Table A.10

PR EOS Interaction Parameters for Carbon Monoxide + n-Paraffins Systems Using the New α Function: N_{ij} And M_{ij} Approach

		Case Number									
		2		3		4			5		
CN	T, K	N_{ij}	%ADD	$M_{ij}(T)$	%ADD	N_{ij}	M_{ij}	%ADD	$N_{ij}(T)$	$M_{ij}(T)$	%ADD
3	273.15	0.008	3.6	0.001	5.0	0.085	1.682	1.6	0.088	1.719	1.7
	298.15			0.019	1.8				0.060	1.393	0.4
	323.15			0.002	3.2				0.025	1.393	7.2
6	323.15	-0.023	1.2	-0.027	0.4	-0.009	1.039	1.2	-0.037	0.972	0.3
	373.15			-0.017	0.9				-0.002	1.042	0.8
	423.15			-0.022	0.4				-0.004	1.059	0.3
8	463.15	-0.043	1.5	-0.024	0.1	-0.191	0.764	1.3	-0.052	0.946	0.1
	473.15			-0.029	0.1				-0.052	0.955	0.1
	483.15			-0.036	0.2				-0.037	0.998	0.2
	493.15			-0.045	0.4				-0.020	1.056	0.3
	503.15			-0.060	0.3				-0.095	0.936	0.4
	513.15			-0.079	0.4				-0.275	0.740	0.3
	523.15			-0.085	1.0				0.020	1.286	0.5
	533.15			-0.148	0.3				-0.310	0.809	0.3
10	310.93	-0.026	3.5	-0.033	0.5	-0.034	0.988	3.5	-0.046	0.980	0.3
	344.26			-0.024	0.3				-0.030	0.990	0.3
	377.59			-0.015	0.5				-0.031	0.971	0.1
12	344.26	-0.022	3.6	-0.029	2.2	0.042	1.103	2.6	0.000	1.042	1.5
	377.59			-0.023	2.6				0.036	1.092	1.3
	410.93			-0.010	0.7				0.012	1.035	0.6
	344.26			-0.028	1.8				0.000	1.040	2.3

Table A.10

PR EOS Interaction Parameters for Carbon Monoxide + n-Paraffins Systems Using the New α Function: N_{ij} And M_{ij} Approach - *continued*

		Case Number									
		2		3		4			5		
CN	T, K	N_{ij}	%ADD	$M_{ij}(T)$	%ADD	N_{ij}	M_{ij}	%ADD	$N_{ij}(T)$	$M_{ij}(T)$	%ADD
20	323.15	-0.018	6.6	-0.030	0.8	0.034	1.057	6.2	-0.059	0.977	0.3
	373.15			-0.015	0.9				-0.042	0.976	0.3
	423.15			-0.004	1.2				-0.046	0.961	0.2
28	373.15	-0.019	3.3	-0.017	0.7	-0.030	0.992	3.3	-0.036	0.988	0.3
	423.15			-0.010	0.9				-0.019	0.993	1.0
	348.15			-0.023	2.5				-0.107	0.957	0.6
	373.15			-0.022	0.4				-0.025	0.998	0.3
	423.15			-0.014	1.8				-0.001	1.009	1.8
36	373.15	-0.031	3.6	-0.037	2.1	0.040	1.047	2.9	-0.001	1.020	0.9
	473.05			-0.022	2.1				0.039	1.041	1.0
	572.95			-0.022	1.3				0.032	1.037	0.7
RMSE			2.363		1.417			1.896			2.709
BIAS			-0.286		-0.130			0.008			-0.203
%AAD			3.2		1.3			2.64			0.84
NPTS			182		182			182			182

Table A.11

PR EOS Interaction Parameters for Carbon Dioxide + n-Paraffins Systems Using the New α Function: C_{ij} And D_{ij} Approach

		Case Number									
		2		3		4			5		
CN	T, K	C_{ij}	%ADD	$C_{ij}(T)$	%ADD	C_{ij}	D_{ij}	%ADD	$C_{ij}(T)$	$D_{ij}(T)$	%ADD
5	273.41	0.120	3.1	0.120	3.1	0.093	0.026	0.5	0.093	0.026	0.5
6	313.15	0.118	5.0	0.094	1.6	0.081	0.043	3.3	0.078	0.019	0.8
	303.15			0.124	1.8				0.107	0.021	0.4
	323.15			0.113	4.9				0.077	0.046	1.3
	353.15			0.134	2.6				0.107	0.028	0.7
	393.15			0.141	1.7				0.108	0.030	1.5
7	310.65	0.102	2.5	0.108	2.2	0.098	0.004	2.4	0.102	0.005	1.8
	352.59			0.103	0.8				0.100	0.003	0.9
	394.26			0.083	2.4				0.121	-0.039	1.9
	477.21			0.091	1.0				0.158	-0.055	0.6
10	377.59	0.118	2.9	0.110	0.5	0.100	0.013	1.9	0.111	-0.001	0.5
	310.93			0.129	1.0				0.114	0.008	0.2
	344.26			0.113	1.9				0.102	0.009	1.2
	310.93			0.119	1.1				0.096	0.020	0.0
16	463.05	0.072	4.9	0.056	0.6	0.213	-0.052	4.7	0.045	0.004	0.6
	542.85			0.066	1.0				0.147	-0.030	0.2
	623.55			0.150	0.7				0.225	-0.030	0.1
	663.75			0.272	1.0				0.370	-0.047	0.4
18	396.60	0.045	3.9	0.051	1.0	0.108	-0.021	3.8	0.047	0.001	1.0
	463.30			0.039	5.0				0.204	-0.052	1.8
	534.90			0.015	5.7				0.298	-0.091	1.6

Table A.11

PR EOS Interaction Parameters for Carbon Monoxide + n-Paraffins Systems Using the New α Function: C_{ij} And D_{ij} Approach - *continued*

		Case Number									
		2		3		4			5		
CN	T, K	C_{ij}	%ADD	$C_{ij}(T)$	%ADD	C_{ij}	D_{ij}	%ADD	$C_{ij}(T)$	$D_{ij}(T)$	%ADD
18	605.40			0.081	1.1				0.152	-0.025	0.2
	673.20			0.160	0.0				0.238	-0.025	0.0
19	313.15	0.097	3.0	0.104	0.6	0.098	0.000	3.0	0.103	0.000	0.6
	333.15			0.093	1.5				0.092	0.001	1.6
20	373.15	0.090	3.8	0.072	1.4	0.101	-0.004	4.0	0.094	-0.007	0.2
	323.15			0.097	1.1				0.107	-0.003	0.5
	373.15			0.083	0.3				0.081	0.001	0.3
21	318.15	0.090	2.8	0.095	1.2	0.101	-0.005	2.1	0.100	-0.003	0.4
	338.15			0.084	2.3				0.096	-0.005	1.0
22	323.15	0.081	4.8	0.095	1.7	0.108	-0.010	3.1	0.104	-0.004	0.7
	348.15			0.076	3.0				0.101	-0.009	1.0
	373.15			0.065	2.4				0.090	-0.007	1.4
24	373.15	0.076	3.5	0.076	3.5	0.078	0.000	3.4	0.078	0.000	3.4
28	373.15	0.060	7.2	0.058	5.7	0.116	-0.015	3.0	0.111	-0.013	0.4
	348.15			0.076	6.4				0.113	-0.011	0.3
	423.15			0.027	6.2				0.109	-0.018	1.9
36	373.15	0.024	5.3	0.032	5.0	0.103	-0.013	2.6	0.101	-0.011	0.7
	423.15			0.009	5.0				0.113	-0.017	0.4

Table A.11

PR EOS Interaction Parameters for Carbon Monoxide + n-Paraffins Systems Using the New α Function: C_{ij} And D_{ij} Approach - *continued*

44	373.15	0.011	7.0	0.002	7.3	0.123	-0.014	2.2	0.132	-0.170	7.3
	423.15			0.000	6.6				0.133	-0.017	0.5
RMSE			2.3237		1.8412			1.298			0.8217
BIAS			0.2714		0.3509			-0.0439			0.0544
%AAD			4.15		2.64			2.92			1.11
NPTS			328		328			328			328

Table A.12

PR EOS Interaction Parameters for Carbon Dioxide + n-Paraffins Systems Using the New α Function: N_{ij} And M_{ij} Approach

		Case Number									
		2		3		4			5		
CN	T, K	N_{ij}	%ADD	$M_{ij}(T)$	%ADD	N_{ij}	M_{ij}	%ADD	$N_{ij}(T)$	$M_{ij}(T)$	%ADD
5	273.41	-0.284	3.1	-0.284	3.1	-0.216	1.171	0.5	-0.216	1.171	0.5
6	313.15	-0.197	4.7	-0.154	1.6	-0.135	1.215	3.2	-0.128	1.098	0.8
	303.15			-0.209	1.8				-0.178	1.110	0.4
	323.15			-0.188	4.9				-0.126	1.242	1.3
	353.15			-0.223	2.6				-0.175	1.147	0.7
	393.15			-0.232	1.7				-0.173	1.154	1.5
7	310.65	-0.132	2.7	-0.142	2.2	-0.125	1.021	2.7	-0.134	1.022	1.9
	352.59			-0.133	0.8				-0.130	1.009	0.9
	394.26			-0.104	2.4				-0.155	0.835	1.9
	477.21			-0.111	1.0				-0.201	0.769	0.6
10	377.59	-0.096	3.1	-0.089	0.5	-0.080	1.042	2.1	-0.090	0.997	0.5
	310.93			-0.107	1.0				-0.094	1.026	0.2
	344.26			-0.092	1.9				-0.083	1.027	1.2
	310.93			-0.098	1.1				-0.078	1.063	0.0
16	463.05	-0.033	4.9	-0.026	0.6	-0.112	0.875	4.5	-0.021	1.009	0.6
	542.85			-0.030	1.0				-0.070	0.932	0.2
	623.55			-0.071	0.7				-0.111	0.931	0.1
	663.75			-0.139	1.0				-0.204	0.896	0.4
18	396.60	-0.018	3.9	-0.021	1.0	-0.046	0.954	3.8	-0.019	1.004	0.9
	463.30			-0.016	5.0				-0.091	0.889	1.8
	534.90			-0.006	5.7				-0.141	0.812	1.6

Table A.12

PR EOS Interaction Parameters for Carbon Dioxide + n-Paraffins Systems Using the New α Function: N_{ij} And M_{ij} Approach - *continued*

		Case Number									
		2		3		4			5		
CN	T, K	N_{ij}	%ADD	$M_{ij}(T)$	%ADD	N_{ij}	M_{ij}	%ADD	$N_{ij}(T)$	$M_{ij}(T)$	%ADD
18	605.40			-0.033	1.1				-0.065	0.946	0.2
	673.20			-0.067	0.0				-0.106	0.946	0.0
19	313.15	-0.039	3.0	-0.042	0.6	-0.039	1.000	3.0	-0.042	1.000	0.6
	333.15			-0.037	1.5				-0.037	1.002	1.7
20	373.15	-0.034	3.9	-0.027	1.4	-0.038	0.993	4.0	-0.036	0.985	0.2
	323.15			-0.037	1.1				-0.041	0.993	0.5
	373.15			-0.031	0.3				-0.045	0.964	0.0
21	318.15	-0.033	2.8	-0.035	1.2	-0.037	0.990	2.2	-0.037	0.995	0.4
	338.15			-0.030	2.3				-0.035	0.989	1.0
22	323.15	-0.028	4.8	-0.033	1.7	-0.038	0.980	3.1	-0.036	0.992	0.7
	348.15			-0.026	3.0				-0.035	0.982	1.0
	373.15			-0.022	2.4				-0.031	0.985	1.4
24	373.15	-0.024	3.5	-0.024	3.5	-0.024	1.000	3.5	-0.024	1.000	3.5
28	373.15	-0.016	7.3	-0.016	5.7	-0.033	0.974	3.0	-0.031	0.976	0.4
	348.15			-0.021	6.4				-0.032	0.980	0.3
	423.15			-0.007	6.2				-0.031	0.968	1.9
36	373.15	-0.005	5.3	-0.007	5.0	-0.023	0.978	2.6	-0.023	0.981	0.7
	423.15			-0.002	5.0				-0.026	0.971	0.4

Table A.12

PR EOS Interaction Parameters for Carbon Dioxide + n-Paraffins Systems Using the New α Function: N_{ij} And M_{ij} Approach - *continued*

44	373.15	-0.002	7.0	-0.003	7.4	-0.024	0.977	2.2	-0.023	0.979	0.5
	423.15			0.000	6.6				-0.026	0.973	0.5
RMSE			2.2407		1.6008			1.3557			0.4748
BIAS			0.1643		0.2363			-0.0486			0.0045
%AAD			3.98		2.29			3.03			1.01
NPTS			328		328			328			328

VITA

Wuzi Gao

Candidate for the Degree of

Doctor of Philosophy

Thesis: HIGH PRESSURE SOLUBILITY MEASUREMENTS FOR SELECTED ASYMMETRIC MIXTURES AND EQUATION-OF-STATE DEVELOPMENT

Major Field: Chemical Engineering

Biographical:

Personal Data: Born in Shannxi, P. R. China, on January 6, 1969, the son of Shuenyu Gao and Xiaolan Wang. Married to Liwei Cai in March, 1995.

Education: Graduated from No. 3 High School, Zhouzhi, Shannxi, P. R. China in July, 1986; received Bachelor of Science degree in Mechanical Engineering from Xi'an Jiaotong University, Xi'an, PR China in July, 1990 and Master of Science degree in Mechanical Engineering from Beijing Institute of Chemical Technology, Beijing, P. R. China in July, 1993. Finished the work for the Master of Science degree in Computer Science at Oklahoma State University, Stillwater, USA, in August, 1999. Completed the requirements for the Doctor of Philosophy degree in Chemical Engineering at Oklahoma State University in December, 1999.

Experience: Teaching and Research Assistant, School of Chemical Engineering, Oklahoma State University, August, 1995, to December, 1999; Engineer, Beijing HuanQiu (HQ) Chemical Engineering Corporation, P.R. China, July, 1993, to July, 1995.

Membership in Professional Societies: American Institute of Chemical Engineers; Omega Chi Epsilon.